University of Stavanger

Faculty of Science and Technology

MASTER THESIS

Study program/ Specialization: MSc Drilling & Well Engineering	Spring semester, 2015 Open
Writer: Reza Mirzai	.... ………………………………. (Writer's signatures)

Faculty supervisor: Mesfin A. Belayneh and Bernt S. Aadnøy

Title of thesis:
Effect of Nano silica in brine treated PAC/ XC/LV-CMC polymer – Bentonite fluid system

Credits (ECTS): 30

Key words: Drilling fluid, Nano Silica, Rheology, Viscoelastic, Hydraulic simulation, Cutting transport , Polymer, XC, PAC, CMC , Bentonite	Pages: ....92.............. + enclosure: ...23.. Stavanger, 15th June/2015

"This thesis is dedicated to my parents and family for their endless love, support and encouragement"

Acknowledgements

This thesis consumed huge amount of laboratory work and research. It wouldn't have been possible if it was not for the support of my supervisors and friends. Therefore I would like to extend my gratitude to all of them.

First of all I would like to express my sincere gratitude to my supervisors, Mesfin A. Belayneh and Bernt S. Aadnøy for their contribution and endless support, excellent guidance, enthusiasm, patience and provision of immense knowledge through the learning process of this master thesis.

I also would like to than my friend and classmate Thomas Sharman for his help regarding the viscoelastic laboratory work.

I am grateful to the Department of Petroleum engineering at UiS for providing me the material and opportunity to fulfill this thesis work.

Stavanger, June 2015

Reza Mirzai

Abstract

In this thesis the performance of Nano silica in polymer based bentonite fluid system was analysed. Several combination of Nano with salt and polymer types were formulated and tested. The effect of temperature, salt, polymer and Nano silica concentration was also investigated and discussed. The Nano silica treated system showed a variation of behaviour in presence of difference salt and polymers. It shows a viscosifying and a thinning effect when treated with Xanthan and PAC, respectively.

After several attempts, this thesis work investigated an optimized nano silica blended system. The system is obtained by the addition of 2.5 g KCl + 0.25 g Nano silica + 0.2 g LV CMC + 0.3 g Xanthan XC in bentonite/H_2O (25g/500g) system, which shows good performance in terms of filter loss and rheology. The viscoelastic properties of Nano-free reference system and Nano-treated system were also measured and compared.

Further the borehole cleaning efficiency and the hydraulic of the formulated system were simulated and the result was compared with the Nano-free reference system.

Contents

List of Tables

List of Figures

List of Abbreviations

BP   British Petroleum

CDV   Critical Deposition velocity

CRV   Critical Suspension Velocity

DP   Degree of Polymerization

DS   Degree of Substitution

ECD   Equivalent Circulating Density

EDS   Elemental Dispersive Spectroscopy

EOR   Enhanced Oil Recovery

GPM   Gallon per Minute

ID   Inner Diameter

LSYS   Low Shear Yield Stress

LV-CMC Low Viscous Carboxyl-methyl Cellulose

MD   Measured Depth

MWD   Measuring While Drilling

OBM   Oil Based Mud

OD   Outer Diameter

PAC   Poly-anionic Cellulose

PPG   Part Per gallon

PSA   Petroleum Safety Authority

PV   Plastic Viscosity

RIH   Run into the Hole

ROOH   Run Out of the Hole

ROP   Rate of Penetration

RPM   Round per Minute

SBM   Synthesis Based Mud

SEM   Electron Microscopy

SPE   Society for Petroleum Engineers

UiS   University of Stavanger

WBM   Water Based Mud

XC   Xanthan gum

YS   Yield Stres

Nomenclatures

C_d Drag Coefficient

G' Storage modulus (Elastic modulus)

G'' Loss Modulus (Viscous modulus)

G^* Complex modulus

N_{Re} Reynold's Number

P_o Pore Pressure

P_{wf} Wellbore Pressure

V_c Cumulative filtrate loss volume

V_d Filtrate loss volume of dynamic filtration

V_s Filtrate loss volume of Static filtration

V_{sp} Filtrate loss volume of Spurt loss

$\bar{v}$ Average flow velocity

v_s Slip velocity

θ_{300} Shear Stress value at 300 RPM

θ_{600} Shear Stress value at 600 RPM

ρ_f Fluid Density

ρ_m Mud Density

σ_h Horizontal/tangential Stress

σ_r Radial Stress

σ_t Tensile stress

σ_θ Tangential Stress

τ_o Yiled Stress

ΔP_{Total} Total pressure drop

ΔP_{ac} Annular Pressure drop across casing

ΔP_{ads} Annular Pressure drop across drill string

ΔP_b Bit Pressure drop

ΔP_{dc} Drilling collar Pressure drop

ΔP_{ds} Drill string pressure drop

ΔP_f Annular friction pressure drop

ΔP_s Surface pressure drop

ΔP Pressure drop

$f_{partial}$ Partial friction factor

$f_{transient}$ Friction factor for Transitional flow regime

$f_{turbulent}$ Friction factor for Transitional flow regime

g Gravitational acceleration

h Depth

P Pressure

A Area

F Force

K Consistency index

L Length of the porous media

Q Flow rate

Re Reynold's number

k Permeability

n Flow index

t Mud cake thickness

t Time

γ Share rate

δ Phase angle

ρ Density

τ Shear stress

ω Angular frequency

1 Introduction

Drilling fluid is an essential part of drilling operation. The main functions of drilling fluid are to cuttings removal, maintaining well pressure and provide a good barrier. Poorly designed drilling fluid causes several drilling related problems such as stuck pipe, circulation loss, shale swelling and well stability problems which increases the operational cost.

On contrary, properly designed drilling fluid reduces borehole instability, formation damage and provides a good sealing performance. It is therefore important to design a drilling fluid having an appropriate density and rheological properties. Experimentally, it is investigated that good mud cake increase wellbore strength, and also reduces filtrate loss. Drilling in a fractured and highly porous formation a huge mud loss can be expected. Treating drilling fluid with solid bridging agents can provides better sealing capacity against the permeable formations especially thief zones. A thin and effective mud cake is also favorable condition to prevent the drill pipe stuck situation to occur. Oil based mud system solve swelling problem, Due to susceptible environment, the common practice is drilling with water based mud system. However in terms of swelling issue, water based mud system doesn't solve the problem.

Recently, the applications nanotechnology on cement, EOR and drilling fluid shows promising results. With the idea of improving the rheological, filtrate and performance efficiency of water based mud system, this thesis work look in to the effect of Nano silica on polymer based mud system. The objective is to formulate a Nano treated system and to characterize it. In addition, to simulate the hole cleaning and hydraulic of the fluid systems comparing with Nano free reference system.

1.1 Background

Well instability problems occur either the well pressure exceeds the fracturing pressure or lower than the well collapse pressure. This results loss circulation and drill string sticking respectively. These problems increase operational cost a lot in the oil industry in term of non-productive time as well. In reservoir section, if the well pressure falls below the formation pressure, a kick will occurs. Prevention of fracture and kick incidences can be controlled by maintaining the well pressure between the collapse and the fracture pressures. Figure 1 shows a well program illustrating allowable operational window.
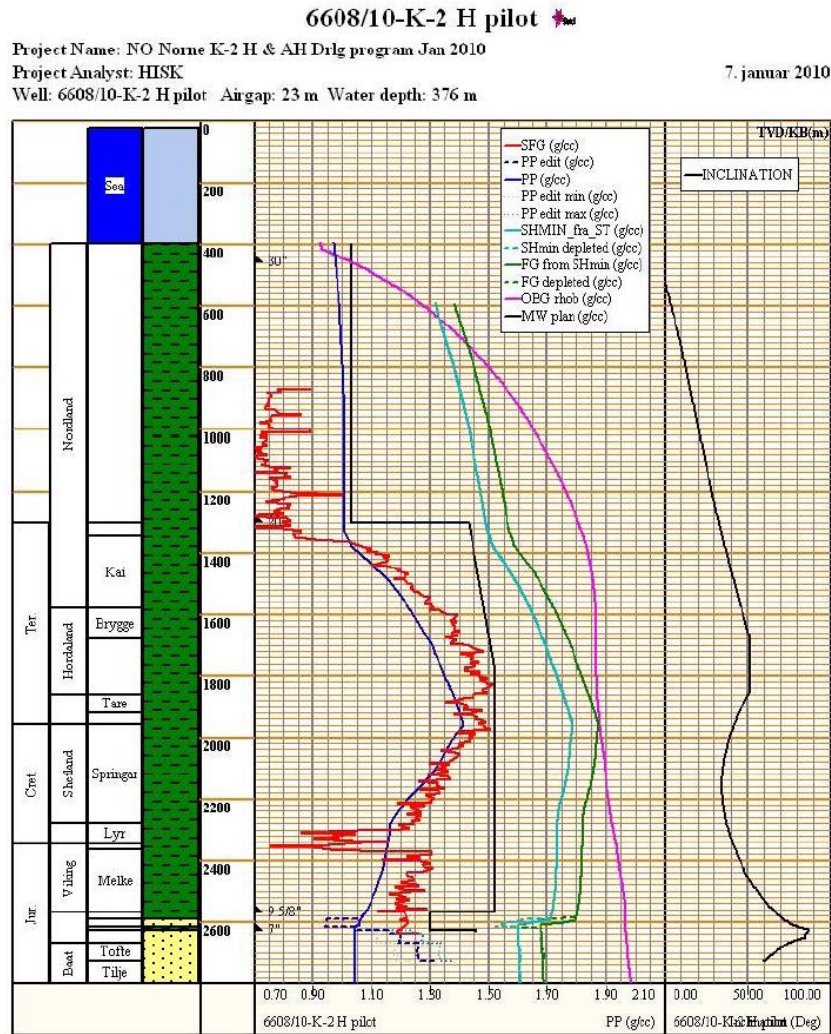
<u>Figure 1 Pore pressure gradient and formation strength and stratigraphic column [30]</u>

The hydrostatic pressure provided by mud is the main factor to control the well. One can calculate the pressure of the well at each depth using the equation (1):

$$P = \rho g h \tag{1}$$

Where the P is pressure [Pa] at the depth h [m] and ρ [kg/m^3] density of drilling fluid and g a free fall acceleration of 9.81 m/s^2.

However there are other parameters which can affect the downhole pressure. Under the dynamic condition the frictional pressure increases the downhole pressure and using the mud density doesn't give any clear picture of the real downhole pressure. To have a better picture and one uses the equivalent circulating density (ECD) as basis to not lead to hole collapse or

formation fracture where the area between these two lines are too narrow. To obtain the value of ECD at the depth of i , equation 2 is used:

$$ECD_i = \rho_m + \frac{\Delta P_f}{g h_i} \tag{2}$$

The frictional pressure loss which contributes to increasing downhole pressure is the annulus pressure ΔP_f for annulus volume above the depth of i .Please notice that the h is the true vertical depth of the point "i". An appropriate drilling mud can reduce the magnitude of the friction to give a better pressure indication. According to Aadnøy (2010) the mud weight must be kept constant for longer period of time to keep the pressure variation as low as possible. It also includes controlling the run into borehole (RIH) and run out of the bore-hole (ROOH) speed, regarding to swabbing and surge effect which may cause borehole collapse or fracturing. This can ensure that well stability with less borehole failure incidents [1].

The ECD in general is a function of the fluid properties (rheology and density) and the dynamic fluid flow rate. Therefore for the prediction of the ECD, the knowledge of the fluid system is important. In addition, the formation damage also can be managed by the property of the fluid system. This thesis is about formulating of Nano treated mud system having good performance.

1.2 Problem description

Shale swelling, sagging and formation damage are associated with the properties of drilling fluid. In principle if the drilling formation is reactive shale, we need to change to OBM from WBM. Recently the application of Nano particles has shown positive results in petroleum industry such as in drilling fluid, cement and EOR. Especially the application of Nano silica is proven in improving cement performance [23]. This thesis therefore addresses issues such as:

- Effect of Nano silica, polymer and salt concentration in bentonite mud system
- The effect of temperature in these systems
- The rheological performance of the Nano-treated system
- The change in viscoelastic properties Nano-treated system and Nano-free reference system
- The cutting transport and hydraulics performance the Nano–treated and Nano-free reference mud systems

1.3 Objective

In order to investigate and analyze the problems defined in previous section, the scope of this thesis is to:

- Review of theories to analyze drilling fluid properties
- Review of the properties of fluid additives to be used for experiment
- To prepare bentonite drilling fluid with and without Nano-treated systems
- To characterize rheological properties the formulated drilling fluid systems
- To perform hole cleaning and hydraulics simulation studies on the newly formulated best Nano system

2 Literature review

2.1 Rock mechanics

The stability of boreholes in addition of drilling mud depends on the stresses around the open-hole section. There are mainly three types of normal stresses which are acting on the wall of wellbore. [1]

- Radial stress σ_r
- Tangential stress σ_θ
- Vertical stress σ_v
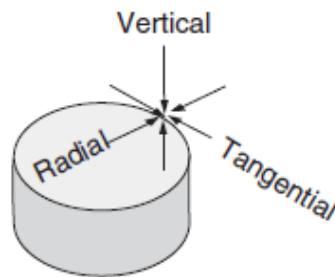
Figure 2 The main stresses acting on wellbore [1]

In case of failure, the well stability is threated and one can expect two types of borehole failure:

- Borehole fracturing
- Borehole collapse

Since wellbore instability has a direct relationship with drilling fluid, this section presents an overview of well fracture and collapse models.

2.1.1 Fracture model

Wellbore fracture when the well pressure exceeds the strength of the formation. The fracturing model depends on the boundary condition at the wellbore. There two boundary condition, namely penetrating and non-penetrating [32]

Fracturing occurs when the fracture gradient of the formation is exceeded. The definition of fracture gradient is amount of pressure before fracture occurs. The reason of fracture is tensile failure at the formation. [23]

Penetrating model: the simplest fracturing model with a clean fluid and no filtrate control, stating that the wellbore will fracture once the minimum horizontal stress σ_h is exceeded.
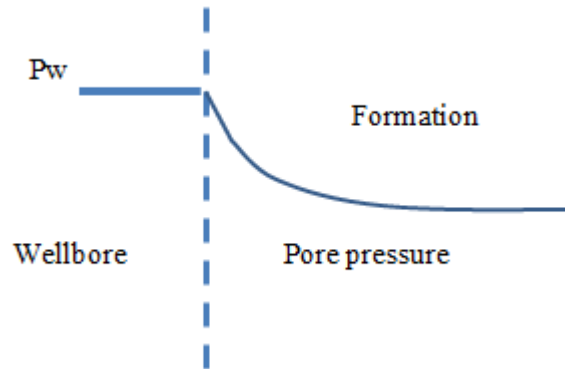
Figure 3 Penetrating fracture model [32]

Non –penetrating model: in this model assumption is based on the presence of the mud cake which will affect the fracturing initiation.
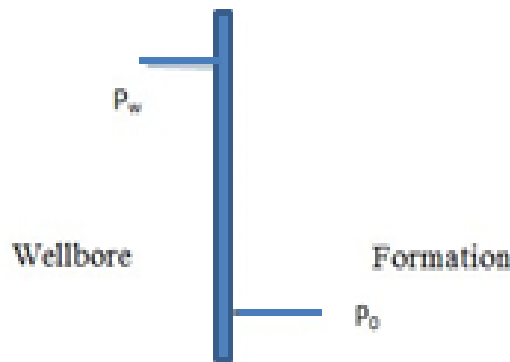
Figure 4 non-penetrating fracture model [32]

The authors have run several well fracturing experiments with various drilling fluid. They have also compared with the commonly used fracture equation given by equation (3).

$$P_{wf} = 2\sigma_h - P_o + \sigma_t \qquad (3)$$

As shown on figure 5 , the discrepancy rate between the model and the experiment is about 70%.
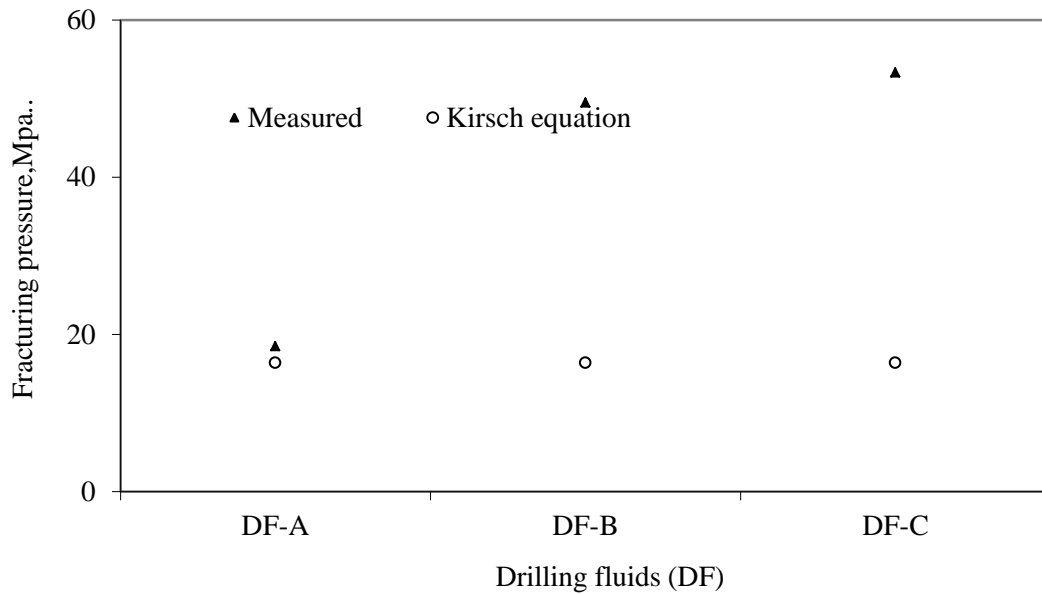
Figure 5 Comparison of measured and modelled fracturing pressures performed on commercial drilling fluids [13] [23].

The result shows that the fracturing pressure depends on the type of drilling fluid. This observation let them o derive a new model by improving the linear elastic material property of the deformation around the wellbore. The mud cake is assumed to behave plastically with a thickness of *t* covering the linear elastic rock. Another assumption is that horizontal stresses are equal ($\sigma_h = \sigma_H$). Aadnøy and Belayneh (2004) described the model by the equation of fracture initiation. [13]

$$P_{wf} = 2\sigma_h - P_o + \frac{2\sigma_h}{\sqrt{3}}\ln(1 + \frac{t}{a})$$

(4)

2.1.2 Collapse model

Borehole collapse as an instability problem is related often to the hole cleaning problems. Borehole collapse means mechanically failure of the wellbore wall due to share failure. It stands for typically 5-10 % of drilling operations cost for exploration and production wells.[11] While the fracture occurs at high wellbore pressure, wellbore collapse is a phenomena related to low wellbore pressure. When the pressure in the wellbore somehow drops below the formation pore pressure, the magnitude of the tangential stress becomes large regarding to radial stress. The rate of radial stress acting on the wall starts to decrease. Due to differential stress between these arise a shear stress which can lead to wellbore collapse. The

wellbore pressure can fall below the pore pressure in different scenarios. It can either happen after a circulation loss or can be caused by the swab effect. There are other parameters which affect the differential pressure in a wellbore collapse failure. These factors are:[10]

- The orientation of the in-situ stresses
- Formation pore pressure
- Rock compressive strength
- Wellbore orientation and diameter

Another definition of shear failure is compressive failure which leads to breakout in the borehole. The direction of the breakout is parallel with the minimum horizontal stressσ_h. It will lead to ovalization of the wellbore [11].
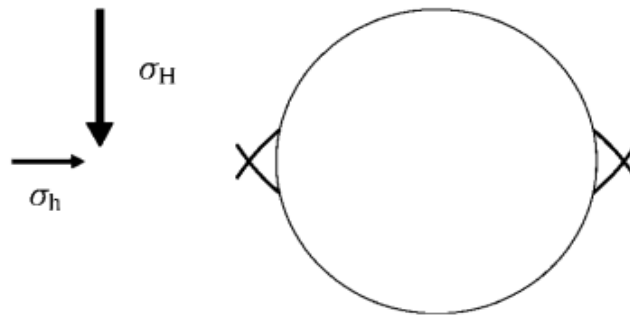
Figure 6 Direction of wellbore collapse regarding to horizontal stresses [11]

2.1.3 Circulation loss

Circulation loss is one of the reasons that increase the cost of drilling operations. In order to continue the drilling operation one has to cure the loss circulation which again increases the cost caused by circulation loss. Pumping lost circulation materials (LCM) is one way to cure or reduce the loss. Circulation loss occurs either through invasion or by fracturing the formation. For the invasion type one can mention shallow sand, coarse and unconsolidated formation and depleted sand formation. The common property of this formation is the high permeability that can lead to mud loss. Fracturing can either be induced by can occur naturally. If one exceeds a critical pressure fracturing takes places at weak zones. The point which is normally fractured is below the previous casing shoe and in this case, the mud loss

can be dramatically high. The fracture can also occur naturally at carbonate or hard shales. Once the fracture is occurs less pressure is needed to propagate the fracture. This makes the curing even more complicated. However some fractures are induced intentionally in case of hydrocarbon bearing, non-permeable shale formations. In these cases acids and fracturing in addition to Proppant are used to create fracture, stimulate and keep the fractures open. The treatment of this type of formation damage can never gain the initial properties. The fracture process occurs in several events stepwise according to B. Aadnøy 2010. These events are as follow:

- 1st. step: Filter cake formation
- 2nd step: Fracture initiation
- 3rd step: Fracture growth
- 4th step: Further fracture growth
- 5th step: Filter cake collapse

2.1 Drilling fluid and function

The definition of drilling fluid is any type of liquid, gaseous fluid, mixture of liquid and solid that is prepared to drill borehole into the earth. However there are other definitions which are used for drilling fluid. Drilling mud is the one normally used in petroleum industry. A drilling fluid consists of a continuous phase and a discontinuous phase. There are mainly three types of drilling fluids. Water based drilling fluid (WBM), oil based drilling fluid (OBM) and gas phase drilling fluid. Drilling fluids are a mixture of gas, liquid and solid to make the drilling wellbores possible. The water based mud has fresh or salt water or both as the continuous phase and a combination of polymers and clay minerals. Other additives are also added to give the suitable properties to the drilling fluid. These are droplets of oil which are emulsified, surfactants and viscosifiers based on the downhole condition.

For the oil based drilling mud a certain amount of water is also added. The water is dispersed at the continuous phase (oil) using emulsifiers. This type of mud stands for 50 % of the drilling operations. Normally deeper sections of wells are drilled by OBM. The disadvantages of OBM are its effect on personals health and the environment. One has to follow the regulation decided by petroleum safety authority Norway (PSA).

As illustrated in Figure 7 drilling fluid is pumped down to the well through drill pile. The functions of drilling mud are as following:

- Remove cutting from the wellbore and transport them to the surface
- Maintain and control the borehole pressure by providing hydrostatic pressure
- Support the borehole from collapse
- Provide and appropriate gel strength to keep the cutting in suspension
- Lubricate the drilling tool during drilling operation
- Provide buoyancy to support the weight of drilling tools ran into the wellbore
- Prevent formation fluid to enter the wellbore
- Prevent the drilling fluid loss into the formation by creating and almost impermeable filter cake

Lubrication & cooling process

In drilling processes, the bit in direct contact with the formation, the generated heat may cause the bit damage if it wasn't for the cooling properties of drilling mud. Mud with lower temperature is pumped through the drilling string and heated mud comes back through the annulus. The lubrication of moving parts is also another function of the mud which must be assured. Lubrication is especially important when there is a drill bit with moving parts like Roller cone type. The objective of lubricator additives was to reduce the bearing wear earlier however with new types of bit (PDC) the lubricator is added to mud to reduce the amount torque and drag resulting from direct contact between bit the formation wall [2]

1 Mud pumps
2 Swivel
3 Kelly
4 Drill bit
5 Drill pipe
6 Annular space
7 Cuttings
8 Shakers
9 Mud pits
10 Rotary table
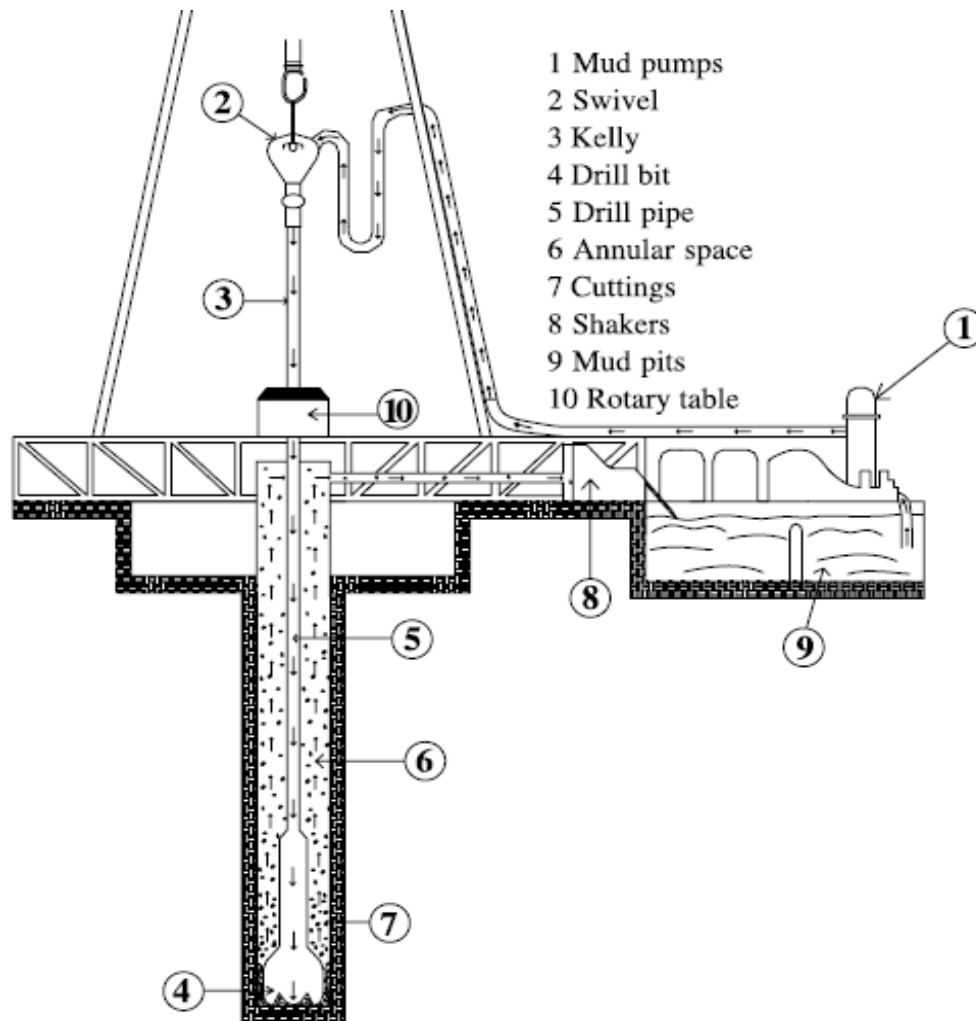
Figure 7 Rotary drilling system [34]

2.2 Types of drilling fluids

There are mainly three types of drilling fluids. The different between them is the continuous phase.

- Oil based muds(OBM)
- Synthesis based muds(SBM)
- Water based muds(WBM)

Oil based muds (OBM) have oil as continuous phase. The oil used in the OBMs is either diesel oil or low toxicity mineral oil. There is also added water emulsifier in case of presence of formation water in OBMs. However OBMs contain around 5% water and in case of increasing water per cent (higher than 5 %) the mud gets contaminated. Synthesis based mud are also provided to reduce the environmental impact of the drilling operations. They provide

performance as much as OBMs with less impact and have synthesis oil as continuous phase. The main reasons using OBMs and SBMs are to minimize borehole instability related to reactive shale, maximize the ROP and lubricity property of the drilling fluid. Disadvantages related to OBMs and SBMs is its expense, contamination of aquifers (groundwater), disposal costs and its health effect on operators and rig personnel [21].

2.3 Water based mud and composition

The focus of this thesis is mainly about the WBMs with polymers so further description about the OBMs and SBMs and their additive will not attempted in this thesis. For the water based mud the water is the continuous phase. WBMs are also known as aqueous drilling fluid which contains more than 90% water or salt water. The main advantage of WBMs is its lower price regarding to OBMs and SBMs and its environmentally acceptable nature. There are however other additives in drilling fluids which have specific function to give to the drilling fluid and the desired property. The interaction between these additives at high temperature may reduce the functionality of them [20]. The composition of water based drilling fluids is divided into three groups:

- **Continuous phase**: Normally fresh water , salt water and saturated salt water

- **Reactive phase**: Additives that are added to give the drilling fluid the particular functionality and property like bentonite, polymers and deflocculates and etc.

- **Non-reactive phase**: Additives which are not meant to react to which the continuous phase or each other like weight materials and cuttings from the boreholes.[19,21]

Water based drilling fluid can be divided into three groups based on the consistence in the water as continuous phase. It can either be fresh water, salt water from the sea or water containing inhibitor to avoid reaction with the formation which we are drilling into. The most conventional type of fresh water based drilling fluid is the bentonite mud. The objective of adding bentonite is to give the drilling viscosity to suspend the solid cuttings. Also filtrate loss control is another function of the bentonite as a reactive phase of the mud system. The main characteristic of bentonite mud is few or no additives and having a low density. There are

easily cleared from cuttings and can easily be turn into inhibitive water based drilling fluid. The main disadvantage of this mud system is that it can easily get contaminated and the viscosity is not easy to control. High viscosity is not desired since it can cause well stability problems. When the drilling fluid is too viscous, the risk of swab and surge effect increases significantly. Drilling with a viscous drilling fluid one can expect kick or circulation loss or both when tripping in and out is too fast. Not to forget the effect of viscosity on ECD when the operational window is too narrow [19].

There is however some criteria regarding to the PH value of the drilling fluid demanding a PH value above 9.5 [29]. The criterion is based on:

- the function of additives like lignosulfonat and lignitt which only gives affect in a drilling fluid with a PH > 9.5
- Degradiation of lignosulfonat decreases at PH >10
- corrosion occurrence in equipment made of steel decreases in PH >10
- The baketrias which may degrade the drilling fluid are no longer a concern having a PH >10

As mentioned earlier clay is the main material to give viscosity to the drilling fluids. Clays are added in from of bentonite where the dominating mineral is montmorillonite. The type of benitonite containing only montmorillonite is called Wyoming bentonite. It is called after bentonite produced from South-Dakota which 100 % consist of Sodium montmorillonite. Clays are classified in several groups:

- Montmorillonite (Smectite)
- Chlorites
- Kaolinites
- Attapulgites
- Illite

The swelling effect of clays depends on the cathion which is absorbed on the surface of clay. The most normal cathion in clays surface are Sodium Na^+ and Calcium Ca^{2+}. In presence of Sodium the volume of swelling clay increases significantly regarding to Clay with Calcium on its surface. This is because of calcium is bound to two crystals and there is less space for water in between crystals. [19]

2.3.1 Clay mineralogy

The main clay minerals are built up by two different fundamental structures. The different of combination of these structures give different type of clays with different properties. The fundamentally structures of clays are called:

- Octahedral layer
- Tetrahedral layer

Octahedral layer (sheet) consists of 2 planes of packed Oxygen (O) or hydroxyls molecules (OH) with aluminum (Al) surrounded in between, having an equal distance from the Oxygen or hydroxyl molecules. The number of Oxygen packed together is six, creating an eight-sided structure. The aluminum can be replaced by magnesium Mg or iron Fe. For Montmorillonite the number of Al replaced by Mg may vary.
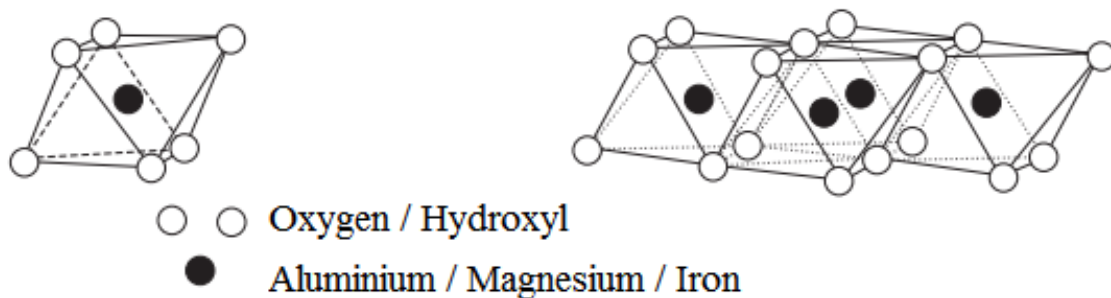
Figure 8 Crystalline structure for octahedral sheet [19]

Tetrahedral layer consist of four Oxygen / hydroxyl packed together surrounding a silicon molecule in between. Six tetrahedral layers are packed together in a hexagonal structure sharing an Oxygen/ hydroxyl molecule. The structure of the hexagonal is in such way that the base of each tetrahedral is on same plane. The structures give these clay layers ability to make thin layers like mica which can easily separate from each other.
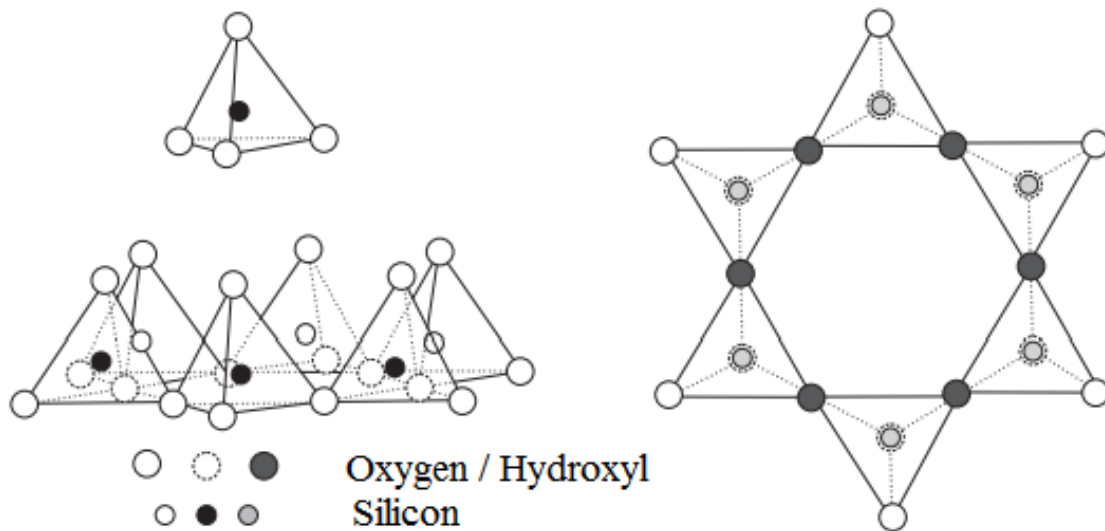
Figure 9 Crystalline structure for tetrahedral sheet [19]

The silicon tetrahedral layer with oxygen/ hydroxyl bounded together and octahedral layer as described above may combine together in a chemical process and create crystalline structure. The crystalline structure of Montmorillonite is created by two silicon tetrahedral layers with one octahedral layer in between which share oxygen as shown in Figure 10 Please notice that hydroxyl cannot be shared as it can for oxygen.
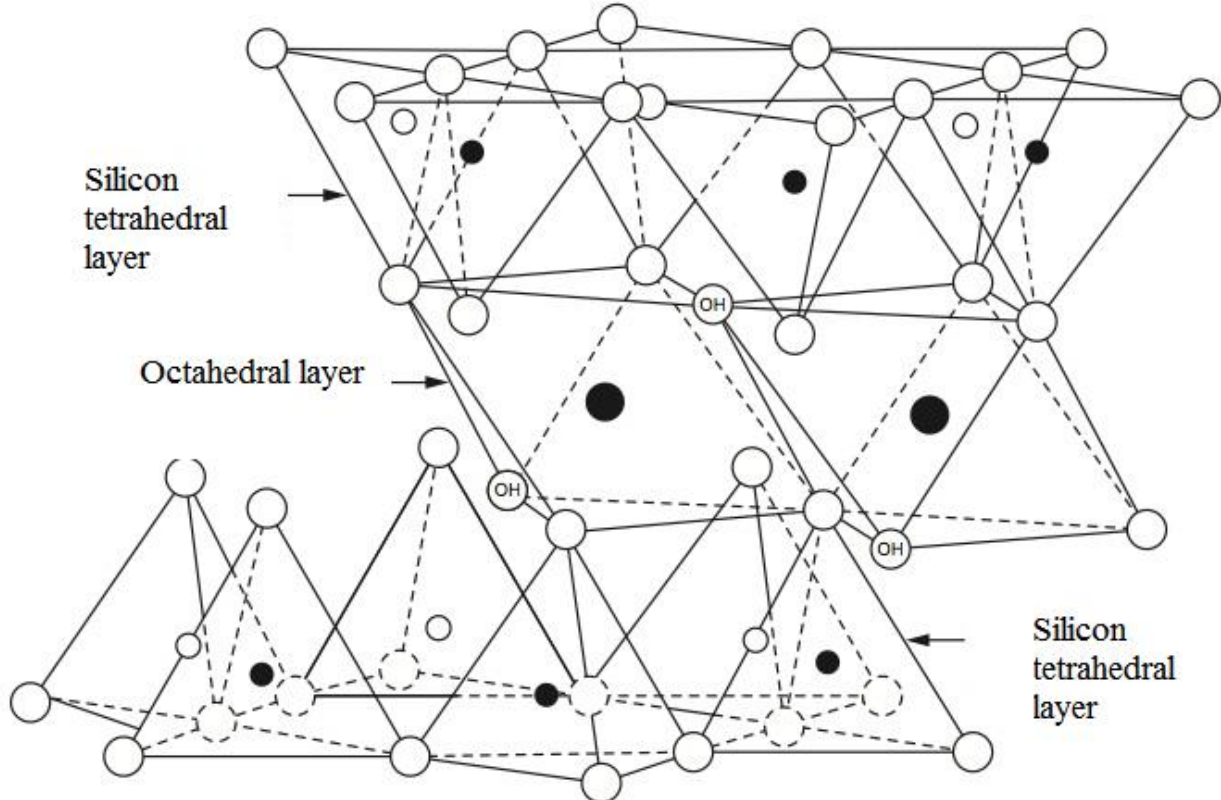
Figure 10 Crystalline structure of Montmorillonite mineral [19]

The layers which are created of silicon-aluminium-silicon plane on top of each other lets the repelling oxygen towards oxygen which is weak bounding it let the water molecules intrude easily in between. In dry condition it leads to shrinkage of the clay layers and in wet condition swelling occurs. The net charge of the crystalline structure of Montmorillonite is -3 and it opens for absorbing cations like Sodium(Na^+), Calcium (Ca^{2+}) , Potasium (K^+) and some other ions. [29]The swelling effect of clays depends on the cation which is absorbed on the surface of clay. The most normal cation in clays surface are Sodium Na^+ and Calcium Ca^{2+}. In presence of Sodium the volume of swelling clay increases significantly regarding to Clay with Calcium on its surface. This is because of calcium is bound to two crystals and there is less space for water in between crystals. [19]
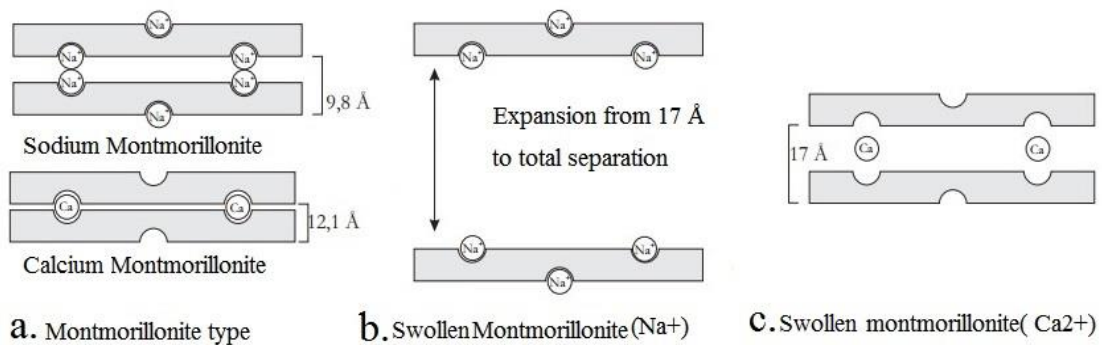
Figure 11 Hydration process for Sodium and Calcium Montmorillonite [19]

The expansion caused by water between calcium Montmorillonite expands negligible regarding to the expansion originated from sodium Montmorillonite (only 10-20 %) and the mechanism behind the water intrusion is also different. The mechanism behind clay swelling is the called the osmotic swelling where ice-like water structure separates the crystalline structures.

The clay present in drilling mud may exist in four states.

- Dispersed deflocculated
- Dispersed flocculated
- Aggregated deflocculated
- Aggregated flocculated

Flocculation is cluster formed particles separated by weak mechanical force. As the negative charges on clay particles surface neutralizes the particles act more independently and dispersion takes place. This state of clay is called deflocculation where clays are dispersed in the liquid phase of the mud system.
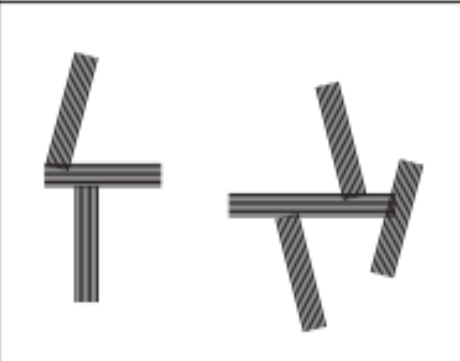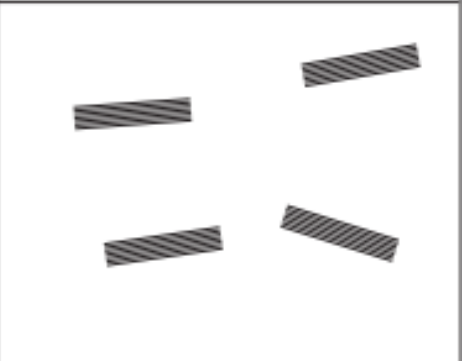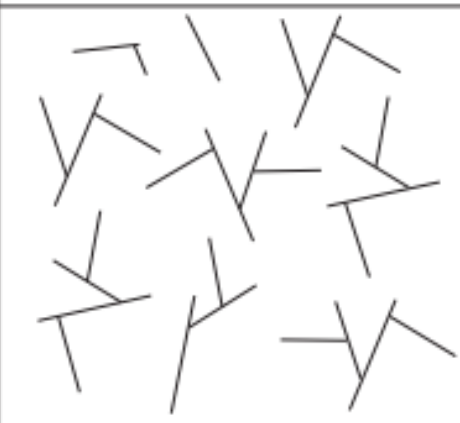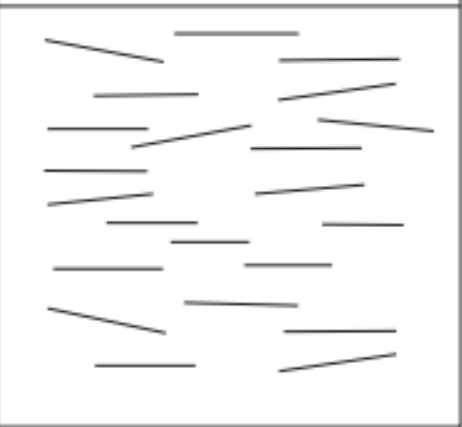
Figure 12 Arrangement of clay particles i drilling fluid [19]

When the parameters such as YS, PV, filtration loss rate and Gel strength change in drilling fluid system the arrangement of clay particles can give a logical explanation about these changes. As it is known the clay platelets are never totally deflocculated-dispersed in water. When the flocculation occurs it increases the Gel strength and yield stress. The change in PV will then determine if the system turns into the aggregated condition or not. When the aggregating takes place among the platelets in decreases the plastic viscosity of the drilling fluid and it is an irreversible process which cannot go back to dispersed condition. The performance of the mud cake is also extremely dependent of the condition of clay platelets. As a consequence of aggregated and flocculated condition the mud cake will has much higher permeability. In order to optimize the mud cake performance chemical additives called as de-

flocculants, thinner and dispersant are added to the mud system. The changes in rheological parameters are described schematically in figure 13.
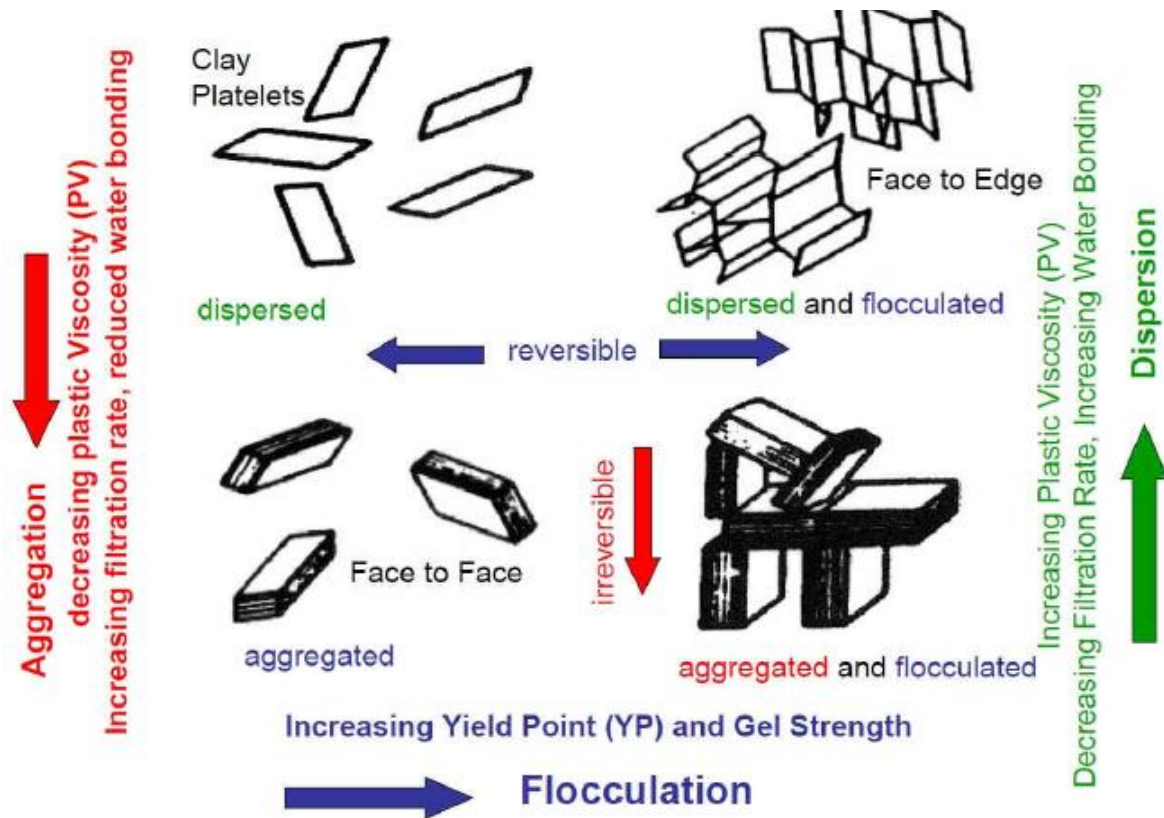
Figure 13 State diagram of colloidal clay platelets suspension in water

In this thesis work, the performance of PAC, CMC and XC and their combined effect will be investigated in the presence and absence of silica Nano-particles.

For situations where the properties of clay are not desired polymers are added to the mud system in order to give the sufficient viscosity. One of the advantages of polymers is that the change in solid content of the mud is negligible. Polymers structure is built up by basic units called monomers. They are bound together in longer chain crating polymers. They are anionic, cationic or non-ionic. The main types of polymers used in petroleum industry are:

- CMC (Carboxyl-methyl Cellulose)
- PAC (Poly-anionic Cellulose)
- Xanthan Gum

2.3.2.1 **Carboxyl-methyl Cellulose (Na) (CMC)**

Carboxyl-methyl Cellulose Sodium (CMC) is normally used as viscosifier and filer loss control in drilling fluid muds [19]. The polymer is a cellulose derivative obtained by chemical reaction of alkali cellulose with Sodium Monochloroacetate under controlled condition. The chain length of a typical CMC used in drilling fluid is normally between 500-5000 glucose units. The properties of CMC solutions are thickening, emulsifying stabilizing, membrane shaping and dispersing regarding to other solutions [22]. The salt tolerance is affected by DS (degree of substitution) of the polymer. The effectivity of the CMC based drilling fluid decreases when the concentration of salt exceeds 50000 ppm (part per million). The more the DS factor of the polymer, the more tolerance it has for salts and Ca^{2+}. For solubility in water the DS factor must be higher than 0.45. The range of DS factor of CMC's is normally 0.4-0.8 making them water soluble. The viscosity provided by CMSs depends on the length of their chain and also on DP (degree of polymerization). The longer the chain the more viscous property it provides for the mud system. Molecular Formula: $[C_6H_7O_2(OH)_2CH_2COONa]n$ Structural Formula is shown in Figure 14.

$$R \;=\; CH_2COONa \quad \text{Carboxyl Methyl Cellulose , Na salt}$$
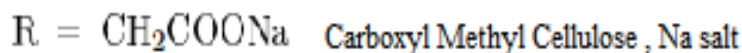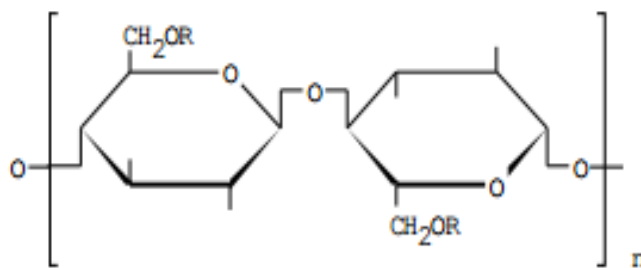
Figure 14 Chemical structure of Sodium Carboxyl methyl Cellulose

2.3.2.2 **Poly-anionic Cellulose (PAC)**

Poly-anionic Cellulose, PACs have the same structure as CMCs but the difference is in their ability of substitution. They have higher DS (0.9-1.0) regarding to CMCs and provide a good filter loss control for the drilling fluids. It also provides a good variation of viscosity and

has higher salt tolerance. There are also used as thickening agent and PAC based drilling fluids are able to handle temperature as high as 150° C. The molecular formula of PAC is $[C_6H_7O_2(OH)_2CH_2COONa]_n$ and its chemical structure is shown in figure 15. [19] [22]
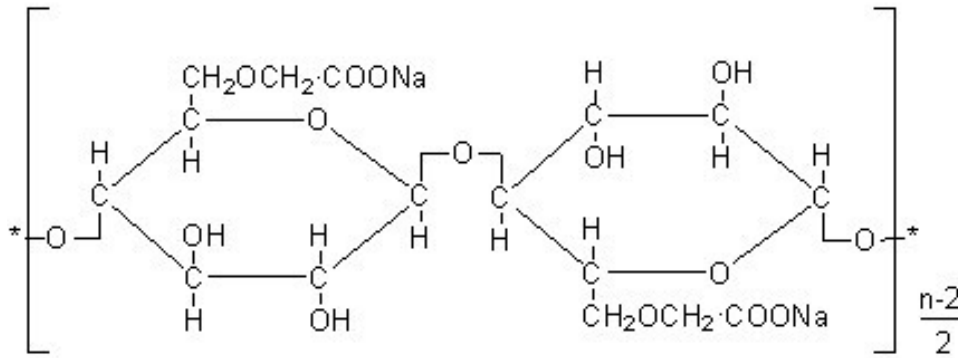
Figure 15 Chemical structure of Poly-anionic Cellulose [22]

2.3.2.3 Xanthan Gum, XC polymer

Xanthan Gum is the only biopolymer used in muds system. [19]. It's a hetero-polysaccharide having a high molecular weight. The chemical structure of Xanthan as same as cellulose molecules in addition of three repeating sugars of Glucose , mannose and monosaccharide.[31] It is produced by carbohydrate from a type of bacteria Xanthamonas Campestris (XC). The polymer is not easier soluble in water unless they are pretreated. The filter loss control is low but the viscosity per weight is higher in Xanthan than other polymers. In the mud system with high solid content Xanthan XC polymer is not advised since it can lead to extra high viscous property due to cross bounding. Degradation of Xanthan based mud system is also well known at higher temperature than 120 ^{o}C [19]. The molecular formula of Xanthan Gum is $(C_{35}H_{49}O_{29})_n$ and its chemical structure is shown in figure 16.
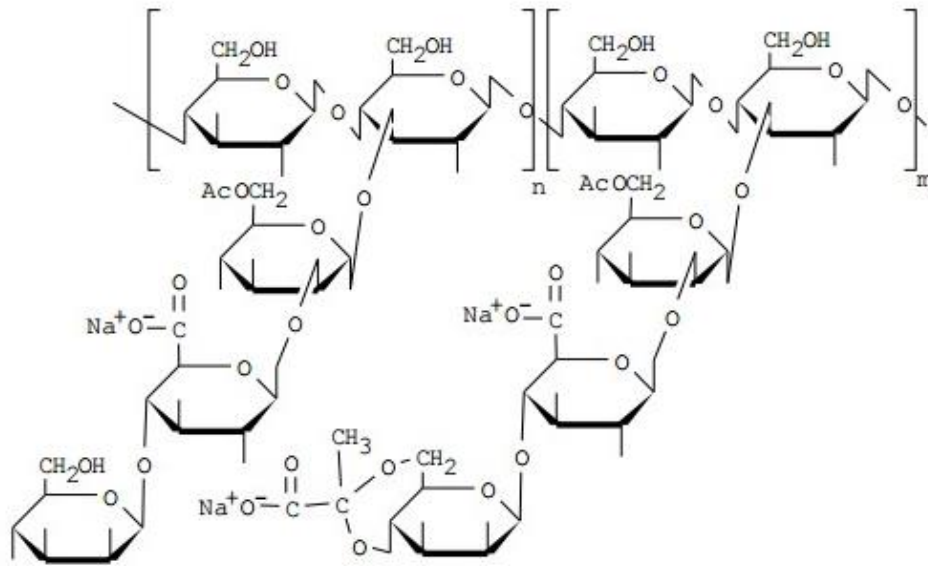
Figure 16 Chemical structure of Xanthan, XC polymer

2.3.3 Weight materials

In order to give the mud system an appropriate density weight material are used. The density of the mud system should always be above the pore pressure and below the fracture pressure of the formation. Other effect of density is related to bore-hole cleaning properties which are not discussed in this chapter. The most known weight material used in petroleum industry is Barite. Due to its low cost and high specific density of the material and its non-reactive property barite is the most popular weight material used around the world. There are other types of weight material which are used in mud systems. Hematite and Ilmenite are two of them. Due to higher specific density which may wear out and erode the equipment they are not used so often as weight materials. [19]

2.4 Characterization of Nano-treated polymer based drilling fluid

This chapter presents a general overview about the properties and behavior of drilling fluids containing Nano particles.

2.4.1 Rheological behavior

Nano technology has provided a new type of application in order to enhance the performance of the material in different industries. However the application of Nano technology in petroleum related industries is recent. It has been proved through several experiments that the Nano technology is able to provide a more positive result in drilling and production operation by increasing the performance of drilling fluid through their rheological

behavior. The focus is especially on drilling fluids which are based on polymer that Nano technology in term of silica Nano particles has given indication of improvement [16]. Nano particles are particles which their size is in a range from 1-100 nm (Nano meter). Their small size which gives the largest surface area per unit volume has given ability to perform differently than micro or macro particles. It gives them chemical, physical and thermal properties which is totally different than their parent material [14].
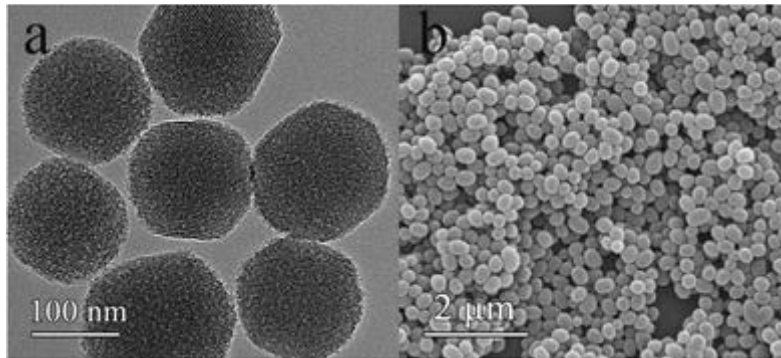
Figure 17 Scale of silica Nanoparticles

Polymer chain in drilling fluid is adsorbed on surface of Nanoparticles and it leads to particle enlargement which creates a three-dimensional network structure that changes the rheological behavior of the fluid [16].Additive NPs have given the drilling fluid a higher solid content which may reduce the ROP according to Amanullah et al. 2011, however it has shown sign of improvement by increasing the plastic viscosity of drilling fluid, reducing API filtration and yield stress of the drilling fluid [38].

2.4.2 Mud cake performance

The Nano based drilling fluid gives a mud cake which is much thinner, well dispersed and tighter mud cake. The thickness measurement of mud cake has direct relation to many drilling and production problems. It can reduce the cost of this type of operation significantly which are directly related to the mud cake performance. The circulation loss and filtrate loss can areas of improvement by applying Nano-treated mud system. Formation damage resulted from spurt loss and mud filtrate invasion is a less concern by application of Nano particles in drilling fluid. Less filtrate is resulted by an effective mud cake where Nano particles have a large areal type contact creating a well dispersed mud cake with low permeability [15,14]. For the unconsolidated formation where the well stability is an issue the performance of Nano-treated drilling fluid has a capacity to reduce the borehole problem by creating a plaster like mud cake. Embedded cutting beds at horizontal and deviated sections which are a

consequence of poor mud cake is also another area of improvement. By plaster like mud cake and no cutting beds on the low side of the wellbore, hole cleaning problem will be a less concerning problem, especially for deviated and horizontal section in extended reach wells [15]. Shale has a tendency to absorb the water from water based mud since it consists of clay. It stands for 90 % of well stability problems according to Cai & Chenevert et al. (2011) and due to environmental reason in some area using WBMs is necessary. However one has to minimize the wellbore instability if there is a shale formation in place. Additive silica Nanoparticles as solid bridging agent has shown positive effect in order to minimize wellbore instability problem [38]. Wellbore instability when drilling through shale formation can be a less concern using Nano-treated fluid. Nanoparticles are smaller than pore throats and will affect the geo-mechanical properties like collapse and fracturing strength of the formation. Less fracture in the formation is associated with less circulation loss. The mud shale interaction will also be eliminated so one can expect less differential sticking and well instability cause by reactive shale.[14] the amount of Nanoparticles have to be at least 5 % by volume of the solid content of the final drilling fluid mix. However the content of the silica Nanoparticle must at least be 10% by volume to plug the pore throats effectively and reduce the permeability which consequently reduces the filtrate loss and shale swelling For the Akota shale the size of pore throats are in a range from 10 to 30 nm. As mentioned earlier the size of Nanoparticles can be up to 100 in diameter and assumption is that only smaller particles than pore throats can reduce the permeability and shale mud interaction [38].

After applying directional drilling technology one had to deal with a larger amount of torque and drag caused by deviated section and bends. It was experimented that micro and macro particles had a limitation to solve torque and drag problems [14]. The Nano-treated drilling fluid with thinner mud cake the contact area between the drilling tools and borehole wall decreases and it consequently will decrease the frictional resistance during the dynamic condition of drilling operation. One will expect a lower value of torque and drag by using Nano-treated drilling fluid [15]. Another theory is that Nano-treated muds creates a thin lubricating layer letting the drilling tools to slide along the wellbore wall resulting less toque and drag in multilateral wells, coiled tubing drilling operations[14]. The properties of Nanoparticles which again make them interesting are the high thermal conductivity, high temperature and pressure tolerance. Thermal degradation of conventional drilling fluid (bentonite) and their viscosifiers is a well know issue in drilling operations in a temperature

above 130°C. Application of Nanoparticles in drilling fluids is essential for HPHT environments. However OBMs are typically used as drilling fluid in such environments [14].

3 Theory

This chapter presents theories used to analyze the experimental results (Chapter 4) and performance simulation studies (Chapter 5).

3.1 Flow in porous media

Whenever a drilling fluid is in contact with a porous medium filtration takes place. Weather the mud is water based or oil based the mobile phase of the drilling fluid will invade the porous formation until a low permeable mud cake is sealing the formation. Mud control actions are necessary to control the filtrate invasion. The amount of filtrate which invades the porous sand formation (thief zones) can affect the properties of the drilling fluid dramatically. It also affects the result of logging tools due to presence of filtrate. However the effect on logging depends of the rate of invasion. The effect is negligible for Measurement while drilling (MWD) tools where the invasion has not taken place yet.

The flow through porous media can easily be visualized a constant flow rate through a porous formation. In this case the fluid doesn't follow the Darcy's law where the flow rate is proportional to differential pressure across the media, flow are and the effective permeability of the porous media.

$$Q = -k \frac{A}{\mu} \frac{\Delta P}{L} \tag{5}$$

Where the Q is filtrate rate [m^3/s], k the permeability of media [m^2], A is diffusion cross section area [m^2], L is length of the media [m], μ is fluids viscosity [cP] and ΔP is differential pressure across the media [Pa]. Due to consistent of drilling mud which is a mixture of solid and liquid one cannot handle it as simple liquid. Due to solid bridging agents which form filter cake the flow rate is varying and slowing after a while when the mud cake is formed. The permeability of filter cake depends on the solid particles ability to for a sealing. However there are other factors which affect the permeability of filter cake are:

- Differential pressure
- Time
- Temperature
- Mud composition
- Mud circulation rate

The filtrate rate is normally measured during static conditions by 30 min API test. At dynamic condition the rate are not easy to predict due to factors like erosion, temperature variation. A mathematical model for invasion rate and invasion length at any given time is introduced by Breitmeier at 1988. The model is based on two assumptions that invasion rate is independent of permeability of formation and its fluids viscosity. Another assumption is a constant filtrate saturation which is a conservative assumptionAccording to Van der Zwaag and Omland the filtration loss volume can be divided to three stages:[43]

- Spurt loss: The volume of the filtrate which enters the formation which is recently drilled just before the solid particles form a filter cake. The volume depends of size and the properties of the solid used in drilling mud. Once the filter cake is formed the spurt loss V_{sp} decreases.

- Static filtration: By the time the mud cake is formed static filtration occurs in pump breaks periods. The volume of filtrate invading the formation slows as the filter cake is getting thicker. According to Van der Zwaag & Omland the volume loss during static filtrating follows the time root relationship:[43]

$$V_s = V_{sp} + m\sqrt{t} \qquad (6)$$

- Dynamic filtration: During the drilling operation and pumping periods the filtrate loss V_d into formation is normally higher due to a thinner dynamic filter cake. The thinner filter cake is a result of shear forces and erosion. Zwaag & Omland says that dynamic filtration volume has also a proportional to the time.

$$V_d = B * t \qquad (7)$$

The cumulative volume of filtrate loss is then the sum of the volumes during these stages [43].

$$V_c = V_{sp} + m\sqrt{t} + B * t \qquad (8)$$

As shown in figure 20 the transient flow regime acts as an interphase between the laminar flow and turbulent flow regime. The turbulent flow affects improves the cutting transport

process but it has also some disadvantages by filter cake erosion, tool erosion and high pressure drops. Another objective of calculating the Reynolds Number is to determine amount of pressure drop due to flow regime. For the laminar flow regime the pressure drop is a function of viscosity while for turbulent flow regime density has the key role to cause pressure drop. [1]. As mentioned earlier the pressure drops in different sections of the wellbore has direct relation to the flow regimes. The flow regime in drilling string is normally turbulent due to high velocity of stream. After a significantly pressure drop across the bit the annular section across the drilling collar gets normally a transient flow regime. However the annulus across the drilling string and riser is laminar [1]

3.2 Rheological models

Definition of rheology means studying flow and deformation of matter. The terms used in rheology are share rate and share stress. These terms are very important to characterize the drilling fluids rheology properties. Fluids are used during the drilling, completion and production operation and must be characterized through their rheological parameters using on or several of the following rheological models:

- The Newtonian model
- The Bingham plastic model
- The Herschel Buckley model
- The power law model
- Robertson and Stiff model
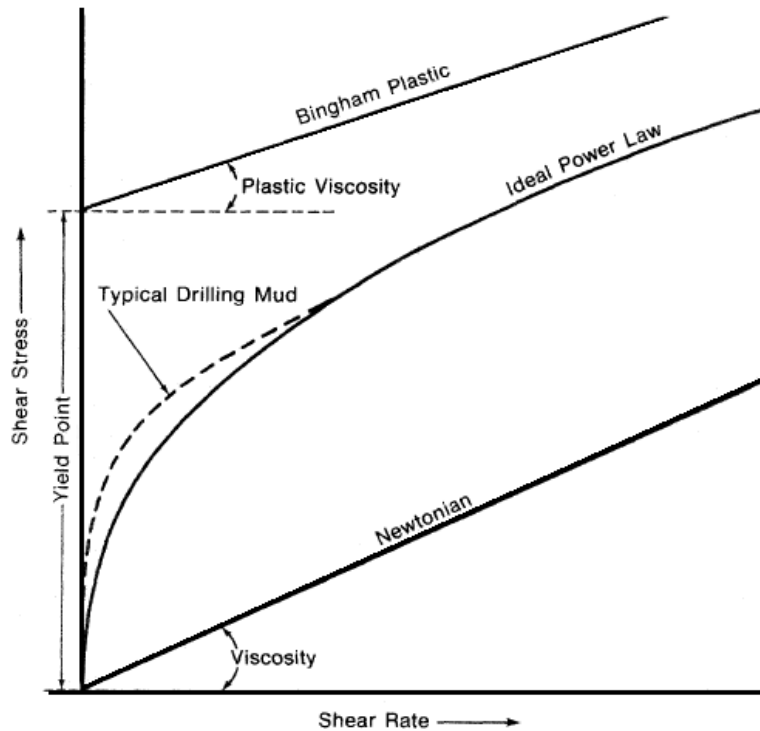
Figure 18 Ideal curves for common rheological models [2]

3.2.1 The Newtonian model

To describe viscous forced acting inside a fluid in motion the term fluid viscosity is defined. To explain the definition of fluid viscosity for to plates with area A parallel to each other with a liquid between them. The upper plate is in motion by a constant velocity V while the lower one is at rest. The distance between plates is L and after a certain distance is passed by the upper plate one has to apply a force F to keep the motion steady.[40] This force has been evaluated experimentally to have a magnitude:[19,40]

$$\frac{F}{A} = \mu \frac{V}{L} \tag{9}$$

The term $\frac{F}{A}$ is called share stress (τ) and it is defined by τ. Thus:

$$\tau = \frac{F}{A} \tag{10}$$

The unit of shear stress is Newton per square meter know as Pascal. According to the Newtonian model assuming constant is the shear rate ($\dot{\gamma}$) of the fluid is defined as:

$$\dot{\gamma} = \frac{v}{L} = \frac{dv}{dL} \tag{11}$$

The share rate is also called the velocity gradient which has a unit of [sec^{-1}]. The Newtonian model states that there is proportionality between shear rate shear stress.

$$\tau = \mu \dot{\gamma} \tag{12}$$

For the equation (12) viscosity is the constant of proportionality which in drilling industry has the centipoises [cP] as unit. Generally viscosity is defined by poises which is equal to 1 [dyn-s/cm^2]. [29,40,19]

3.2.2 The Bingham plastic model

The Bingham plastic is one the most common rheological models which is used in drilling industry. The model includes many types of fluids. It defines a level of shear which must be overcome to initiate the flow. This level of shear stress is called the yield stress [τ_0]. The slope of the line is plastic viscosity μ_p which is shear rate independent. The equation for this model is as follow:

$$\tau = \mu_p \dot{\gamma} + \tau_o \tag{13}$$

However most of the oil fields show the share rate dependent behavior which makes the model deficient for the mud systems. Polymer based drilling fluids also show share rate dependent. [29,40]

3.2.3 The power law model

This model fits the behavior of the oil field fluids very good. The viscosity term is no longer present in the power law equation. A new term, consistency index K is used to describe the behavior of fluids. The n is termed as flow behavior index.

$$\tau = K \dot{\gamma}^n \tag{14}$$

One can determine the value of n and K (lbf s^n/100ft^2) using equations (15) and (16)and data from laboratory experimental data.[19,29,40]

$$n = 3{,}32 \log(\frac{\theta_{600}}{\theta_{300}}) \tag{15}$$

$$K = \frac{R_{300}}{511^n} = \frac{R_{600}}{1022^n} \tag{16}$$

3.2.4 The Herschel Buckley model

Another modified version of the Bingham model is called Herschel Buckley model which describes the behavior of most of fluids in case of share rate dependent. In this case the plastic viscosity is replaces by the term consistency index K to visualize the share rate dependency. After reaching yield strees the behavior is non-linear. If the fluid is doesn't have any yield stress then the model is reduced to the power law model [44].

$$\tau = K\dot{\gamma}^n + \tau_o \tag{17}$$

The *n* and *k* values are determined graphically and τ_0 can be determined by:

$$\tau_0 = \frac{\tau^{*2} - \tau_{min}\tau_{max}}{2\tau^* - \tau_{min} - \tau_{max}} \tag{18}$$

τ^* can be determined by using interpolation method based on the shear strain value given as:

$$\gamma^* = \sqrt{\gamma_{min}\gamma_{max}} \tag{19}$$

3.2.5 Robertson & Stiff model

Robertson and Stiff suggested a three constant which model to describe the rheological behavior of the drilling fluid. It shows relationship between shear stress and shear rate for the drilling fluids and cement slurries [42].

$$\tau = A(\gamma + C)^B \tag{20}$$

Where *A, B, and C* are model parameters. The value of A and B are considered same as K and n for the Power law model. The value of C in other hand is and correction C is called correction factor for the shear rate with $(\gamma + C)$ defined as effective share rate. The parameters are calculated by equation (21) and (22).

$$log\tau = logA + Blog(\gamma + C) \tag{21}$$

B is determined by the slope of the curve and A is the intercept by setting $(\gamma + C) = 1$ and at the end the parameter C can be determined by interpolation.

$$C = \frac{(\gamma_{min}\gamma_{max} - \gamma^{*2})}{2\gamma^* - \gamma_{min}\gamma_{max}} \tag{22}$$

MSc Thesis, 2015

γ^* is usually calculated by interpolation and based on the equation (23) of τ^*[42].

$$\tau^* = \sqrt{\tau_{min}\tau_{max}}$$

(23)

3.3 Fluid flow regimes

To have better understanding of pressure drops and cutting transport one has to flow regime related to that section of the well. There are two types of flow regimes. The first one is called Laminar flow regime. For the laminar flow the fluid is moving as parallel layers to each other and the pipe wall. The center of the stream has the highest flow velocity. The flow will normally be laminar for high viscous fluid with low flow velocity. The second flow regime with a higher flow velocity is called turbulent. For the transient flow the flow is no longer parallel due to high stream velocity. As the flow velocity increases the stream becomes more chaotic.
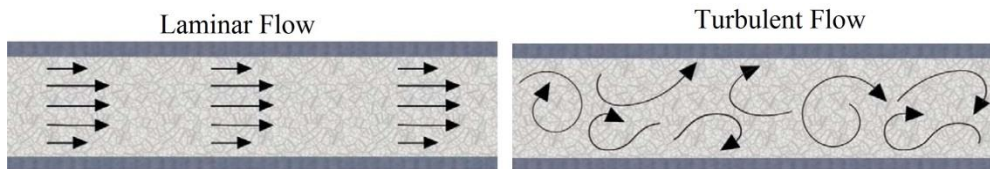
Figure 19 Laminar and Turbulent flow regimes

In order to differentiate the flow regimes the Reynolds Number is presented. It is a dimensionless number representing the ratio of inertial forces to viscous forces. The Reynolds Number for a stream in a tubular pipe can be calculated using the equation (24).

$$Re = \frac{\rho \bar{v} D}{\mu}$$

(24)

Where the Re is Reynolds Number, ρ is the density of the fluid $[\frac{kg}{m^3}]$ $\bar{v}$ is the average velocity of the stream $[\frac{m}{s}]$, D is the hydraulic diameter of the pipe $[m]$ and μ is the viscosity of the fluid $[Pa.s]$. It has been interpreted that when the inertial forces are dominant in the fluid in motion then the flow regimes is turbulent. For the fluid where the viscous forces are dominant over inertial forces one can expect a laminar flow regime. However there is another phase between these two flow regimes. The transitional phase where the flow are no longer parallel .The transitional flow can be characterized for having a Reynolds number between 2000 and 4000. The range of Reynolds number for different flow regimes is visualized figure 20.
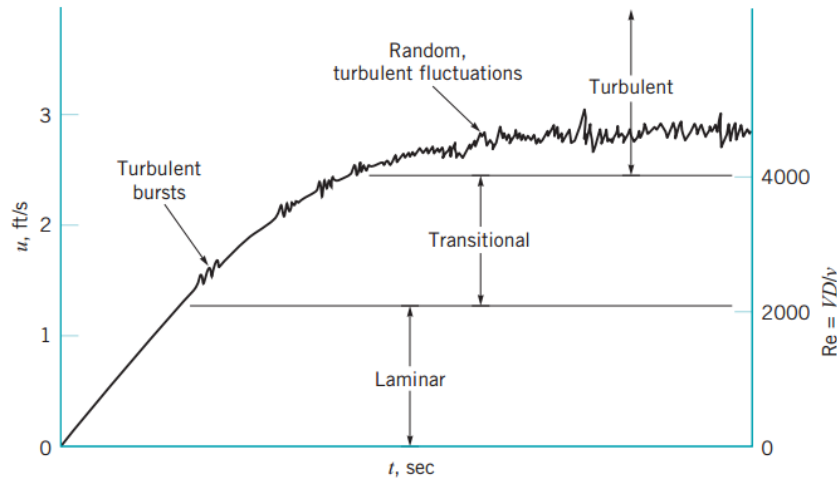
Figure 20 Reynolds number range for different flow regimes

3.4 Hydraulic model

The hydraulic system parameters are determined to for hydraulic optimizations. The main objected is to provide an appropriate nozzle jet impact. However there are other factors which are involved for selection of these parameters. As mentioned earlier critical flow velocity for cutting transport and borehole cleaning are those factors. Due to high variation in hole and tools and pipes dimension the flow regimes are different which also must be taken into consideration.

As mentioned earlier there are both annular frictional pressure and static pressure are factors affecting the downhole pressure. By calculating the ECD one can control the downhole pressure more accurately. ECD is a function of frictional pressure and static pressure. Static pressure is controlled by changing the density of the drilling mud. The frictional pressure is however more complex. The frictional pressure in annulus is affected by following factors:

- Rheological behavior of the drilling fluid
- The flow regime of drilling fluid
- The drilling fluids density
- Drilling string eccentricity
- The flow rate of drilling fluid

In order to overcome the frictional pressure drops in different section of the wellbore, the pump pressure has to deal with following pressure drops:

- Pressure drops thorough the surface equipment like swivel and pipes ΔP_s

- Pressure drops across the drilling stringΔP_{ds} and drilling collar ΔP_{dc}

- Pressure drops across the nozzles of drilling bitΔP_b

- Annular pressure drops outside the drilling collarΔP_{ac}

- Annular pressure drops outside the drilling string and riser ΔP_{ads}
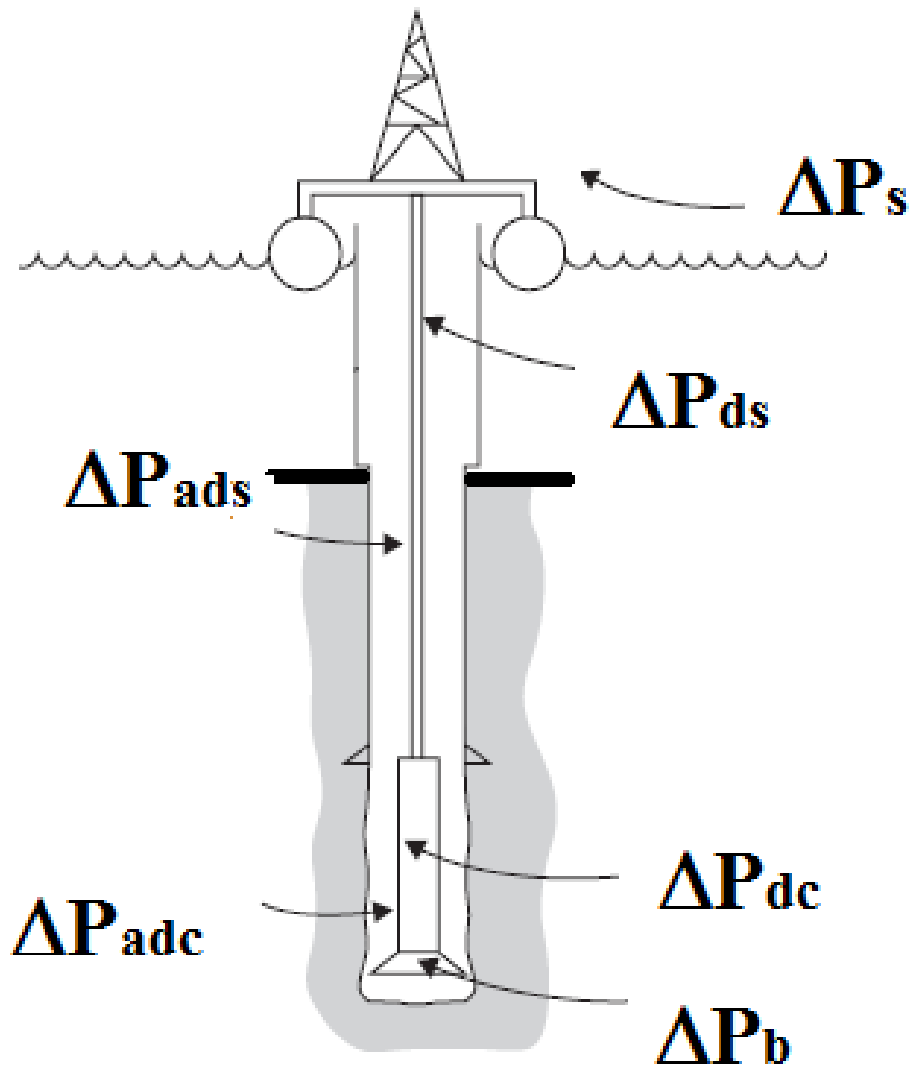
Figure 21 Hydraulic system and pressure drops [modified]

The total pressure drop for the hydraulic system is the sum of the mentioned pressure drops.

$$\Delta P_{Total} = \Delta P_s + \Delta P_{dc} + \Delta P_{ds} + \Delta P_b + \Delta P_{ac} + \Delta P_{ads} \qquad (25)$$

Other pressure drops are not directly related to drilling operation. They are more related to borehole cleaning and pump pressure. Aadnøy (2010) divided these pressures drops into two groups. The pressure drop across the nozzle and other pressure drops known as parasitic pressure drops. The values of parasitic pressure are directly related to the flow regimes. The pressure drop across bit nozzle is not negligible and has an impact on drilling operation. According to Kendal and Goins, for having maximum jet impact force, the bit pressure drop must be close to 49 % of the pump pressure. Another optimization is to provide the maximum bit hydraulic horsepower. In this case the pressure drop across the bit must be kept as high as 66 % of the pump pressure. The fraction must be kept until the target depth is reached or the flow rate is down to minimum annular velocity for cutting transport. [3] The pressure drop across the bit nozzle (ΔP_b) assuming field units, is usually calculated by equation (26):

$$\Delta P_b = \frac{\rho q^2}{12034.7 A^2 {C_d}^2} \tag{26}$$

Where q is the volumetric flow rate across the bit nozzles (GPM), ρ is the density of the drilling fluid (ppg), A is the sum area of the bit nozzles (in^2) and C_d is the bit discharge coefficient which is normally set equal to 0.95. The parasitic pressure drop in annulus and drill pipe is around 10-20 % of the total pressure drop of the system. For calculating annular pressure drop one has to use a rheological model. The Bingham plastic and power law model are best fitted for the mud behavior for pressure drop prediction. The obtained annular pressure drop obtained is normally less accurate due to simplifying assumption. Another reason is the complex behavior of mud as a Non-Newtonian fluid. Another factor which affects the annular pressure drop is the annular wellbore geometry.[5] It is well known that the pressure drop in concentric annular flow is significantly higher than eccentric annular flow. According to Haciislamoglu and Cartalos the pressure drop in fully eccentric pipe can be as low as 40% less than a fully concentric drilling pipe. Eccentricity is not a parameter which can be easily controlled. It is a function of depth and bore inclination.[6] Variation in cross sectional area in the inclined section due to cutting beds which occupy part the area, prediction of pressure drop becomes more challenging. A flow profile for a non-Newtonian in an eccentric drill pipe is shown in figure 22.
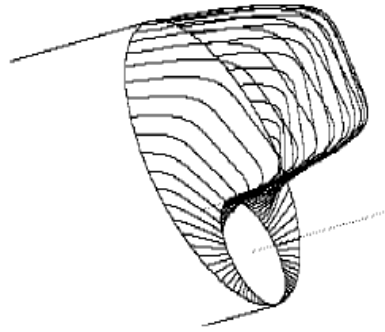
.
Figure 22 Velocity profile of non-Newtonian fluid in an eccentric drill pipe

The unified rheology model is given as [41]:

$$\tau = K\dot{\gamma}^n + \tau_y \tag{27}$$

Where, the shear yield (τ_y), *k* and *n* values are calculated directly from Fann rheology data. Table 1 shows unified hydraulic model, which is used to analyze the best fluid system to be formulated in experimental part of this thesis.

Table 1 Unified hydraulic model [41]

Pipe Flow	Annular Flow
$\mu_p = R_{600} - R_{300}$ $\tau_y = R_{300} - \mu_p$ $\tau_0 = 1.066(2R_3 - R_6)$ $\mu_p = cp$	
$n_{p} = 3.32 \log\left(\dfrac{2\mu_p + \tau_y}{\mu_p + \tau_y}\right)$ $k_p = 1.066\left(\dfrac{\mu_p + \tau_y}{511}\right)$	$n_{p} = 3.32 \log\left(\dfrac{2\mu_p + \tau_{y\,-}\tau_y}{\mu_p + \tau_y - \tau_y}\right)$ $k_p = 1.066\left(\dfrac{\mu_p + \tau_y - \tau_o}{511}\right)$
$G = \left(\dfrac{(3-A)N+1}{(4-A)N}\right)\left(1+\dfrac{A}{2}\right)$ A= 1 FOR ANNULL α= 1 for pipe	
$v_p = \dfrac{24.51\,q}{D_P^2}$	$v_a = \dfrac{24.51\,q}{D_2^2 - D_1^2}$ v=ft/min

$$\gamma_w = \frac{1.6*G*v}{D_{R_1}}$$
$$\gamma_w = sec^{-1}$$

$$\tau_w = [\left(\frac{4-\alpha}{3-\alpha}\right)] \tau_0 + k \gamma_w{}^n$$

$$N_{Re} = \frac{\rho\, v_p}{19.36\tau_w}$$	$$N_{Re} = \frac{\rho\, v_e}{19.36\tau_w}$$
Laminar: $$f_{laminar} = \frac{16}{N_{Re}}$$	Laminar: $$f_{laminar} = \frac{24}{N_{Re}}$$
TRANSIENT: $$F_{TRANSIENT} = \frac{16\, N_{RE}}{(3470 - 1370 N_P)}$$ Turbulent: $a = \frac{\log n + 3.93}{50}$ } $f_{turbulent} = \frac{a}{N}$ $B = \frac{1.75 - LOGN}{7}$ }	TRANSIENT: $$F_{TRANSIENT} = \frac{16\, N_{RE}}{(3470 - 1370 N_P)}$$ Turbulent: $a = \frac{\log n + 3.93}{50}$ } $f_{turbulent} = \frac{a}{N}$ $b = \frac{1.75 - logn}{7}$ }

$$f_{partial} = (f_{transient}{}^{-8} + f_{turbulent}{}^{-8})^{-1/8}$$

$f_p = (f_{partial}{}^{12} + f_{laminar}{}^{12})^{1/12}$	$f_a = (f_{partial}{}^{12} + f_{laminar}{}^{12})^{1/12}$

3.5 Viscoelasticity

Solid particle follow the hooks law and there is proportionality between the shear rate and share stress. The slope of the stress strain is called rigidity modulus G, indicating that the material is rigid.[40]

$$\tau = G\gamma \tag{28}$$

Viscosity is the same constant that relates shear and shear rate for Newtonian fluids. They follow Newton's law. However some materials have the characteristics of both liquid and solids meaning that are both elastic and viscous. Polymer such as Xanthan is an example of such viscoelastic materials. Polymers that are used in drilling mud give the mud the viscoelastic properties. The definition of viscoelasticity can easily be misunderstood by plasticity. Plastic materials like metals are ductile. Ductility is as same as plasticity.

Viscoelasticity is the property of materials and fluids which have the ability to regain the original shape after deformation after a certain period of time. The time it takes is different based on the viscos part of the material. The process of regaining the original shapes starts by the time the load or the force which caused the deformation is removed. Drilling fluids exhibit these properties clearly when they are subjected to the pressure and temperature loading in the wellbore [40].

The viscoelastic property of drilling fluids is very important in order to provide sufficient gel strength during non-rotating periods of operation to keep the cuttings in suspension and to avoid problems like differential sticking, borehole fracturing or borehole collapse. Evidences which indicate the importance of viscoelasticity in drilling mud are effects observed in form of pressure build ups, pressure delays and pressure transient caused by of the drilling fluid flowing through the wellbore. Solids present at drilling mud can result severe problems if the gel strength of the fluid is not sufficient. One has to avoid the barite sag effect by providing and appropriate flow condition.

Oscillatory methods are used to measure viscoelastic properties. This is because it is not possible to measure these parameters for a uniform and steady flow. The rheometer subjects the fluid to a sinusoidal deformation .Then the resulting stress is measured by a transducer. To find out if the fluid is elastic or viscous the phase of stress and stress are then compared. For the elastic fluid the both stress and strain are in phase. For the perfectly viscous fluid the phase is totally opposite [40]
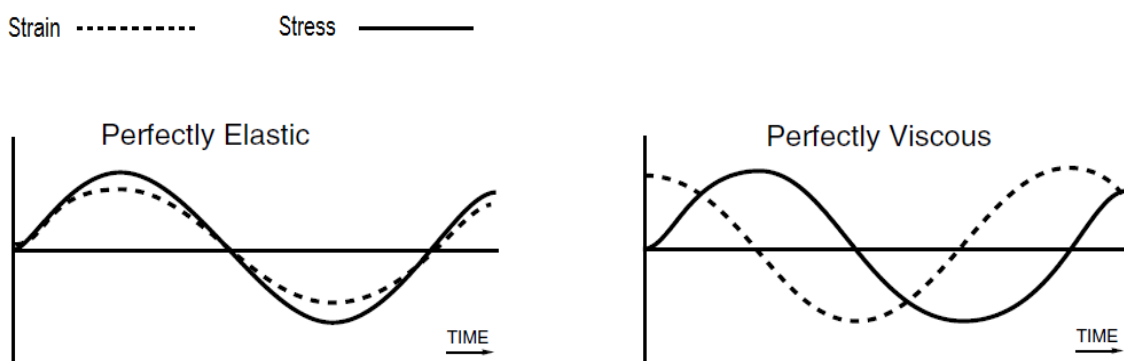
Figure 23 Oscillatory measurement of viscoelasticity behavior[40]

The test which is used to determine the viscoelastic properties is called dynamic test. The oscillatory strain resulted by the sinusoidal deformation is:

$$\gamma = \gamma_0 \sin(\omega t) \qquad (29)$$

Where the γ_0 is the maximum amplitude of strain resulted by deformation, ω is the oscillation frequency [rad/sec] and t is time in sec. The strain results shear stress acting on surface.

$$\tau = \tau_0 \sin(\omega t + \delta) \qquad (30)$$

Where τ_o the maximum amplitude of shear stresses, and δ is phase angle. Using trigonometric and the equation of resulted shear stress one can obtain:

$$\tau = \tau_0 \sin(\omega t)\cos(\delta) + \tau_0 \sin(\delta) \cos(\omega t)] \qquad (31)$$

This again can be written as:

$$\tau = \gamma_0 [\left(\frac{\tau_0}{\gamma_0} \cos\delta \right) \sin(\omega t) + \left(\frac{\tau_0}{\gamma_0} \sin\delta \right) \cos(\omega t)] \qquad (32)$$

In addition to rigidity modulus G, there are some important parameters which are the key to measure the viscoelasticity of drilling fluids. These terms are elastic modulus $G^{\grave{}}$ and viscous modulus $G^{\grave{}\grave{}}$. The elastic modulus $G^{\grave{}}$ is also the storage modulus meaning the storage of elastic energy. The viscous energy is lost and therefore $G^{\grave{}\grave{}}$ is called the loss modulus. One can visualize the elastic modulus vs. viscous modulus as line 90 degrees apart with line in between. The magnitude and direction of the line are called complex modulus G^{*} and phase angle δ respectively. The more viscous the fluid the higher is the slope of the line. The phase angle is 0 for a perfectly elastic fluid and 90 for a perfectly viscous fluid.
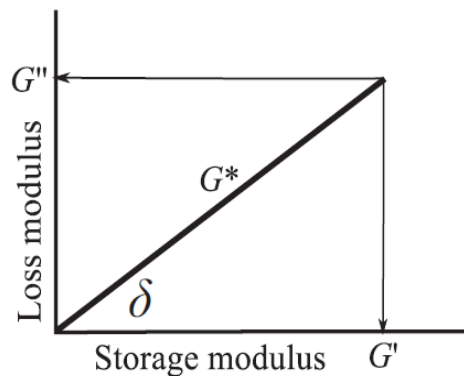
Figure 24 Storage modulus vs. loss modulus[40]

By using the above equation the definition of elastic modulus G' and viscous modulus G'' are as follow:

$$G' = \frac{\tau_0}{\gamma_0} cos\delta \tag{33}$$

$$G'' = \frac{\tau_0}{\gamma_0} sin\delta \tag{34}$$

The absolute value of complex modulus G^* is:

$$G^* = \sqrt{G'^2 + G''^2} \tag{35}$$

The ratio of viscous modulus to elastic modulus corresponds to the tangent of the phase angle:

$$tan\delta = G''/G' \tag{36}$$

3.5.1 Measurement method

3.5.1.1 Amplitude sweep

The test method is to keep the frequency constant and increasing the amplitude. The test is done in oscillation in order to measure linear viscoelastic (LVE) range. For the fluid within LVE range the behavior will be according to the Hooke's law and elastic[18]. The fluid sample is in so called undisturbed condition. The test measures the elastic modulus G' and viscous modulus G'' respectively. If magnitude of the elastic modulus is greater than the viscous modulus the behavior of the fluid is viscoelastic solid or gel ($G' > G''$). An example can be the drilling fluid in rest having gel strength during static condition. Even if the gel structure is weak stability is expected from them. If the magnitude the viscous modulus is higher than the elastic modulus the sample has viscoelastic fluid properties. It defines that the sample is flowing even within the LVE range. The motion of G' and G'' at maximum amplitude is plotted against the deformation in figure 25.
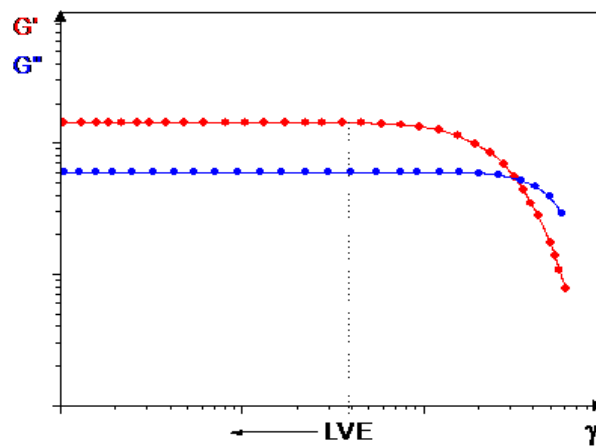
Figure 25 Elastic and Viscous modulus plot against deformation in amplitude sweep test [17]

By the time the modulus start to decrease the fluid is in disturbed condition. The elastic modulus then crosses the viscous modulus in a point called the flow pointτ_f. The plateau value of G' describes the rigidity of the sample and the plateau value G'' is measure of viscosity for an un-sheared sample. The more the difference between $G'$and G'' the more visible is the characteristic of the pure solid or liquid in the sample. Thus the test method opens for determining the end of the LVE range, yield pointτ_y and flow point. [17]

3.5.1.2 Frequency sweep

Frequency sweep are oscillatory tests performed by decreasing the frequencies from a maximum value downward while the amplitude is held constant [17]. The tests are also referred as dynamic oscillation tests. Since the frequency is inverse value of the time the test is used to measure time dependence deformation. Short term behavior is characterized by rapid motion at high frequencies and long term behavior is characterized by slow motion at low frequencies. [18] However the frequency tests are less informative for dispersions like paint and cosmetics. [17]The test is used to measure viscoelastic property and evaluate the long term dispersion storage stability of samples for example the drilling fluid which is at rest (static condition). The behavior at LVE range is important and normally an Amplitude tests is carried out before the frequency sweep test. Figure 26 show the curve for $G'$and G'' against angular frequency. The point where the $G'$and G'' cross each other is where the liquid like behavior becomes dominant.
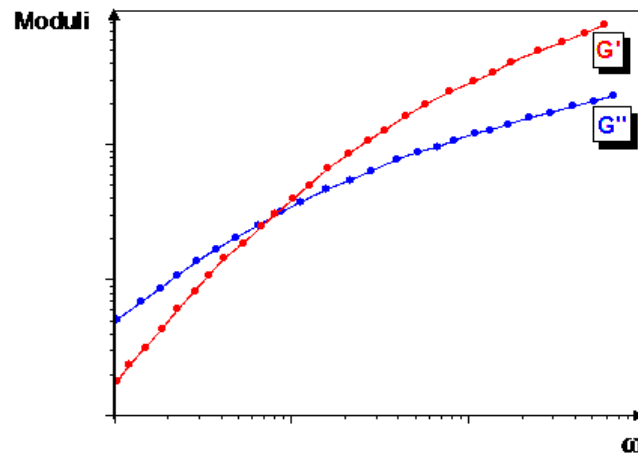
Figure 26 Frequency sweep test, Elastic and Viscous modulus plot against frequency [17]

The test is also very important for the polymers. Other characteristics like melting point, glassing transition and enlargement density can also be determined by performing the test at different temperatures. [17]

3.6 Cutting Transport & Suspension

As mentioned earlier removing the formation cuttings is the one the primary function of the drilling mud. If the cutting removal somehow fails the drill string may get stuck. It also may fracture formation if the size of cutting is large enough to overcome the gel strength and settles, borehole fraction becomes a potential risk and circulation loss occurs. Normally larger hole size has larger cutting which are difficult to remove. Based on pump capacity and the flow rate provided by them, by using simulator it is possible to obtain the minimum flow rate necessary to ensure cutting transport. Cuttings tend to settle due to gravity. There are some parameters which are critically for cutting removal process:

- Flow velocity
- Rate of penetration (ROP)
- The flow regime
- Borehole inclination
- Drilling mud rheology
- Hole angle
- Hole size
- Mud weight

The well inclination is very critical. The inclined section of the well often experiences cutting transport problems. However the continuous rotation of drilling tools and mud circulation makes cutting transport process easier (dynamic condition). The parameters mentioned above are those which are possible to control. Other factors which cannot be controlled are cutting density and cutting size. [1]

The borehole inclination is more critical for angles of 40 to 60 according to Torbjørnsen et al.(1994). The cutting slide along the borehole and accumulate affected by three types of forces. These forces are hydrodynamic forces, static forces and colloidal forces. Field experience indicates that however small sand particles are most difficult to remove. Small particles can easily form bed at high angle and horizontal section by the time mud circulation stops. Once the bed is formed the re-suspension and bed erosion is difficult to achieve for small sand particles as the bed is more compact than large particles. This may even make the casing running difficult or almost impossible in case of long extended reach with length of 20000 ft. due to excessive torque and drag [19, 37].

Drill cutting suspension is also a critical property of drilling fluid. In order to doing operation which demands static condition may take long time like tripping out, mud has to suspend the particles and keep a constant density constant. This property of drilling fluid must make sure that mud degradation or cutting settlement does not occur. This property is called gel strength. The polymers which are added to drilling mud have the same property to form a gel after a certain period of time. Once it occurs, the strength increases by the time. This phenomen is called Thixotropy The gel-like structure and the time it takes to act like a gel in drilling mud must be as short as possible. However after rotation and pumping starts again the fluid must regain the flow property. The force needed to initiate the flow is something else than the yield stress which is time independent.

3.7 Cuttings transport models

There are several studies considering the cutting transport performance. The cuttings are assumed to have irregularly shaped. They can be divided into two groups.

- Empirical
- Mechanistic

Chen has presented two empirical correlations regarding to settling velocity in rotary drilling operation. One for cuttings settling in slip regimes and the other is for turbulent-slip

regime. According to Chien et al. (1994) the settling velocity depends on the diameter of particle but it is not proportional. He divided the settling velocity into three groups. Laminar slip settling velocity for particles where the diameter is less than 0.018 cm, where the settling velocity increases proportionally with d^2. The main factor affecting this settling velocity is fluid density and rheology properties. Turbulent slip settling velocity for particles with a diameter larger than 0.13 cm, where the setting velocity increases by square root of the diameter.[8] Factors which affect this velocity are surface characteristic of the particle in addition to fluid density. The particle with diameter between these values had the transient slip regime.

Definition of slip velocity is important in order to understand the cutting transport process. Transporting velocity V_T cutting is assumed to be slip velocity subtracted from the fluid velocity in the annulus [35].

$$v_T = v_f - v_s \qquad (37)$$

Cutting are subjected to several forces are acting on a particles. Gravitation forces F_g, drag forces F_d and Van der Waals mentioned earlier as colloidal forces between particles. However there are also some other forces like buoyancy force, F_b and lift force F_l. For a vertical wellbore the gravitational and drag forces on a spherical solid particle are illustrated.
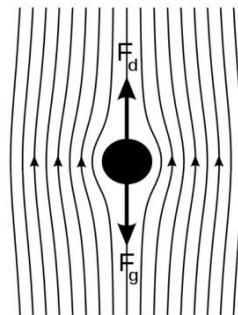
Figure 27 Drag and gravitational force acting on a solid particle[33]

To understand how suspension of cutting occurs one has to define the amount of energy to overcome the acting drag force. It is defined by drag coefficient. This coefficient is basically the fraction of the energy to overcome the drag force. Particles Reynolds number have also a key role to determine the settling velocity or particles. It is a function of particles diameter, settling velocity and particles and fluids density.

$$C_D = 1308.7d(\rho_p - \rho_f)/v_s^2\rho_f \qquad (38)$$

Chien et al 1994, then defines the equation for settling velocity for irregular particles to be:

$$v_s = 120 \left(\frac{\mu_e}{d\rho_f}\right) \left[\sqrt{1 + 0.0727d\,(\rho_p/\rho_f\ - 1)(d\frac{\rho_f}{\mu_e})^2} - 1\right] \qquad (39)$$

As mentioned earlier the particles Reynolds number defines which setting velocity equation must be used. For settling velocity for particle with $N_{Re} < 1$ a more simple equation is presented by Stoke. According to Stokes law the settling velocity and drag coefficient are defined by [35].

$$v_s = \frac{gd^2\left(\rho_p - \rho_f\right)}{18\mu_e} \qquad (40)$$

$$C_D \approx 24/N_{Re} \qquad (41)$$

In order to prevent the settlement process denser fluid and dynamic condition is advised to disrupt the process. For the dynamic condition one has to make sure a turbulent flow regime with high flow velocity. This condition can in some case help to erode the beds which are already deposited. The difficulty of the bed removal depends on the size and characteristics of the particle. The drilling tool in this area is normally lying on low side and when bed formation starts a bed ring around the tool can lead to settlement and bed rings around the drill pipe.
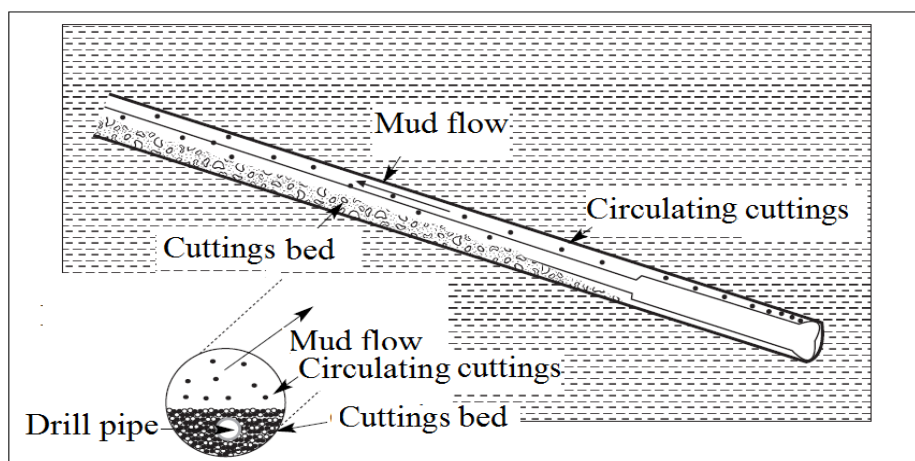
Figure 28 Cutting beds in inclined section of wellbore [36]

The bed ring can cause stuck pipe situation when bottom-hole assembly (BHA) with a larger diameter is pulled out of the hole. The rotation is also more difficult than a concentric

drilling pipe. These beds are difficult to erode once they are formed. Mitigating drilling practices must be emphasized to prevent these incidents [36].

3.8 Torque and drag

Reducing torque and drag is an essential part of the planning and design phase of drilling operation. The limited capacity of top-drive due to excessive torque, inability to slide tubular due to excessive drag forces especially in oriented wells. In order to reduce torque and drag one has to optimize to reduce the negative effect of each component which contributes in inefficiency of the drilling system. The optimization has to happen in the planning stage, well profile, casing and tubular design and the type of drilling fluid and its lubricator. As mentioned in earlier OBMs have a better lubricating effect than WBMs [36].Due to economical reason one has to use a certain type of drilling mud in each well section. After optimization during the planning if the torque and drag problems are still a concern one has to consider more specific modifications. The torque basically is defined by the definition of friction factor which determines the magnitude of the torque. For the water based system the lubricant is the key factor for torque and drag reduction. Table 2 shows the friction factor for different mud systems obtained from BP's laboratory tests [7].

Table 2 Mud type vs. friction factor [7]

Mud type	Friction factor
Water	0.67-0.76
Xanthan solution	0.52
KCl/PHPA	0.39-0.45
Amethyst WBM	0.39-0.45
Low solid WBM	0.41-0.50
Bentonite mud	0.40-0.46
Silicate mud	0.39-0.43
80/20 field OBM	0.19-0.21

The friction factor was reduced by adding lubricant into the mud system. However the compatibility of the lubricant and mud system must be taken into account. One can see clearly

MSc Thesis, 2015

that the additives like polymers and lubricants reduce the friction factor. The reduction is highest once changing to OBMs. At the area which is exposed to direct contact with drilling tools the friction factor is increased. The forces acting on drilling tubular are illustrated in t figure 28. The drag and frictional torque are directly related to the surface area which is in contact with the tools. At the deviated and horizontal sections of the well, due to possibility of cutting deposition the frictional forces and the incident like stuck pipe and fatigue is frequently higher. The torque and drag optimization depends on hole cleaning ability of drilling mud and its lubricator to minimize the friction factor and cutting beds deposition. In addition to factors mentioned like flow characteristics and mud property, other factors like well profile and geometry. These beds are more likely formed at high inclined section with and angle between 40 to 60 degrees.
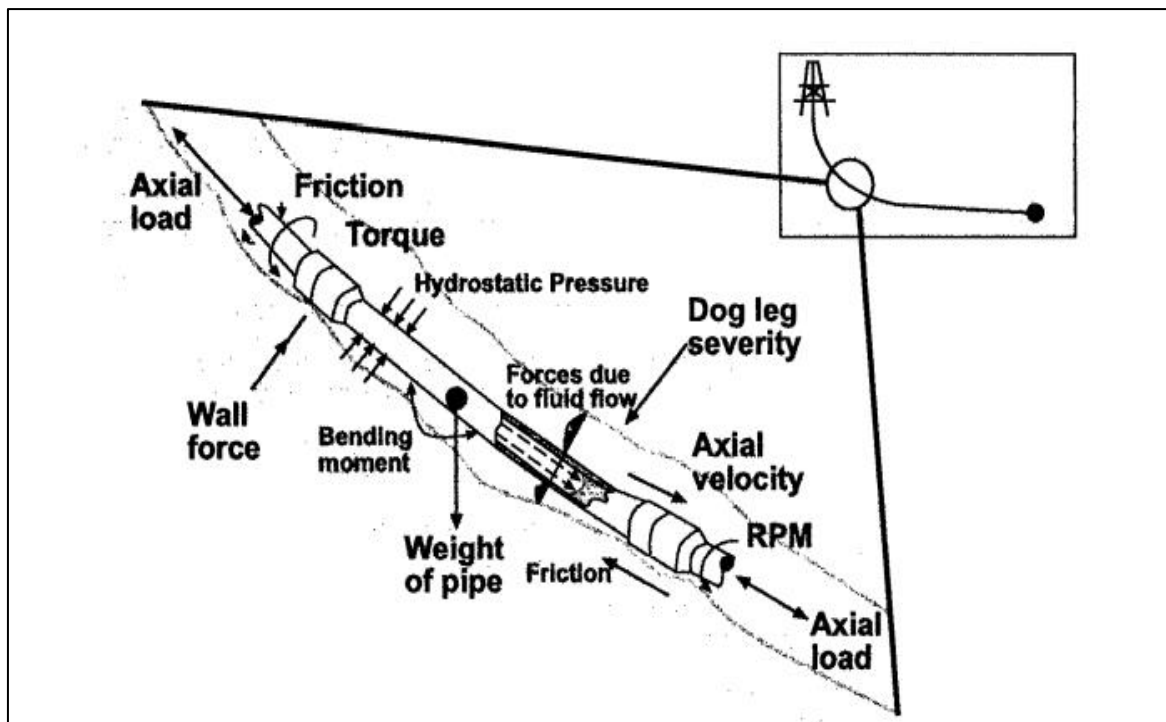
Figure 29 Schematic forces acting on drilling tubular in deviated wells [7]

4 Experimental works

Performance of Nano-treated water based drilling fluids has been of interest to find out if there possibility for improvement by applying Nano-technology into drilling fluid technology. As it was mentioned earlier the rheological behavior of drilling fluid is essential for the cutting transport, drill sting mechanics and annular pressure drop. The main idea behind application of Nano silica is an improvement in cementing technology which has given the cement slurry higher mechanical strength. Due to its fine size the Nano silica has been used to reduce the permeability and porosity of set cement. [23]

In this chapter we are going to investigate the rheological behavior and performance of WBMs by varying the condition, composition and concentration of different additives especially the Nano silica. The investigation methodology is divided into 2 parts.

- **Part I : Experimental part**
    - Rheology
        - ➢ Effect of temperature
        - ➢ Effect of polymer concentration
        - ➢ Effect of salt type and concentration
        - ➢ Effect of Nano silica concentration
    - Viscoelastic characterization
        - ➢ Amplitude Sweep test (Ref. system Vs. Nano-treated system)
        - ➢ Frequency Sweep test (Ref. system Vs. Nano-treated system)
    - Flow through porous media (Ref. system Vs. Nano-treated system)

- **Part II : Performance Simulation part**
    - Cutting transport simulation
        - ➢ Cuttings bed height
        - ➢ Minimum flow rate
    - Hydraulic simulation
        - ➢ Total pressure drop(Selected system)
        - ➢ Annular pressure drop(Selected system)
        - ➢ ECD (Selected system)

The objective of the rheological test is to study the effect of single and combined additives on rheological parameters and filter loss to screen out the right amount of each additive (salt, polymer, Nano silica) for nest experiment to finally provide a superior Nano-treated drilling fluid with high performance. The viscoelastic study of the selected Nano-treated drilling fluid will also be performed through experiment for characterization and comparison with reference system.The last experiment is to test and compare the diffusion of filtrate into a sand package for reference system and Nano-treated system in order to observe filtrate invasion in high porous high permeable media. Further we are going to test the selected drilling fluid using simulation software in order to evaluate its hole cleaning performance in real well geometry. The simulation result will be compared with reference system and 2 other similar mud systems. The final section of the simulation work is about hydraulic simulation of the different pressure drops in a designed well using the unified hydraulic model.

4.1 Description of Nano silica (SiO$_2$)

The size range of the Nano Silica which was used in the experimental part is the 15 nm sized Nano silica which are provided by EPRUI Nanoparticles & Microspheres Co. Ltd, China. However the detail regarding to the particles were not specified an Elemental Dispersive Spectroscopy (EDS) was used to characterize the Nano-particle for identification by Scanning Electron Microscopy (SEM). In order to imaging and analysis of the particles palladium was used to coat particles, the particles were coated with ***Palladium*** (Pd). Figure 30 shows the SEM image and EDS analysis of Nano-particle is shown in figure 31. Please notice that in addition of silica and oxygen a very little amount of carbon was also observed in the sample.
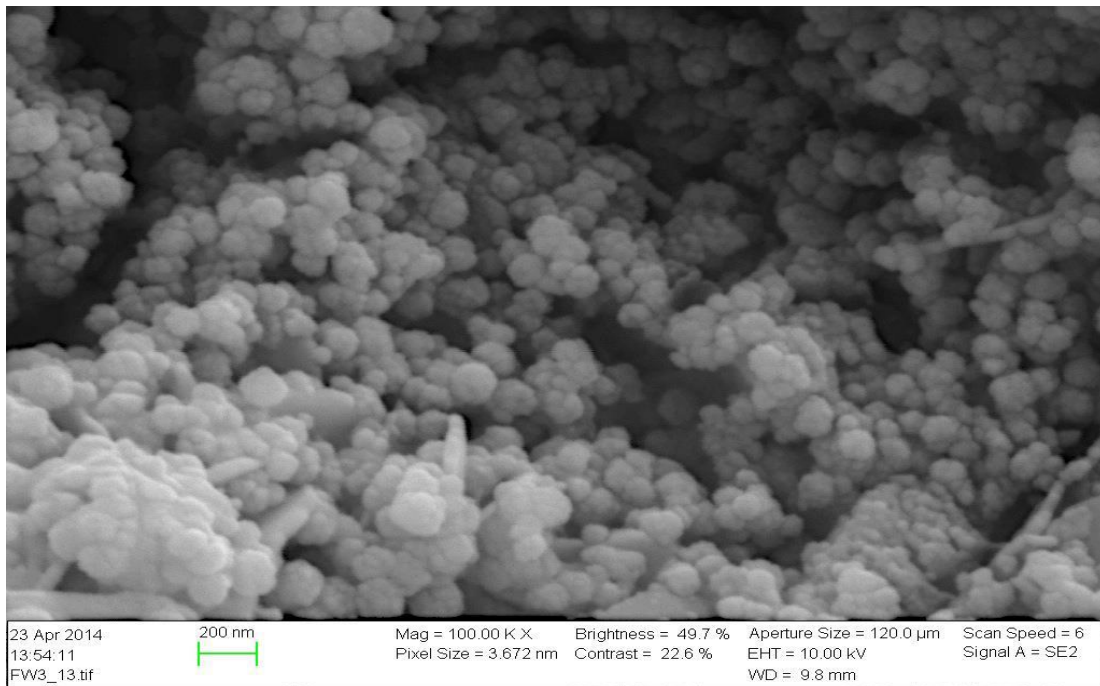
Figure 30 Scanning electronic microscope picture of the used Nano Silica
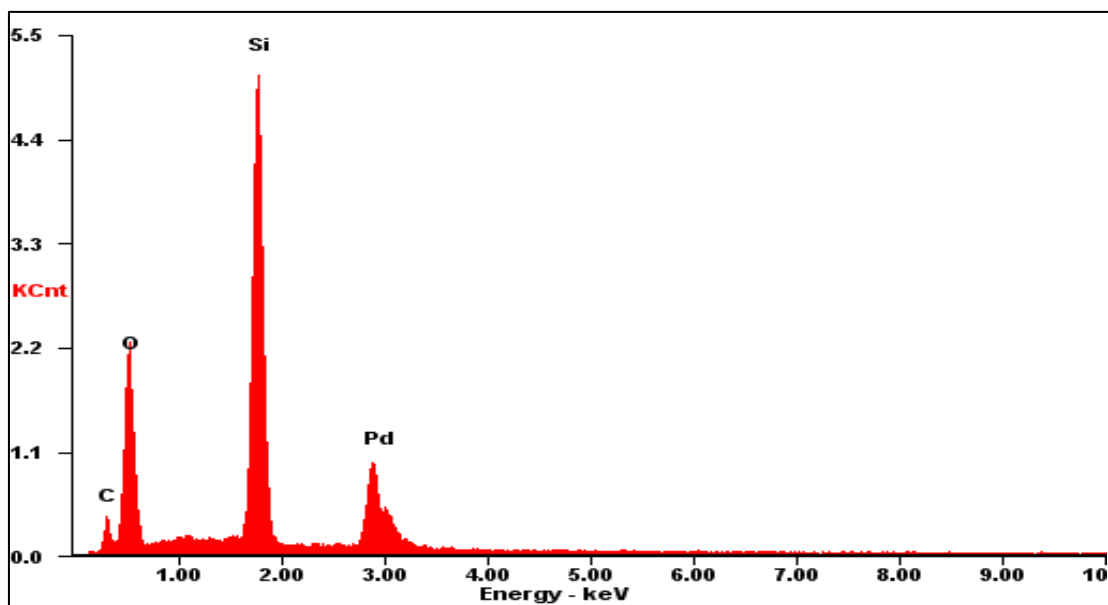
Figure 31 EDS analyses of the Nano silica

4.2 Effect of temperature in Nano-treated polymer based WBMs

The effect of temperature is of interest because well temperature increases as we drill into deeper sections. The increasing temperature is due to geothermal gradient of the formation which is usually about $3^{o}C$ per 100 meters. It is critically important to ensure drilling fluid properties are maintained and it performs its functions during the drilling operation even at higher temperatures.

4.2.1 Description of Drilling Fluid system

For the investigating of the temperature effect, there was designed and prepared several stable drilling fluid systems containing PAC, NaCl and Nano silica. The test matrixes are shown in table 3:

Table 3 Reference test matrix

Nr.	Mud system	Bentonite	H$_2$O	PAC	Nano	NaCl
#1	Reference	25 g	500 ml	0	0	0
#2	Ref. + salt	25 g	500 ml	0	0	4 g
#3	Ref.+ poly.	25 g	500 ml	0.25 g	0	0
#4	Ref.+Poly.+Nano	25 g	500 ml	0.25 g	1	0
#5	Ref.+Poly.+Nano+salt	25 g	500 ml	0.25 g	1	4 g

The effect of temperature on Nano-treated polymer based WBMs was studied by conducting the thermos cup and measuring the temperature after heating up the sample up to 72 ^{o}F , 110 ^{o}F and 130 ^{o}F.

The mixing procedures were adding the Nano silica, salt and then polymer at first stage respectively and bentonite at final stage. All the samples were then stored for minimum 24 hours in order to let the bentonite platelets react completely.

4.2.2 Test result and discussion

The measurement result of all samples during rheological work are presented as Shear stress and Shear rate with the units lb/100ft^2 and RPM respectively. The filter loss test was performed by measuring the amount of filtrate after 7.5 minutes.

To visualize the change in rheological behavior at mentioned temperature, rheological parameters of each system such as PV, YS, n, K, LSYS (law shear yield stress) and YS/PV were calculated and presented at Appendix B. The measurement data for the sample #4 and #5 are shown as examples in figure 32.
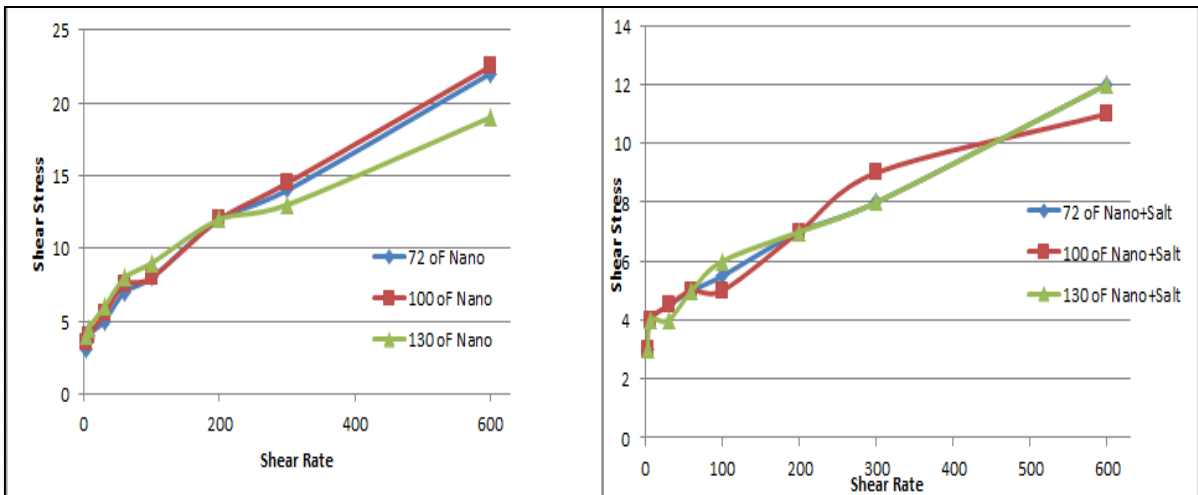
Figure 32 1 Comparison of shear rate shear stress curve for the sample #4 (left)and #5 (right) at three different temperatures
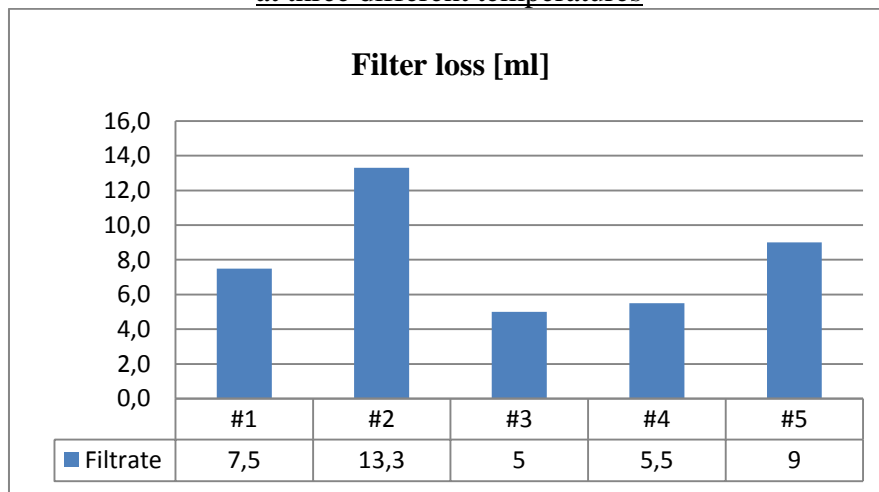
Figure 33 Comparison of dynamic filter loss measured for the mud system at room temperature

Measured data at different temperature indicated that temperature's affect the rheological behavior of any of samples is different for each sample. The highest change was observed in the reference system showing higher shear stress values when the temperature was raised. The value of YS and LSYS was increased as temperature was raised for the reference system.

One can observe the effect of each additive such as NaCl, polymer and Nano silica on rheological parameters by comparing their values. The salt additive in #2 and Nano silica in sample #4 led to a thinning effect on the drilling fluid system and decreasing the YS and LSYS regarding to their previous samples which lack these additives (#1 and #3). The change of shear stress for the systems containing Salt, Nano silica and Polymer was not substantial. However the uncertainties regarding to temperature measurement are high as it can be observed on measured data which creates a wavy curve. Filter loss measurement showed a significant variation for the systems where the highest value were after adding the salt. The

investigation of the temperature effect will not be attempted further in this thesis as it doesn't show any clear effect in presence of Nano silica.

4.3 Effect of polymer concentration in WBM

In this section we are going to investigate the effect of polymer concentration in WBM. For this part the PAC polymer was used in three different concentration to indicate how sensitive the rheological parameters are when the amount of polymer changes. The mud systems contained all the KCl salt to provide inhibitive drilling fluid. The effect of salt on the performance of the polymer is of interest. KCl will shorten the polymer chain and thus affect the rheological behavior of the system [25].
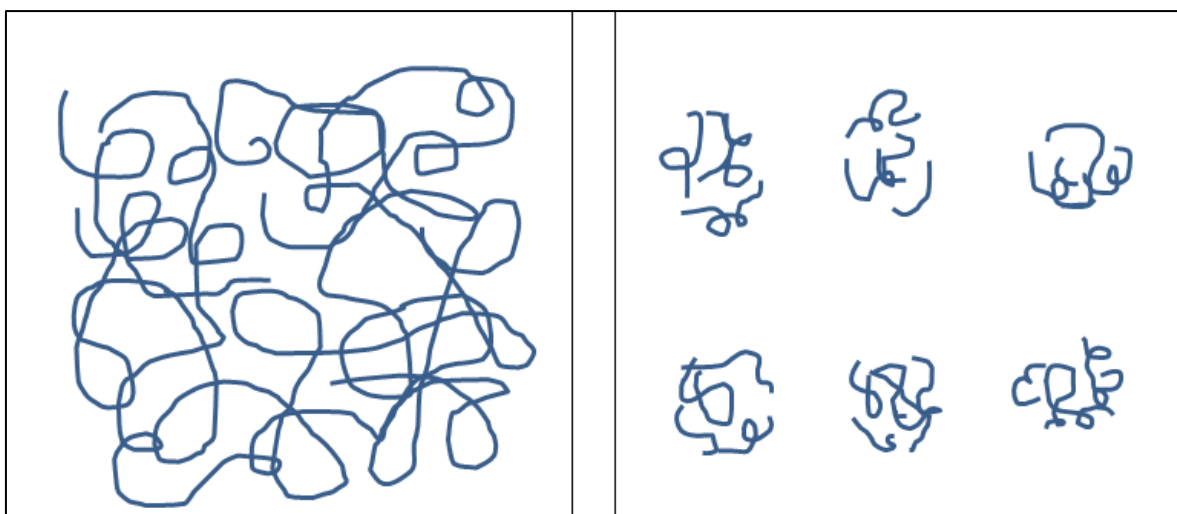
Figure 34 The Structure of the polymer chains in absence (left) and presence (right) of the salt additives

4.3.1 Description of Drilling Fluid system

There were prepared the 4 samples of drilling fluid systems with the composition described in table 4:

Table 4 Test matrix with different PAC concentrations

Mud system	Bentonite	H_2O	PAC	KCl
Ref. #1	25 g	500 ml	0.0 g	2.5 g
Ref +0.1 PAC #2	25 g	500 ml	0.1 g	2.5 g
Ref+0.3 PAC #3	25 g	500 ml	0.3 g	2.5 g
Ref+0.5 PAC #4	25 g	500 ml	0.5 g	2.5 g

4.3.2 Test result and discussion

The data measured for each system indicates that the addition of polymer has visible effect on the rheological behavior by decreasing the shear stress of drilling fluid. The more the concentration of PAC, the lower is the measured shear stress of the system. The shear stress-

MSc Thesis, 2015

shear rate of all 4 systems is plotted in the figure 35. Since the Nano silica also gives lower value of shear stress, there was not used any Nano silica in this test to make sure the change is caused by PAC concentration.
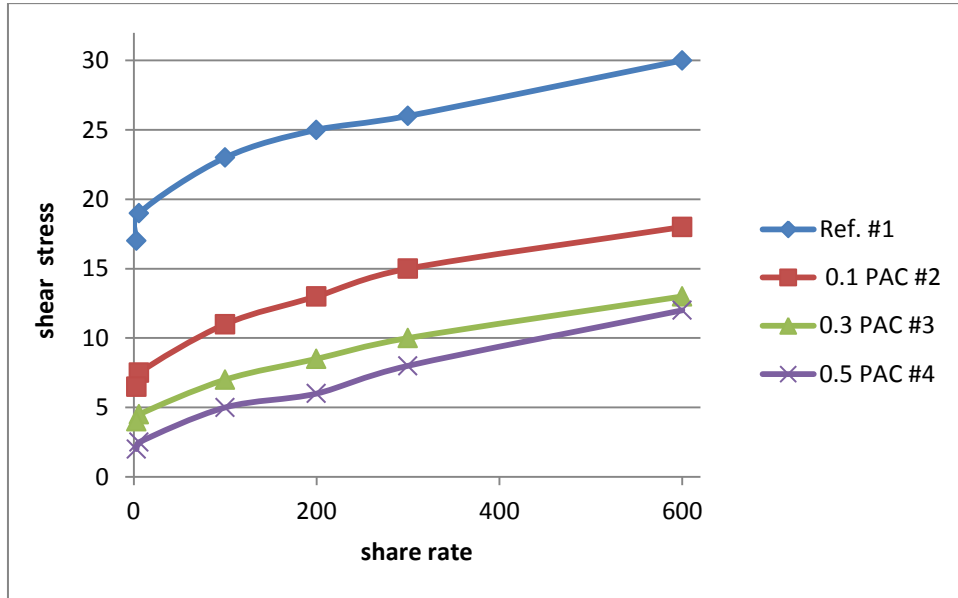
Figure 35 Comparison of Shear rate shear stress curve for samples with different PAC concentrations

	Ref. #1	0.1 PAC #2	0.3 PAC #3	0.5 PAC #4
■ Filter Loss [ml]	14,0	11,5	7,5	5,5
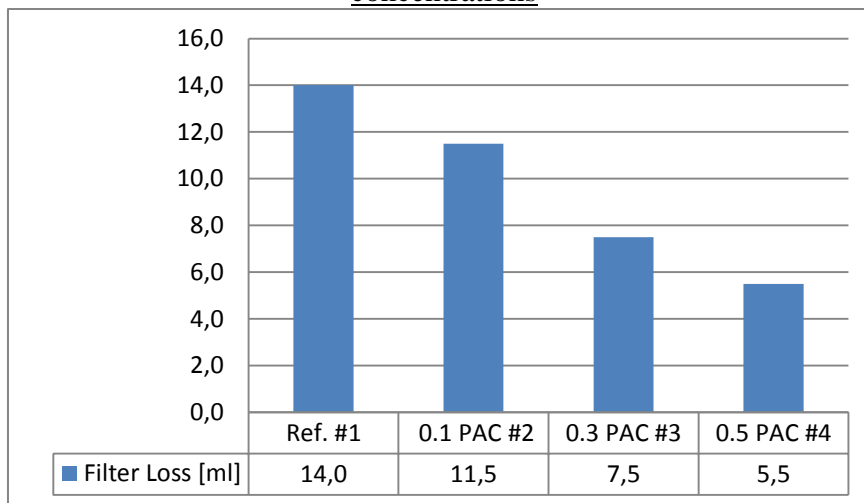
Figure 36 Filter loss of mud systems with different PAC concentrations

The polymer has not been acting as viscosifier where the polymer chains were broken in presence of KCl. By calculating the rheological values of system and showing those in a diagram one can compare the values which are most affected as a consequence of higher PAC concentration. It led to lower YS, K and LSYS values as PAC concentration increased. This indicates a deflocculating process among clay platelets which have reduced the Gel Strength and YS. The drilling fluid with lower YS and of course lower LSYS has less ability for

MSc Thesis, 2015

cutting suspension which might led to cutting bed in lower side of borehole at the inclined section of the well [29].The values of PV seem to be almost unaffected by lower polymer concentration indicating that bentonite platelets are gone from dispersed to aggregated arrangements [29]. However the PAC added to the system will optimize the filter loss into the formation which is favorable. For further experiment 0.5 g of polymer will be used to keep the filter loss low.

	PV	YS	n	k	LSYS
Ref.	4,0	22,0	0,2	7,2	15,0
0.1 PAC	3,0	12,0	0,3	2,9	5,5
0.3 PAC	3,0	7,0	0,4	0,9	3,5
0.5 PAC	4,0	4,0	0,6	0,2	1,5
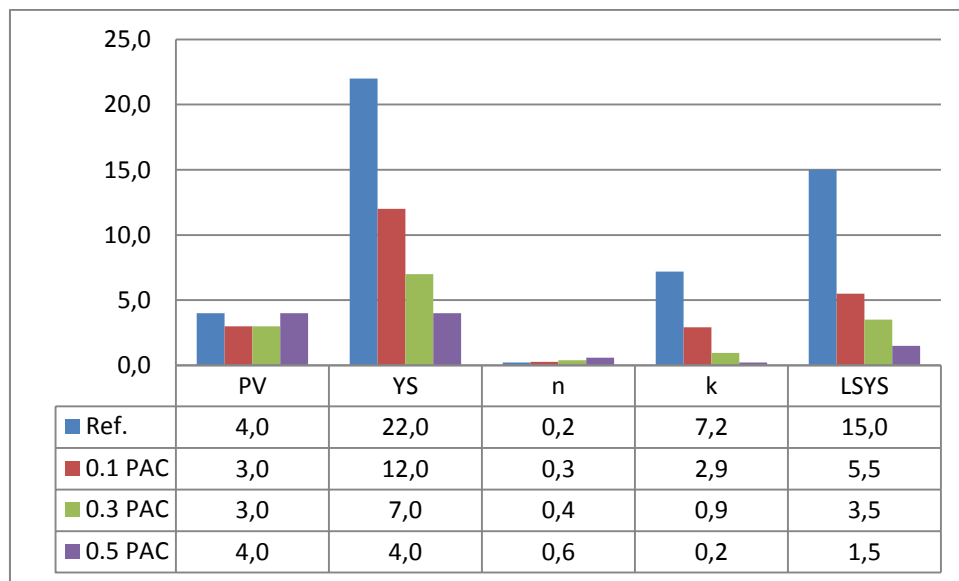
Figure 37 The calculated rheological parameters of the drilling fluid systems

4.4 Effect of salt type and concentration in polymer based WBMs

In this test we are going to investigate the effect of the salt type which is compatible with the drilling fluid and optimize the concentration which is to be used in the Nano-treated WBM system. Due to swelling effect of Montmorillonite which exists in shale formations one has mitigate the swelling by adding salt. The fresh water as continuous phase in WBMs is not inhibitive unless salt is added into system. This makes the drilling fluid favorable and mitigates stuck pipe situations to occur. The polymer added to the system contributes also as inhibitor by reducing the contact between clay platelets and water.

The types of salt which are selected to be investigated are NaCl, KCl and $CaCl_2$. As we know the PAC polymer is a modified version of CMC polymer and has higher DS factor. For this test CMC polymer was used as filter loss controller in all samples.

4.4.1 Description of Drilling Fluid system

There were prepared 13 different mud systems, in 4 different concentrations as shown in tables 5, 6 and 7. The concentration was increased slightly for each sample. The KCl is the main salt which gives the best inhibitive WBM. However the effect of NaCl and $CaCl_2$ are also investigated to document the effect. In order to compare the salt effect, there were prepared 2 system of the sample #1. The salt additive was added once before the bentonite and once after it to investigate and compare the ex-situ and in-situ effect of salt.

Table 5 Test matrix for WBMs with different NaCl concentrations

Mud system	Bentonite	H_2O	CMC	NaCl
#1	25 g	500 ml	0.5 g	0.75 g
#2	25 g	500 ml	0.5 g	1.50 g
#3	25 g	500 ml	0.5 g	2.25 g
#4	25 g	500 ml	0.5 g	3.00g

Table 6 Test matrix for WBMs with different KCl concentrations

Mud system	Bentonite	H_2O	CMC	KCl
#5	25 g	500 ml	0.5 g	0.75 g
#6	25 g	500 ml	0.5 g	1.50 g
#7	25 g	500 ml	0.5 g	2.25 g
#8	25 g	500 ml	0.5 g	3.00g

Table 7 Test matrix of WBMs with different CaCl2 concentrations

Mud system	Bentonite	H_2O	CMC	$CaCl_2$
#9	25 g	500 ml	0.5 g	0.75 g
#10	25 g	500 ml	0.5 g	1.50 g
#11	25 g	500 ml	0.5 g	2.25 g
#12	25 g	500 ml	0.5 g	3.00g

4.4.2 Test result and discussion

The data measured during the test are plotted to give a clear picture of how the shear stress shear rate curve is affected as a result of higher salt concentration. The CMC polymer has lower salt tolerance than PAC and XC. By keeping the polymer concentration (0.5 g) constant a thinner drilling fluid system was observed as salt concentration increased. By comparing the measured data for in-situ and ex-situ, the NaCl didn't manage to reduce the viscosity provided by bentonite as much as it did for the in-situ sample. This might an effect of having drilling fluid where the salt has not dissolved in the sample perfectly homogenously. The reduction of

shear stress was more critical in cases where KCl was used than NaCl. Regarding to the CaCl$_2$, the mud system which contained higher than 0.75 g of CaCl$_2$ totally failed and the bentonite was deposited and separated form water. This can be explained by exceeding the CMCs salt tolerance as number of Ca^{2+} ions increased. Please notice that the thinning effect and reduction of shear stress measured was almost equal for 0.75 g CaCl$_2$ and 2.25 KCl.

When the concentration of Cl increases, the clays ability for hydration decreases. The Cl- will at first stage react with Ca2+ and Na+ which already exists in the drilling fluid. The amount of KCl desired for the drilling fluid varies based on the formation which is about to be drilled. In case of using NaCl in the drilling fluid not only provide Cl- ion, it will also increase the concentration of Na+ ion in addition to Na+ cations which preexisted in the system[29]. This might explain the less thinning effect of NaCl compared to KCl. Based on the measurements and thinning effect of salt in order to provide inhibitive mud 2.5 g of Salt is used for further experiments.
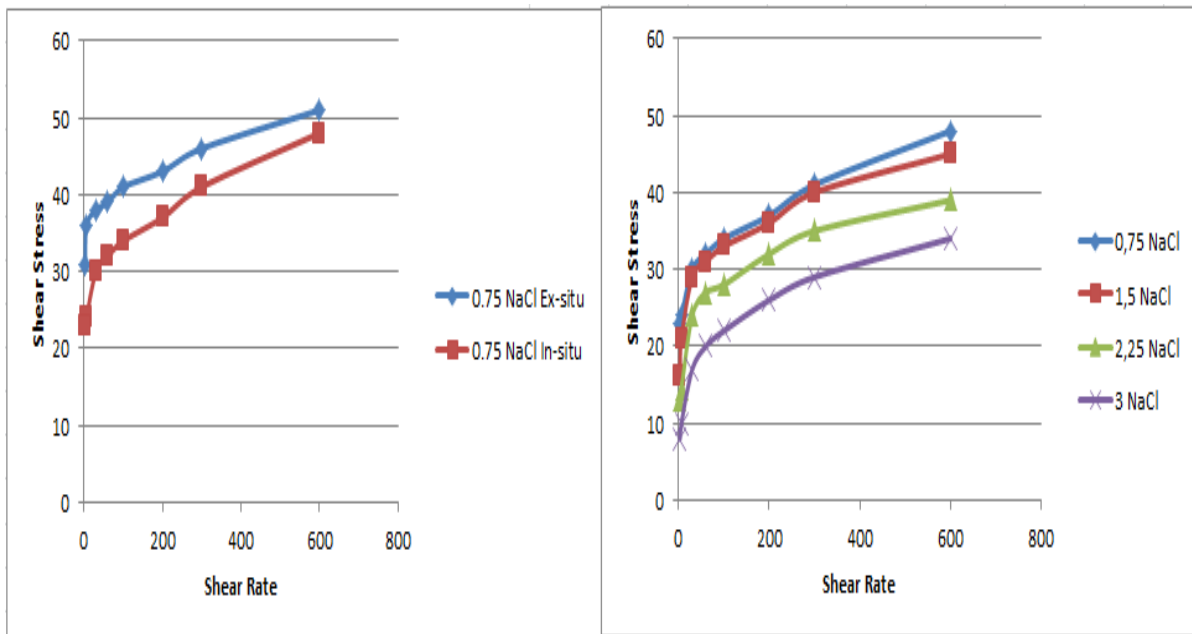
Figure 38 Comparison of Shear rate shear stress for Ex-situ, In-situ salt effect (left) and WBMs with different NaCl concentrations
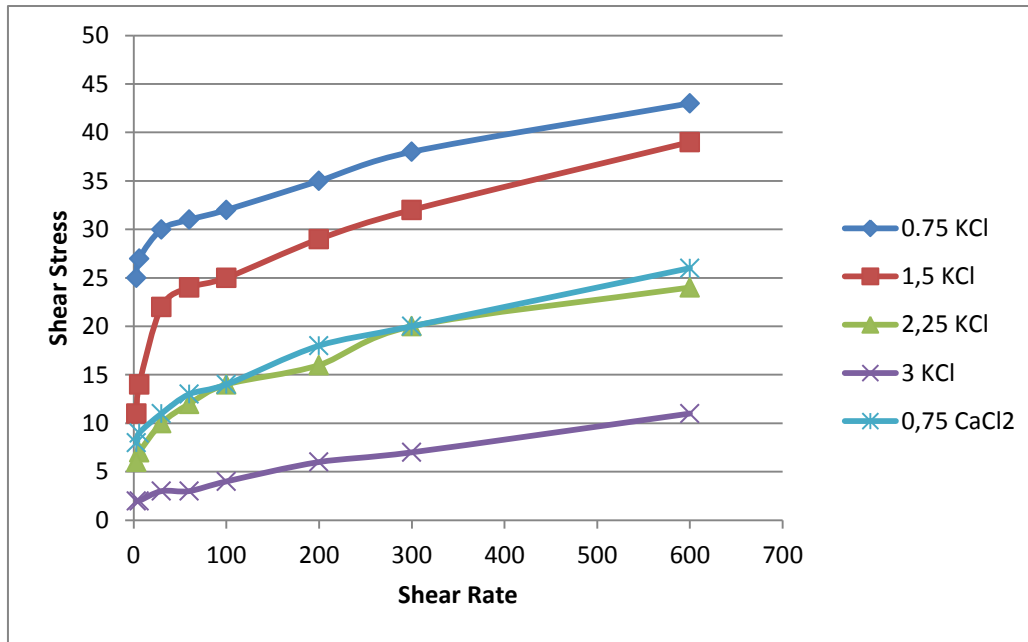
Figure 39 Shear rate shear stress curve for WBMs with different salt concentrations

4.5 Effect of Nano silica concentration in polymer based WBM

The concentration of the Nano silica which was added to the system in the first experiment seems to be too high for the reference system. Based on that evaluation we are going to investigate the appropriate concentration of Nano silica and the type of polymer which is compatible with Nano silica.

4.5.1 Description of Drilling Fluid system

For this test at first stage the PAC was used once with NaCl and once with KCl containing 3 different concentrations of Nano silica.

Table 8 Test matrix for WBMs with different Nano concentrations (PAC+NaCl)

Mud system	Bentonite	H_2O	PAC	NaCl	Nano silica
Ref #1	25 g	500 ml	0.5 g	2.5 g	0.0 g
Ref+ 0.15 Nano #2	25 g	500 ml	0.5 g	2.5 g	0.15 g
Ref+ 0.30 Nano #3	25 g	500 ml	0.5 g	2.5 g	0.30 g
Ref+ 0.45 Nano #4	25 g	500 ml	0.5 g	2.5 g	0.45 g

Table 9 Test matrix for WBMs with different Nano concentrations (PAC+KCl)

Mud system	Bentonite	H_2O	PAC	KCl	Nano silica
Ref #5	25 g	500 ml	0.5 g	2.5 g	0.0 g
Ref+0.15 Nano #6	25 g	500 ml	0.5 g	2.5 g	0.15 g
Ref+0.30 Nano #7	25 g	500 ml	0.5 g	2.5 g	0.30 g
Ref+0.45 Nano #8	25 g	500 ml	0.5 g	2.5 g	0.45 g

In order to have more variation among salt used in the mud systems PAC was also used by using a mixture of NaCl and KCl. The total amount of salt maintained at 2.5 g with having 1.25 g of KCl and 1.25 g NaCl. The test matrix is shown in table 10.

Table 10 Test matrix for WBMs with different Nano concentrations (PAC+NaCl+KCl)

Mud system	Bentonite	H$_2$O	PAC	NaCl	KCl	Nano silica
Ref #9	25 g	500 ml	0.5 g	1.25 g	1.25 g	0.0 g
Ref+ 0.15 Nano #10	25 g	500 ml	0.5 g	1.25 g	1.25 g	0.15 g
Ref+ 0.30 Nano #11	25 g	500 ml	0.5 g	1.25 g	1.25 g	0.30 g
Ref+ 0.45 Nano #12	25 g	500 ml	0.5 g	1.25 g	1.25 g	0.45 g

For the second part two different fractions of XC and PAC were used. The salt type was KCl and also a blend of KCl+NaCl as previous samples to indicate how the rheological behavior of drilling fluid will change as a consequence of increasing Nano silica concentration. For this purpose, the following test matrixes were prepared is shown in table 12.

Table 11 Test matrix for WBMs with different Nano concentrations (PAC+XC+NaCl)

Mud system	Bentonite	H$_2$O	PAC	Xanthan	NaCl	Nano silica
Ref #13	25 g	500 ml	0.4 g	0.1 g	2.5 g	0.0 g
Ref+ 0.15 #14	25 g	500 ml	0.4 g	0.1 g	2.5 g	0.15 g
Ref+ 0.30 #15	25 g	500 ml	0.4 g	0.1 g	2.5 g	0.30 g
Ref+ 0.45 #16	25 g	500 ml	0.4 g	0.1 g	2.5 g	0.45 g

Another 4 mud systems were prepared with a lower amount of PAC and increasing the amount of Xanthan XC to 0.2 g. It will indicate the effect and grade of compatibility between Xanthan XC and Nano silica. The test matrix is presented in the table 13.

Table 12 Test matrix for PAC+XC+KCl +NACl mud systems with different Nano concentrations

Mud system	Bentonite	H$_2$O	PAC	Xanthan	NaCl	KCl	Nano silica
Ref#17	25 g	500 ml	0.3 g	0.2 g	1.25 g	1.25 g	0.0 g
Ref+0.15 Nano#18	25 g	500 ml	0.3 g	0.2 g	1.25 g	1.25 g	0.15 g
Ref+0.30 Nano#19	25 g	500 ml	0.3 g	0.2 g	1.25 g	1.25 g	0.30 g
Ref+0.45 Nano#20	25 g	500 ml	0.3 g	0.2 g	1.25 g	1.25 g	0.45 g

The same amounts of polymers were used for the next 7 mud systems. The only parameter that differentiates them from #17 - #20 is the 2.5 g KCl and no use of NaCl. In this samples

the range of Nano silica additive were increase by only 0.05 g at the time starting from Reference system with no Nano silica. The test matrix is presented at table 14.

Table 13Test matrix for PAC+XC+KCl mud systems with different Nano concentrations

Mud system	Bentonite	H_2O	PAC	Xanthan	KCl	Nano silica
Ref#21	25 g	500 ml	0.3 g	0.2 g	2.5 g	0.00 g
Ref+0.05 Nano#22	25 g	500 ml	0.3 g	0.2 g	2.5 g	0.05 g
Ref+0.10 Nano#23	25 g	500 ml	0.3 g	0.2 g	2.5 g	0.10 g
Ref+0.15 Nano#24	25 g	500 ml	0.3 g	0.2 g	2.5 g	0.15 g
Ref+0.20 Nano#25	25 g	500 ml	0.3 g	0.2 g	2.5 g	0.20 g
Ref+0.25 Nano#26	25g	500 ml	0.3 g	0.2 g	2.5 g	0.25 g
Ref+0.30 Nano#27	25g	500 ml	0.3 g	0.2 g	2.5 g	0.30 g

The next test matrixes were prepared by eliminating the PAC from the system. The low viscosity CMC was combined with Xanthan and KCl was used as inhibitive agent as shown in table 15.

Table 14 Test matrix for CMC+XC+KCl mud systems with different Nano concentrations

Mud system	Bentonite	H_2O	LV CMC	Xanthan	KCl	Nano silica
Ref#28	25 g	500 ml	0.2 g	0.3 g	2.5 g	0.00 g
Ref+0.20 Nano#29	25 g	500 ml	0.2 g	0.3 g	2.5 g	0.20 g
Ref+0.25 Nano#30	25 g	500 ml	0.2 g	0.3 g	2.5 g	0.25 g
Ref+0.30 Nano#31	25 g	500 ml	0.2 g	0.3 g	2.5 g	0.30 g

4.5.2 Test result and discussion

The test matrixes were mixed for sample #1 to #8 and tested to find out if the performance of the new developed show any sign of improvement regarding to the reference system. Increasing Nano silica concentration led to lower values of shear stress than the reference system both with KCl and NaCl.
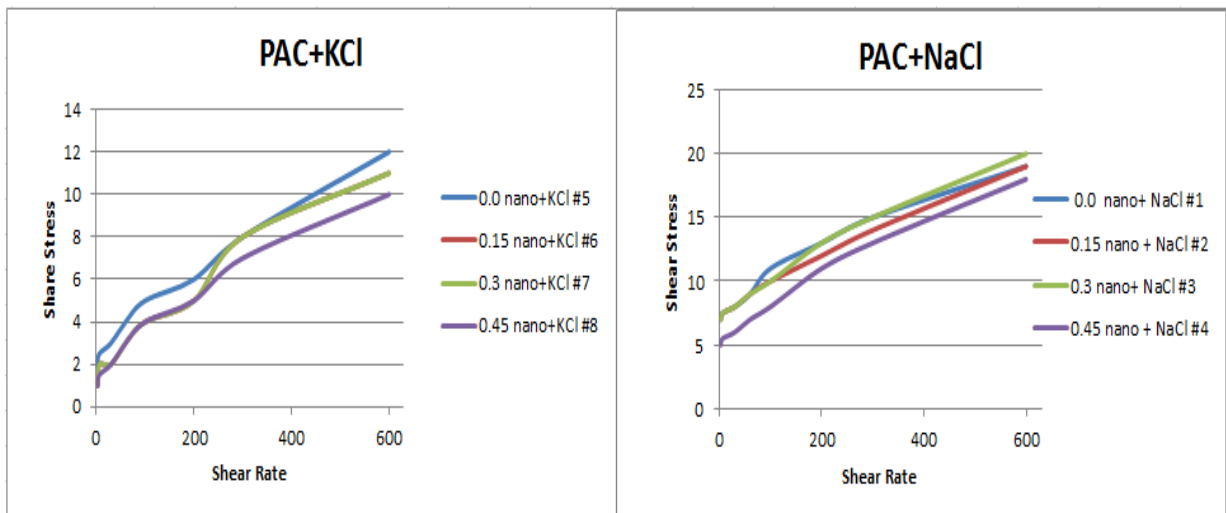
Figure 40 Comparison of shear rate shear stress curve for PAC+KCl (left) and (PAC+NaCl) right with different Nano concentrations

The rheological parameters confirm the indication that no improvement has been achieved for the PAC system. Considering the e reference systems containing no Nano silica, the performance of new systems with Nano was even less favorable than reference system as shown in figure 41.
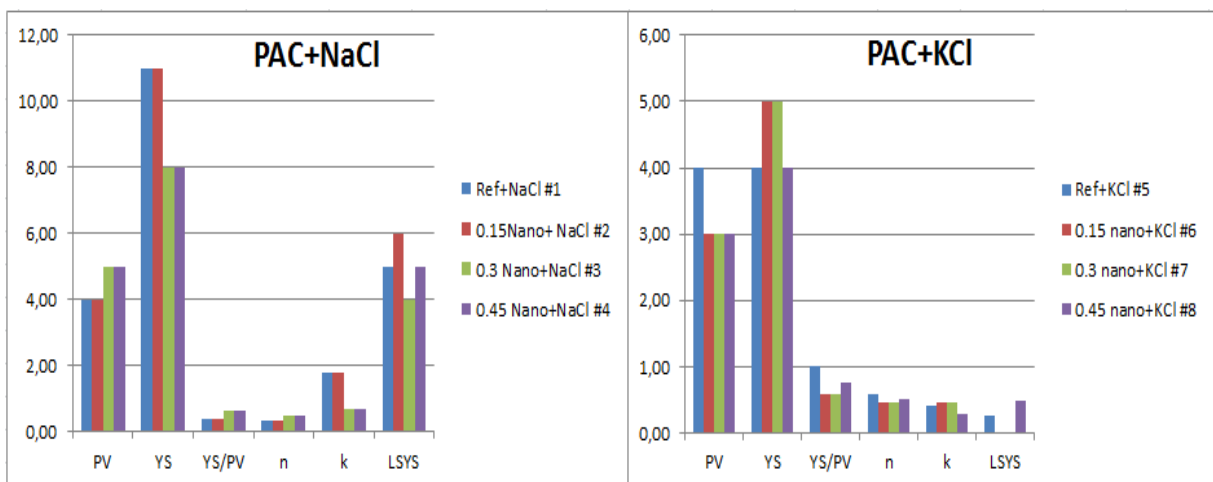
Figure 41 Comparison of rheological parameters for PAC+NaCl (left) and PAC+NaCl (right) with different Nano concentrations

The next blends were a mixture of NaCl and KCl in presence of PAC and three Nano silica concentrations. The measurements are plotted in figure 42.Nano silica containing samples (#10, #11, #12) has a lower shear stress regarding to the reference (#9). The higher shear stress values of #12 regarding to #11 shows an interesting behavior of the drilling fluid. By taking to account the thinning effect of Nano silica, it was expected lower shear stress value for sample

#12. However the shear stress values for high shear rates are higher for sample #12 than the sample #11. It can be explained by the existence of certain Nano silica concentration which raises the shear stress and thus provides a better cutting transport than the reference system (#9).
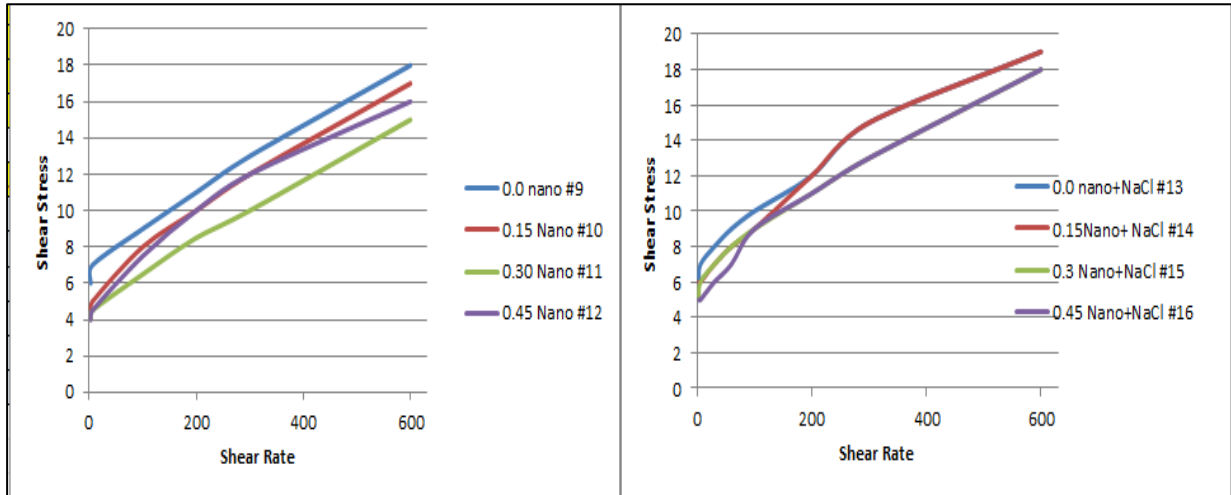
Figure 42 Comparison of shear rate shear stress curve for PAC+NaCl+KCl (left) and PAC+XC+NaCl (right) mud systems with different Nano concentrations

	0.0 nano #9	0.15 Nano #10	0.30 Nano #11	0.45 Nano #12
Filter loss[ml]	5,5	5,5	5	5,5
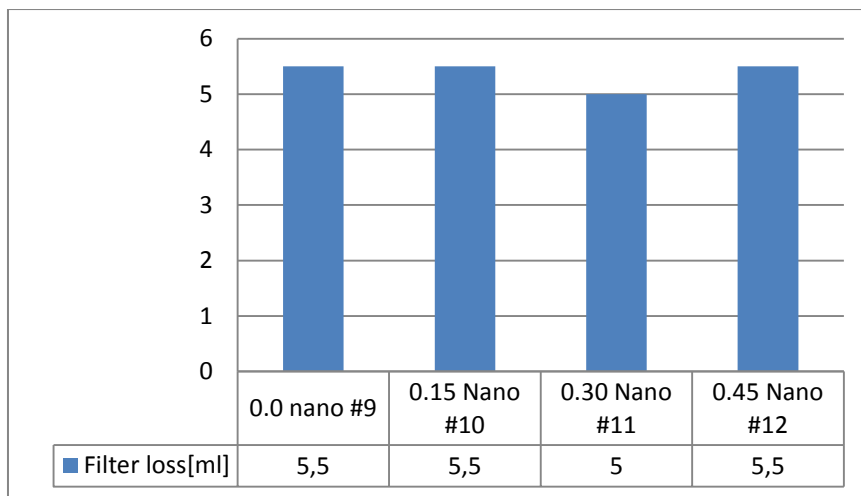
Figure 43 Filter loss measured for PAC+KCl+NaCl mud systems with differenct Nano concentrations

Due to poor result of the first test sample the PAC concentration was reduced and Xanthan XC was also added to the systems (#13, #14, #15, #16). The shear stress measured did not change significantly. The poor rheological values are shown are shown in figure 44 and the data are presented at the appendix C. The samples #15 and #16 provided higher PV but their value for YS has decreased regarding to the reference system. The only parameters differentiating the sample #14 and the reference system is LSYS which optimizes the cutting

transport slightly. However the optimization is so little that modification of the reference system is possible with cheaper alternative than adding Nano silica and the system is not as inhibitive as those with KCl.
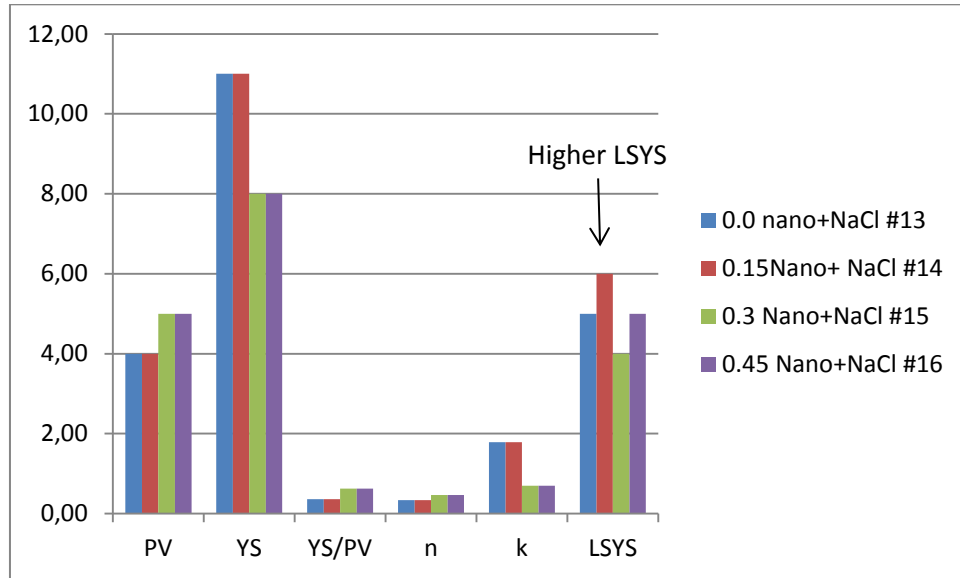
Figure 44 Comparison of rheological parameters for PAC+XC+NaCl mud systems with different Nano concentrations

The second mixture of PAC and XC polymer and KCl and NaCl as salt was then made and measured. (#17, #18, #19, #20) .The descriptions of the samples are presented at table 12.

Considering the result of the system made by mixed salt, the reduction of KCl has not affected the reference so much. The change is most visible only at the sample #20 where a higher concentration of Nano silica in presence of the salts shows poor measured values of shear stress regarding to the reference system.
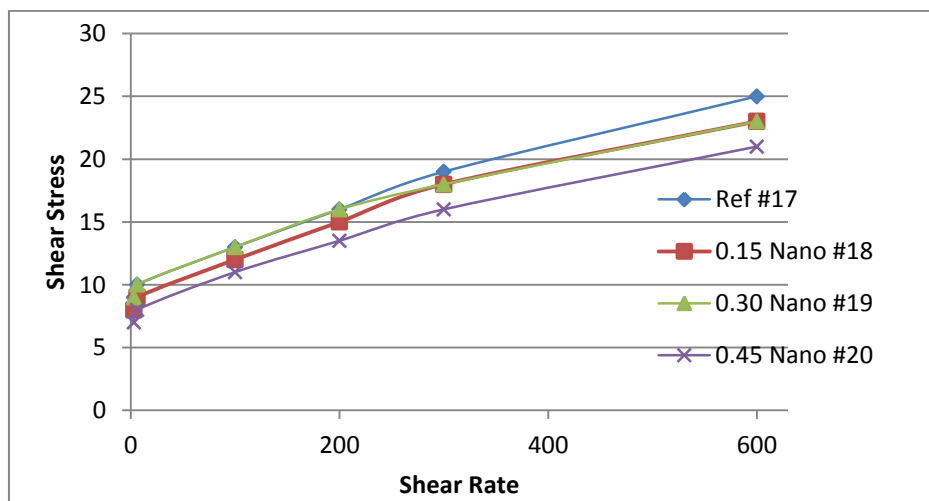
Figure 45 Comparison of shear rate shear stress curve for PAC+XC+KCl+NaCl mud system with different Nano concentrations

	Ref #17	0.15 Nano #18	0.30 Nano #19	0.45 Nano #20
Filter loss[ml]	5,25	5,5	5	5,5
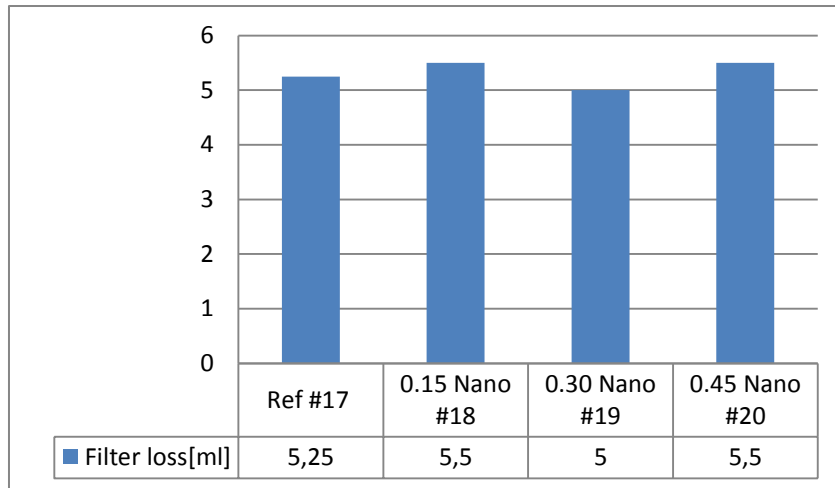
Figure 46 Comparison of filter loss measured for XC+PAC+NaCl+KCl mud system with different Nano concentrations

The concentration of 0.45 seems to be too high for such amount of bentonite and polymer. It was decided to use lower concentration of Nano in order to determine the right concentration with best performance. The presence of KCl is essential in order to keep the system inhibitive. By only using KCl as inhibitor, Xanthan XC and PAC as polymer the following measurement data were registered for sample #21 to #27 shown in figure 47.
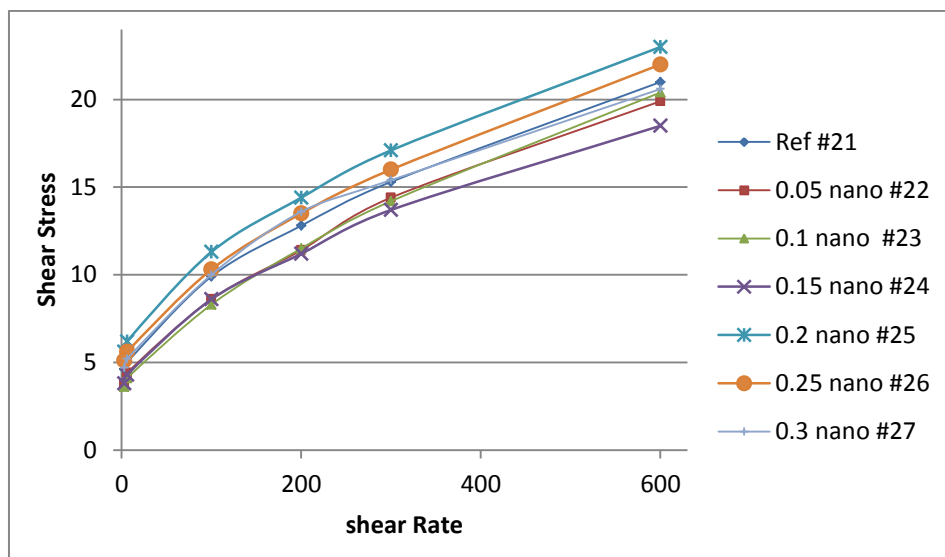
Figure 47 Comparison of shear rate shear stress curves for PAC+XC+ KCl mud systems with different Nano concentrations

Experiment result indicates the addition of Nano silica led to a system with higher values of shear stress for the sample #26 and #27. The shear stress value is higher at higher shear rate and at lower share rate it approaches the reference system. The calculated rheological parameters are shown in figure 48.
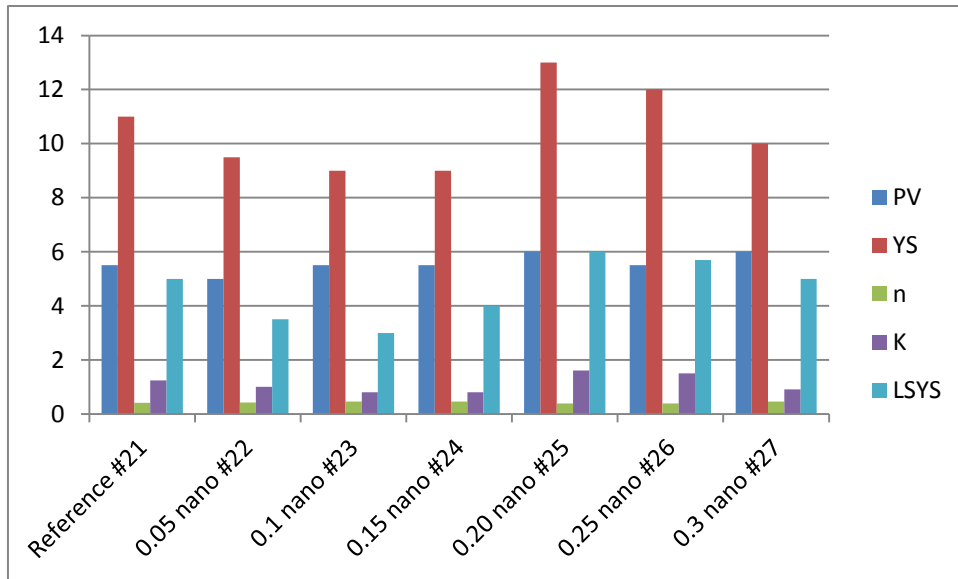
Figure 48 Comparison of rheological parameters for PAC+XC+ KCl mud systems with different Nano concentrations

	Ref 0.00 nano #21	0.05 nano #22	0.10 nano #23	0.15 nano #24	0.20 nano #25	0.25 nano #26	0.30 nano #27
Filter loss [ml]	6,5	7,25	6,75	6,5	6	6,5	6,8
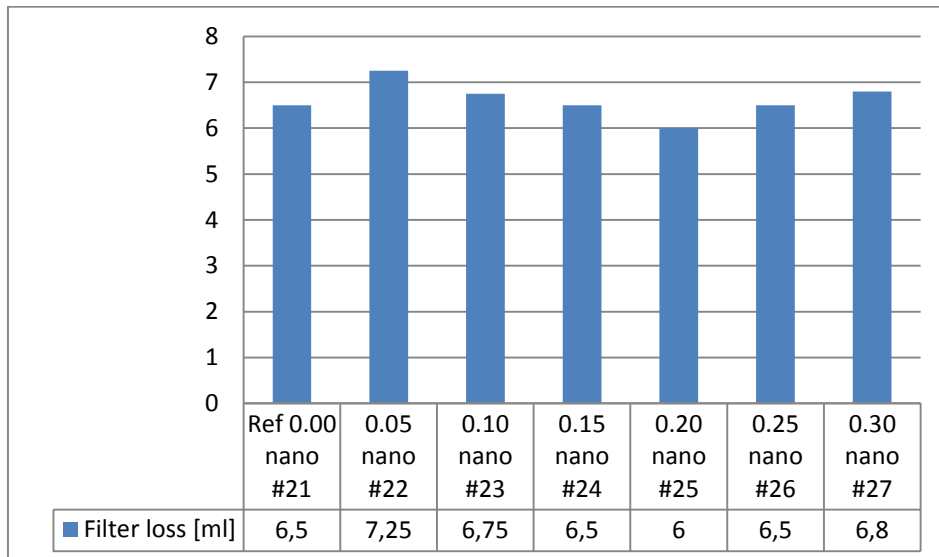
Figure 49 Comparison of filter loss measured for PAC+XC+ KCl mud systems with different Nano concentrations

The system #25 and #26 show higher values for YS and LSYS value compared with the reference system. The filter loss regarding to the sample #25 showed also lowest value indicating a more effective mud cake than the reference system. The interesting observation is a clear variation in filter loss and rheological behavior only by small amount of Nano silica added to the system. Filter loss, YS and LSYS follows a wavy pattern by increasing at start decreasing and then increasing again as the Nano concentration increased slightly.

Based on the results obtained from experiment the PAC polymer is not considered as compatible polymer in Nano containing systems. However Xanthan shows more compatibility at lower concentration of Nano silica. In order to test new polymer in addition to Xanthan it was decided to test the LV CMC to investigate rheology behavior of the system. The test matrixes of the samples are presented at table 15 for samples #28, #29, #30 and #31. The following data were obtained after the measurement as shown at table 16.

Table 15 Measured rheological data for CMC+XC+KCl mud systems

RPM	Ref #28	Ref+0.2 Nano #29	Ref+0.25 Nano #30	Ref+0.3 Nano #31
600	22	24,5	31	26
300	16,5	19	25,5	21
200	14	17	23,1	19
100	11	14	20,5	15,8
6	8	10	16,5	11,5
3	7	9	16	11

In order to compare samples, the main rheological parameters were calculated and presented in the figure 52. Comparison of the rheological parameters indicates a significant change in LSYS, YS and K values which are essential for the cutting transport and hole cleaning process. The value of PV is almost constant indicating no change at higher shear rates. The system which is most interesting one is #30 which has:

- The highest value of LSYS.
- Highest value of YS
- Lowest rate of filter loss (more effective mud cake)
- Highest YS/PV

It's important to remind that the higher yield stress (Yield point) obtained by the Bingham plastic model can also affect the drilling operation in a negative way. The negative effect is noticed at lost circulation and kick situations. [29] .The calculated value of YS is however assumed to be the higher than the real yield stress of the drilling fluid. Actually the calculated value is more close to the shear stress equivalent to share rate around the borehole (annulus). That is why YS is a good indicator for fluids cuttings suspension property. According to Bern et al. (1996) the minimum value for barite suspension is must be in a range between 7-15 lb/100ft^2 which for the sample #30 show the LSYS the highest value and equal to 15 lb/100ft^2.[27] Another indication for the cutting suspension and transport is the YS/PV ratio

which in addition of low value of n ensures a more laminar flow in the annulus which indicates a good cutting suspension and transport performance [28] For the sample #3 with 0.25 g Nano silica the highest YS and an equal value for PV compared to reference system the YS/PV is at its highest.

According to Skjeggestad et al, (1989) the risk of corrosion in equipment such as drill pipe, and other degradation of drilling fluid and its additives is reduced as long as the PH stays above 9,5[38] The mud systems were tested for PH using PH-meter at the laboratory. All the samples indicate a PH value close to 9.00. The mud system will not cause any corrosion to the steel equipment with this PH value. PH values for mud system are presented in figure 53. Mud cakes for the reference system and Nano systems are presented in figure 52. The thickness of the mud cakes was almost same for all four systems.
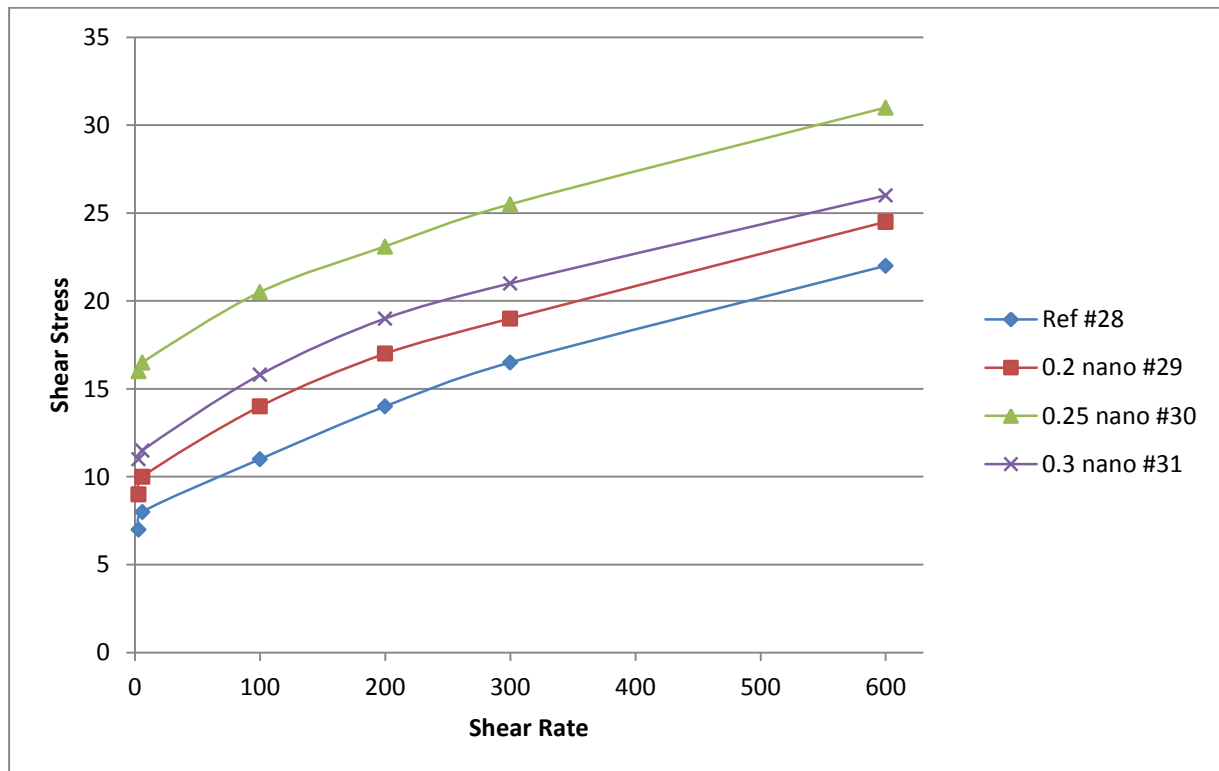
Figure 50 Shear rate-shear stress curve for the CMC+XC+KCl drilling fluid systems with different Nano concentrations

Filter loss (7.5 min) [ml]

	Ref 0.00 nano #28	0.20 nano #29	0.25 nano #30	0.30 nano #31
Filter loss[ml](7.5min)	5,75	6,25	5,5	6,5
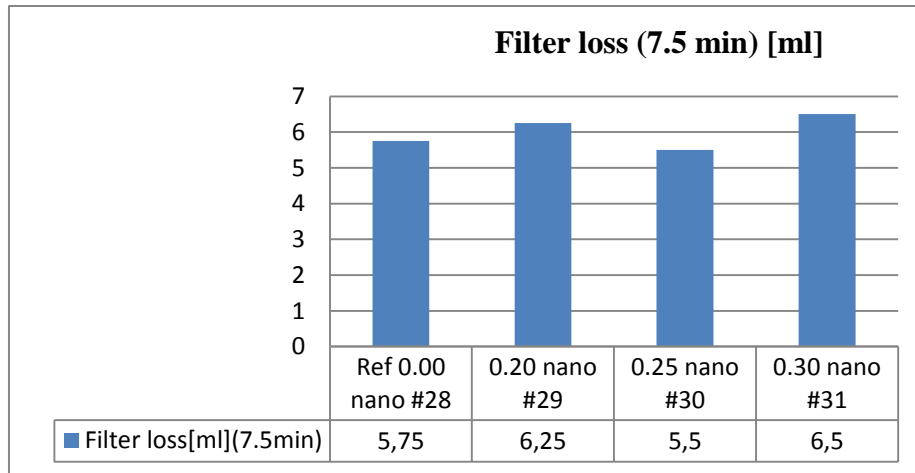
Figure 51 Comparison of Filter loss measurement for CMC+XC+KCl mud system with different Nano concentrations

Rheological Parameters

Higher YS and LSYS

	PV	YS	n	K	LSYS
Ref 0.00 nano #28	5,5	11	0,41	1,24	6,00
0.20 nano #29	5,5	13,5	0,37	1,93	8,00
0.25 nano #30	5,5	20	0,28	4,40	15,50
0.30 nano #31	5	16	0,31	3,08	10,50
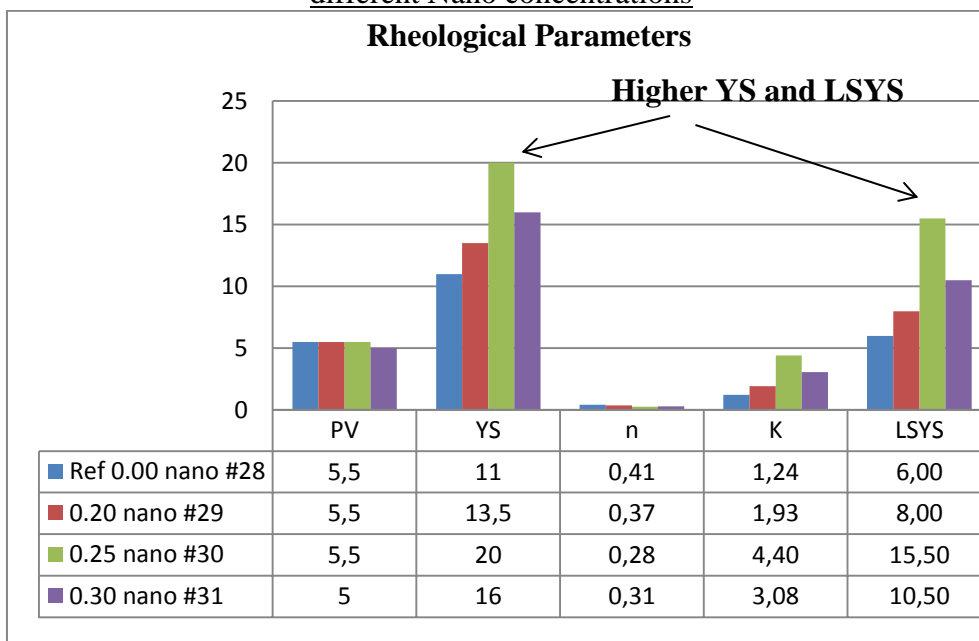
Figure 52 Comparison of rheological parameters for CMC+XC+KCl mud system with different Nano concentrations

PH Value

	Ref 0.00 nano #28	0.20 nano #29	0.25 nano #30	0.30 nano #31
PH Value	9,1	9	8,95	9
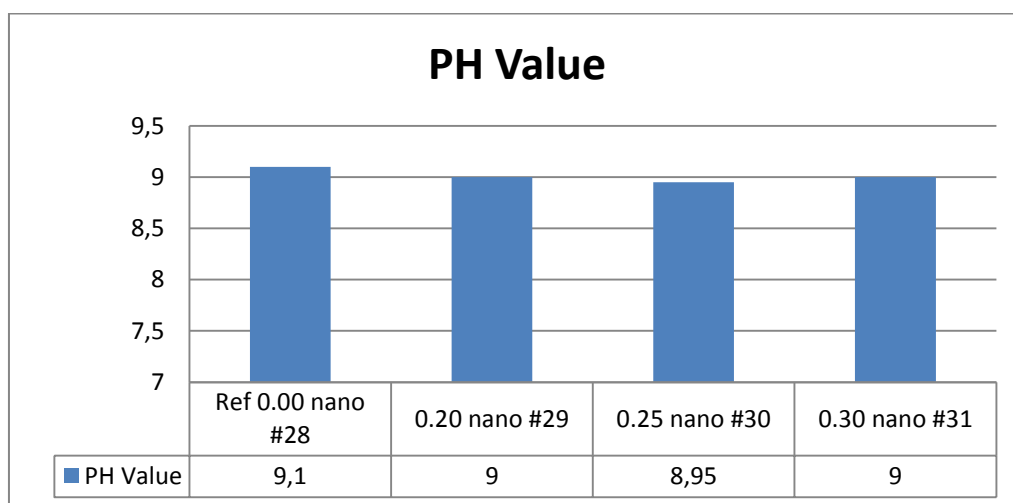
Figure 53 PH value for CMC+XC+KCl drilling fluid system
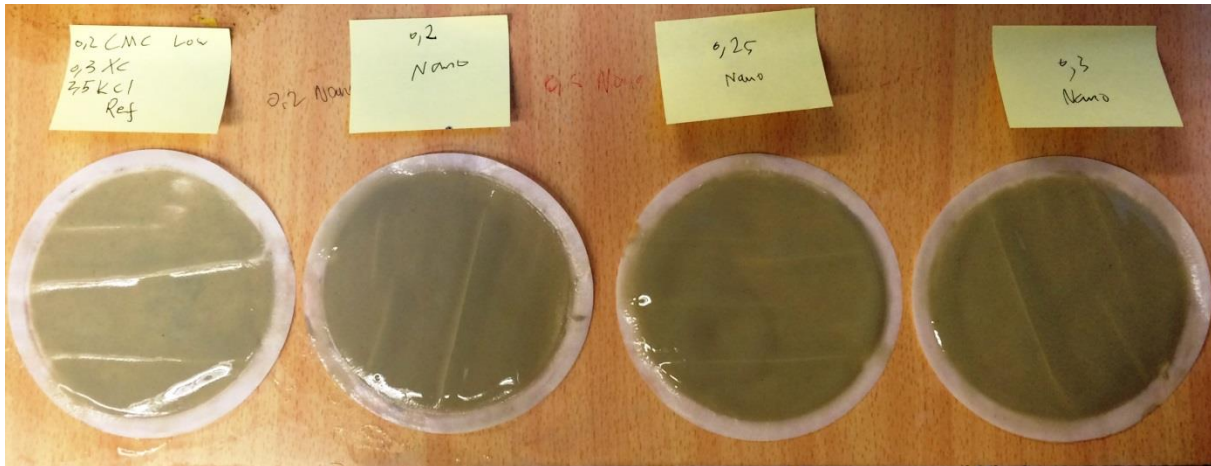
Figure 54 Mud cakes for CMC+XC+KCl drilling fluid systems with different nano concentrations

4.6 Viscoelastic properties of drilling fluids

The reference mud system and the selected Nano-treated mud with 0.25 g Nano system were then subjected to the strain and angular frequency in order to measure the viscoelastic properties of the drilling fluid. The Anton Paar rhoemeter was used to perform the viscoelasticity tests. The main tests which were performed during the lab were the Amplitude Sweep test and the frequency sweep tests. The principal of the test is measure the fluids reaction when it is subjected to deformation.

The question to be raised is that do the viscoelastic tests give any indication of improvement for the Nano-treated drilling fluid?

4.6.1 Amplitude Sweep

In order to perform the amplitude sweep tests were conducted with a constant frequency of 10 rad/s or [s^{-1}] and the amplitude was increasing. Another name of amplitude test is the strain sweep test.

4.6.2 Test result and discussion

The data are plotted and shown in figure 55 and figure 56. As it was expected the value of the storage modulus G´ was higher than the loss modulus G´´, indicating the dominance of the elastic behavior at early stage of the test with lower value of strain is applied to the sample. For the strain values where the storage modulus is linear, the sample is able to act elastically and go back to the first phase. As strain increases the LVE limit is reached where the sample is no longer at the reversible phase. The zone after the LVE is exceeded and G´ is still greater than G´´ is called the yield zone or yield/flow transition range [18].The value of yield point

where the storage modulus behaves linearly and the flow point flow point where G´=G´´ are determined graphically both for the reference system and the Nano-treated system. Measured data are presented in appendix E. The interesting part of data regarding to τ_f determination are available at the table 17 and table 18.

Table 16 Amplitude Sweep test data for τ_f determination for the reference system

Measure Point	G'' [Pa]	γ(%)	τ [Pa]	G' [Pa]	G'-G'' [Pa]
36	9,83	51,71	**7,49**	10,63	0,80
37	8,26	71,91	**8,07**	7,59	-0,67

Table 17 Amplitude Sweep test data for τ_f determination for the Nano-treated system

Measure Point	G'' [Pa]	γ(%)	τ [Pa]	G' [Pa]	G'-G'' [Pa]
36	12,42	56,9	**11,15**	15,15	-2,73
37	10,42	79,34	**11,36**	9,82	0,60

The value of LVE limit (τ_y) was graphically determined and shown in the figure 57. It is important to mention that the LVE range is exceeded at the point where one of the functions G´ or G´´ leaves the plateau value .In both cases is the storage modulus G´ which leaves the pleateau.

The modified drilling fluid containing Nano silica has a more elastically behavior by having a higher τ_y. It can be explained by a higher value of shear stress which they can be subjected to by the drill cuttings before the fluid yields and lets the cutting to deposit. Yield point τ_y was 0.55 [Pa] for the reference system and approximately 1.33 [Pa] for the Nano-treated system. By this we mean an improvement in the suspension property of the Nano-treated system. It's of interest to compare the value of Yield stress obtained from the Bingham plastic.

The value of the flow point (τ_f) where the phase angle is 45° and G´=G´´ is determined by reading the shear stress equivalent for that values. The τ_f value appears to be around 7.8 [Pa] for the reference system. The treatment of the reference system by 0.25 g Nano silica increased the yield shear stress up to 11.2 [Pa]. At higher shear stress than the flow point shows the liquid like characteristic.

The amplitude sweep curve show an increasing in the loss modulus G´´ before it decreases. The peak occurs even after the LVE rang is exceeded .The increasing of G´´ right before the flow point can be explained by assuming a network structure built in the sample at rest. The

structures do not collapse by increasing the shear strain at first stage when the shear strain increases. Another reason might be first the forming of micro cracks and then growing of cracks into the macro cracks which at the end (at peak) collapses right before the crossover point $(G´=G´´)$[18].
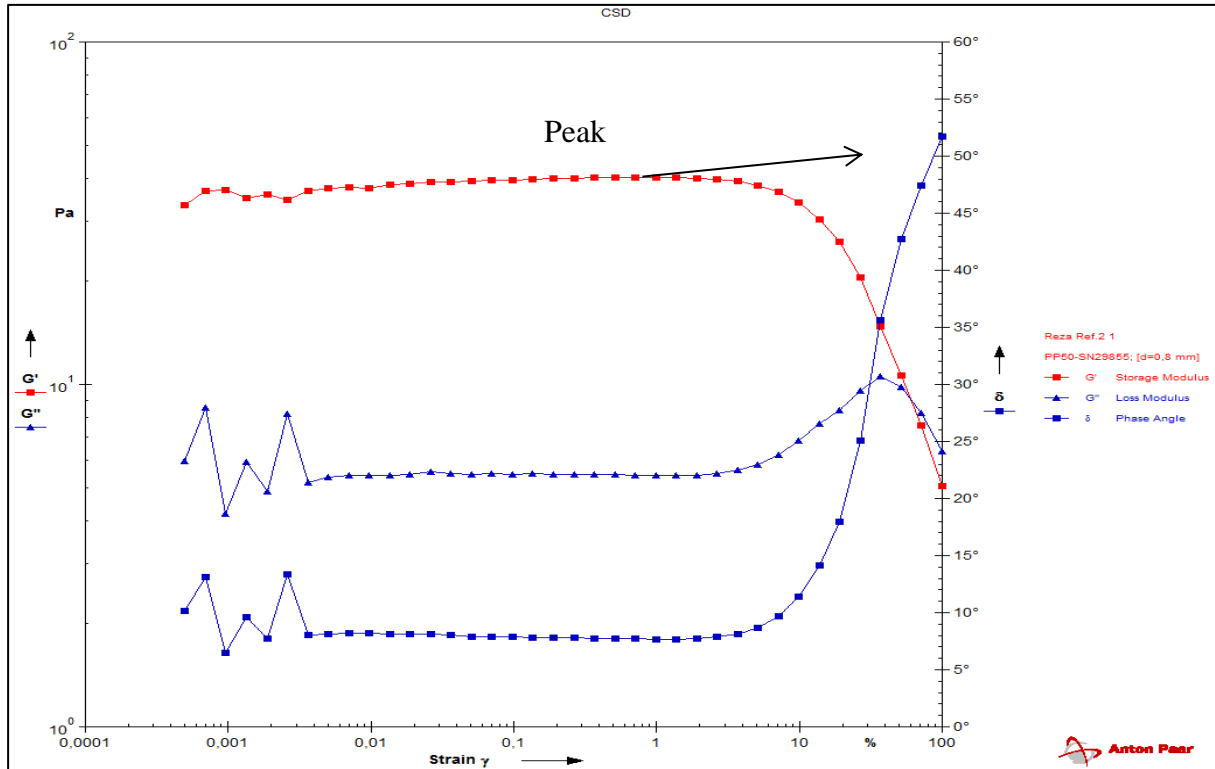
Figure 55 Amplitude Sweep test curve for the reference system
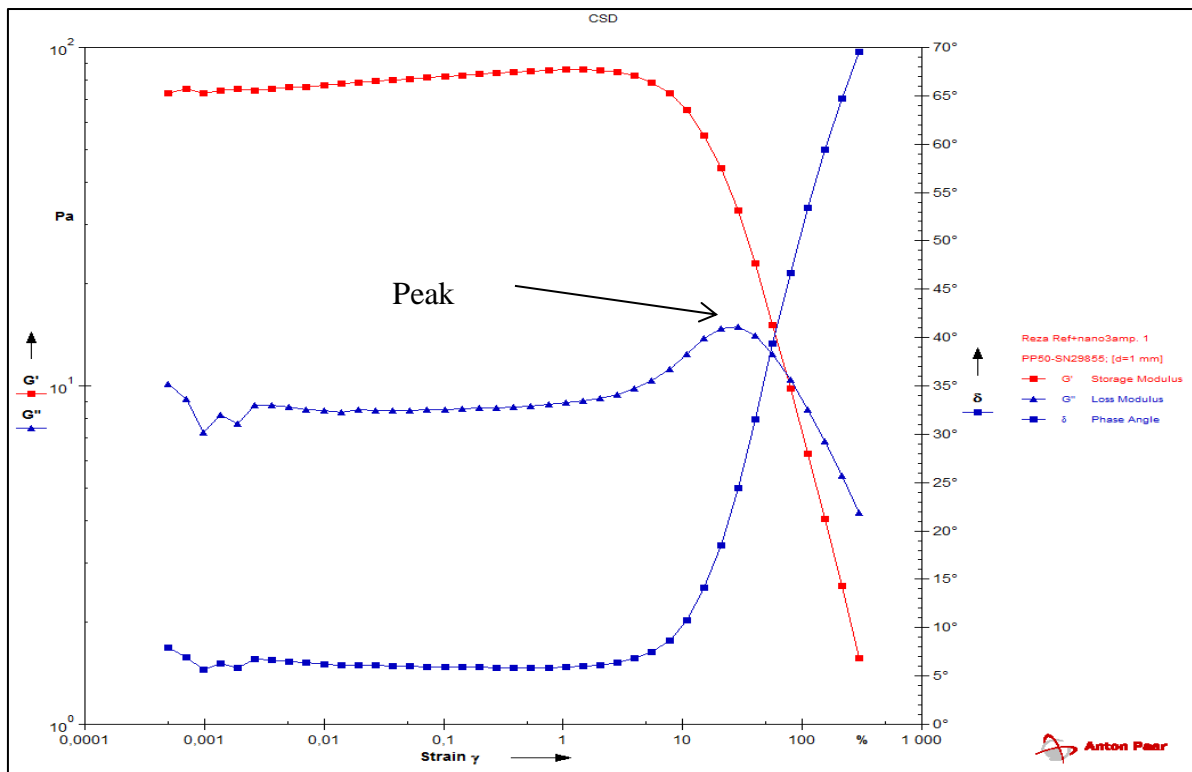
Figure 56 Amplitude Sweep test curve for the Nano-treated system
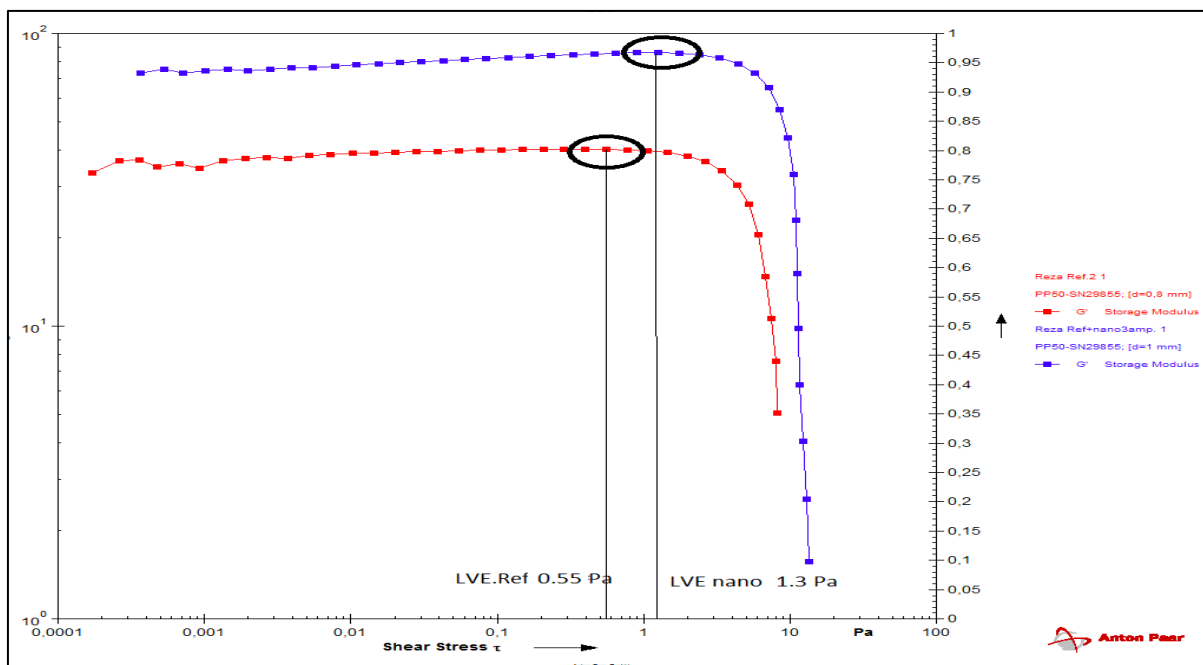
Figure 57 LVE range and yield point (τ_y) determination for the reference and Nano-treated systems
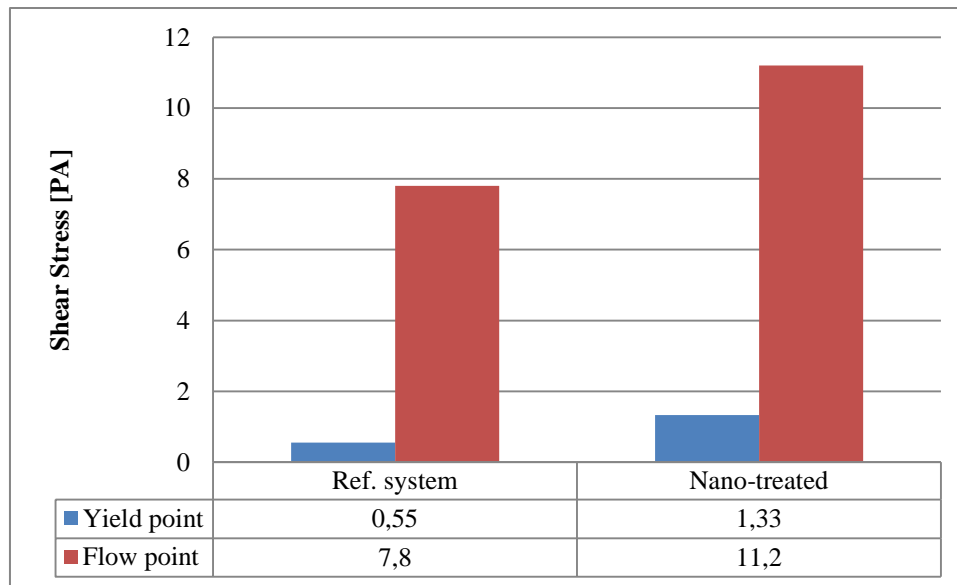
Figure 58 Comparison of Yield point (τ_y) and Flow point (τ_f) for reference and Nano-treated systems

4.6.3 Frequency sweep test

In this section were going to investigate the viscoelastic properties of the reference system and the Nano-treated system by performing the frequency sweep test. The test is to investigate the timed dependence deformation of the samples. In order to perform the test angular frequency was varying during the test while keeping the amplitude constant and measurement was performed by the Rheometer. The result of the amplitude sweep test recommended a strain of 0.1 % for the reference system and 0.05 % for the Nano treated system. The range used for the angular frequency was downward and from 100 to 0.01 s^{-1}. The storage modulus G´, loss modulus G´´ and the complex viscosity was measured and plotted against the frequency as show in the figure 59.

4.6.4 Test result and discussion

For the frequency range of the samples G´ is greater than the G´´ indicating a stable gel-like structure. The plot of both sample show the elastic behavior which as favorable for cutting suspension ability of the drilling fluid[24]. Due to the limited range of frequency during the test the crossing point between G´ and G´´ was not obtained. However there is no evidence confirming that any crossing point exists at lower frequency. In that case the fluid will act different against fast and slow deformation. The point where G´ falls below the G´´ is where the liquid-like behavior dominates for the sample [18]. The main different observed is the values of storage modulus G´ and loss modulus G´´ have increased after adding Nano-Silica compared to the reference drilling fluid. The rising value is higher for Storage modulus

as it is shown is in figure 59. The complex viscosity is also decreasing at extremely low frequencies.
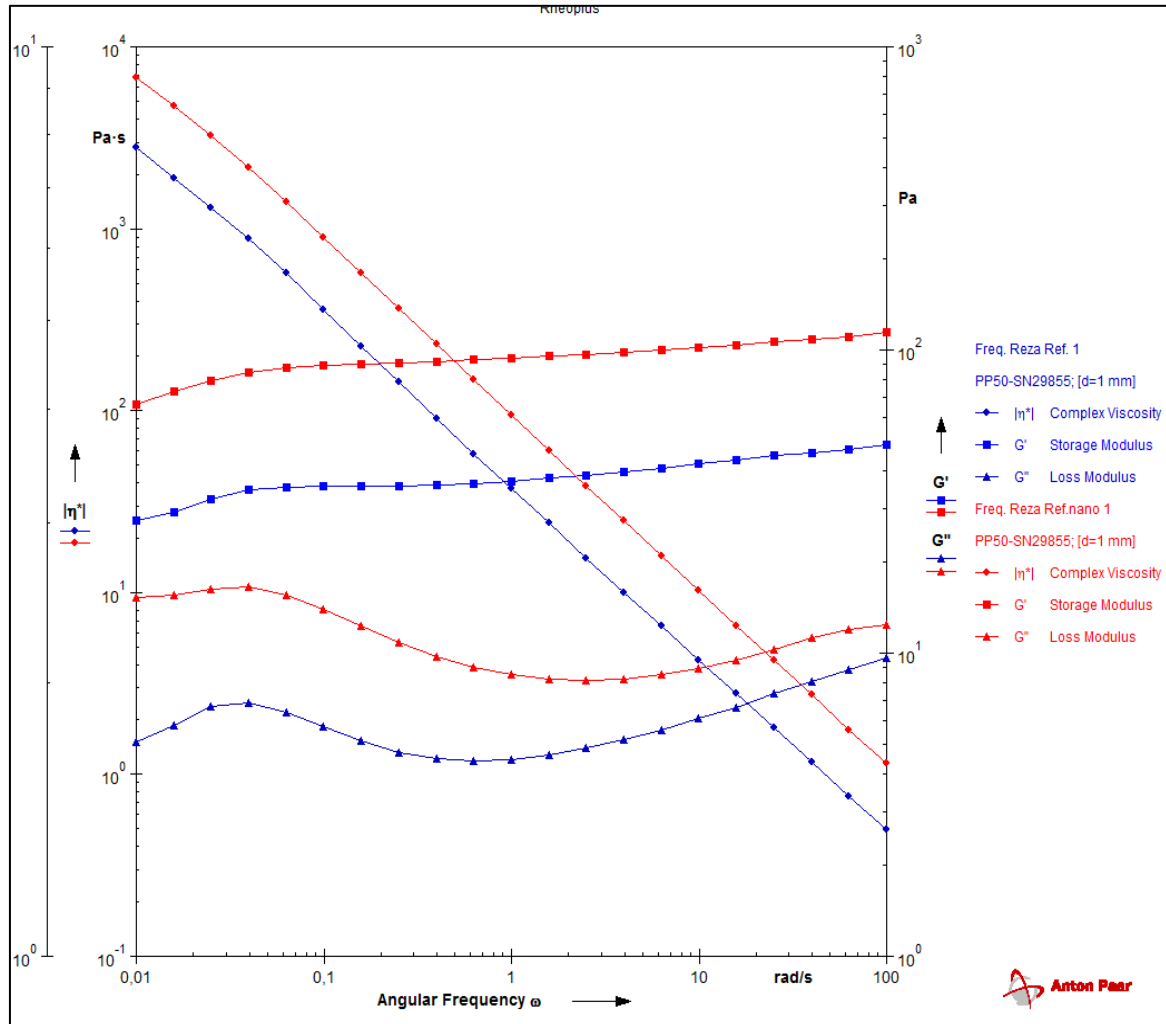
Figure 59 Comparison of frequency sweep test curve for the reference system and Nano Treated system

4.7 Nano-treated WBM flow through porous media

In this section the filtrate invasion of a sand package as a porous media is investigated. The main objective of this part of experiment is to compare the rate of invasion for the reference system and Nano-treated system through a practical experiment.

4.7.1 Experiment setup

For this experiment a transparent pipe was filled with sand until a certain point. A column of the drilling fluid was placed on top of the sand and the depth of the invaded zone was measured once after 30 min. and once after 60 min. The porosity of the sand packages was same both for reference system and for Nano-treated system. Due to equal densities the column height of the mud had same height in order to provide an equal bottom hole pressure at the top of the sand package.

4.7.2 Test result and discussion

Comparison of the rate of invasion exhibits a much more effective drilling fluid system. The observed lower spurt mud was lower for the Nano-treated system compared to the reference system. The rate of filtrate invasion for the Nano-treated system and reference system are presented in table19.

Table 18 Depth of invasion for Reference system and Nano-treated system

Δt	Reference system	Nano treated system
30 min.	2.8 cm	1.5 cm
60 min.	3.4 cm	1.8 cm

According to the Darcy's law for filter loss a lower filtrate rate is a result of higher viscosity of the drilling fluid and less permeable filter cake where the particles easily block the pores at early stage [29]

Filtrate invasion of the sand package by reference system after 30 min(left) and 6 (right)	Filtrate invasion of the sand package for the Nano-treated system after 30 min(left) and 6 (right)
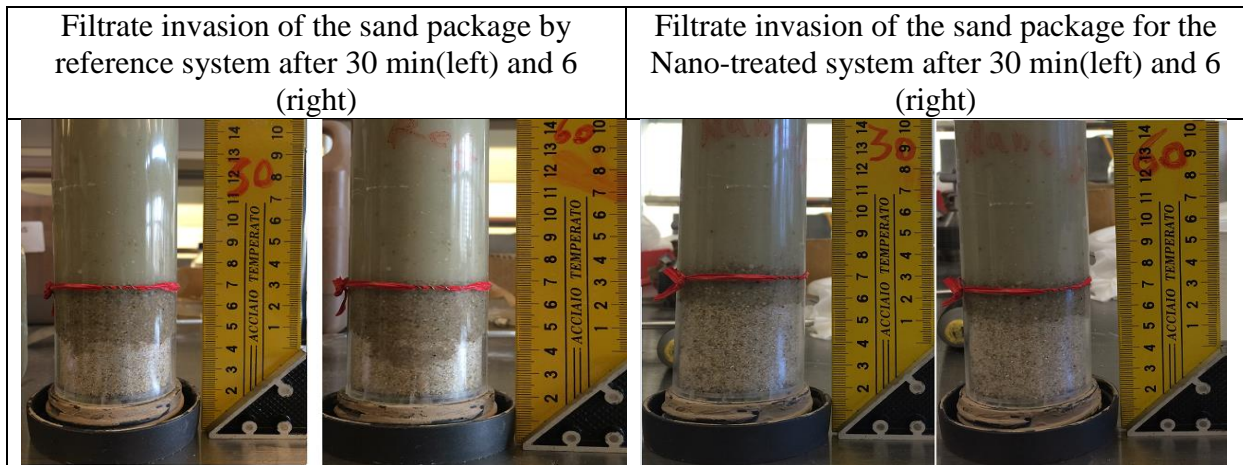
Figure 60 Illustration of the filtrate invasion of sand package by reference system (left) and Nano treated system (right)

5 Drilling fluid performance simulation study

5.1 Cuttings transport simulation

The drill cutting removal has been investigated for decades in order to deal with the hole cleaning problems. The cuttings which are drilled out from the deep formation of the well are normally the most challenging one to transport. The inclination of the well makes it even more challenging in order to clean out the wellbore and mitigate occurrence of stuck pipe situation. [37]

It is also proven the inefficient removal of small sized cutting are the main reason behind the excessive torque and drag. The process of cuttings transport is influenced by many factors such as forces which are acting on the cuttings. These forces determine the mechanism of cuttings to become transported, deposited or suspended. The hydrodynamic forces, static forces and colloidal forces are those which act on cuttings in the annulus. Annulus is the most critical section of the well due to limitation of pumping capacity and high pressure drops through the drill pipe and the drill bit.

The characterization of the drilling fluids is directly related to their ability for cleaning the wellbore. However the properties of the cutting and operational parameters are also factors which in addition of the drilling fluid properties play a key role to ensure a perfectly cuttings free wellbore. The cleaning process is explained by defining two definitions. The critical suspension velocity (CRV) is the minimum flow velocity for initiation of bed erosion and the critical deposition velocity (CDV) which is the minimum flow velocity to prevent bed formation. CRV and CDV are function of the necessary flow rate to clean the wellbore[37].

In this section we are going to investigate the cutting transport characterization of reference system and Nano-treated drilling fluids by holding the operational parameters and cutting size density constant. The cutting transport simulation is performed in a real well geometry having vertical section, bend and inclined section.

5.1.1 Simulation setup

The well depth was designed to be 11003 ft and the size of casing and the open borehole are 12,615 "and 12,250 "respectively. The drill pipe outer diameter (OD) is 5" and the bottom hole assembly (BHA) are also included into the design parameters. The detailed data regarding to the size of drill pipe, BHA and casing are presented in the appendix F. The

simulation was performed by using the Well-Plan Software. The well schematic designed for simulation is shown at the figure 62. Operation parameters are presented in table 20.

Table 19 Operation parameters for the cuttings transport simulation

Cuttings diameter [in]	Cuttings density [sg]	Bed porosity [%]	ROP [ft/hr]	Rotary speed [rpm]	Bit diameter [in]	Annulus diameter [in]	Joint diameter [in]	Minimum/maximum pump rate [GPM]	Increment pump rate [GPM]
0.120 in	2.500	36.00	62.5	100	8.50	8.50	5.50	100/1000	200

13 3/8 in. casing 55.5 ppf J-55

4012,5 ft.

12,250 in. OH

6990,50 ft.

Figure 61 Schematic diagram of the designed well for cuttings transport simulation

5.1.2 Drilling fluids

The density of the drilling fluids was 1.02sg and the rheology data are given in table 21. The reference mud system was formulated by mixing the 0.2gm low viscous CMC and 0.3gm XC in 25g Bentonite/500gm H2O with 2.5kcl. The test matrix is presented in table 20.

Table 20 Test matrix for the mud systems used for cuttings transport simulation

Mud system	Bentonite	H$_2$O	LV CMC	Xanthan	KCl	Nano silica
Ref #1	25 g	500 ml	0.2 g	0.3 g	2.5 g	0.0
#2	25 g	500 ml	0.2 g	0.3 g	2.5 g	0.2
#3	25 g	500 ml	0.2 g	0.3 g	2.5 g	0.25
#4	25 g	500 ml	0.2 g	0.3 g	2.5 g	0.3

The rheological data in table 21 were used in order to perform the simulation for the cutting transport. The objective is to compare the system and determine whether the Nano treated drilling fluid provide better hole cleaning than the reference system or not.

Table 21 Rheological data for the mud systems used for cuttings transport simulation

RPM	Ref #1	0.2 Nano #2	0.25 Nano #3	0.3 Nano #4
600	22	24,5	31	26
300	16,5	19	25,5	21
200	14	17	23,1	19
100	11	14	20,5	15,8
6	8	10	16,5	11,5
3	7	9	16	11

5.1.3 Simulation result and discussion

The Cutting transport simulation was performed through the height of the cutting bed given a certain rate of penetration (ROP) and pump pressure. The removal of the drill cutting is critical at inclined section and the designed well has an inclination of almost 40 ^{o} at its highest.

5.1.3.1 Bed height

The cutting deposited in the figure 63 show the sensitivity of the cutting bed creation regarding to the well inclination. The vertical section which is cased and cemented the no cutting bed is observed neither for the reference system or the Nano-treated system. The increment of the well inclination results a higher cutting deposit for the reference system where the bed height is around 5 in. at its highest. Comparison of the 0.3 and 0.2 Nano systems indicates that any modification of the drilling fluid system will only delay the bed deposition by 150 ft and prevention of cutting bed is not an alternative. However the system which had the best performance with no deposition of cutting down to 10500 ft. MD was the 0.25 Nano-treated systems. The most critical part is the section with 38 ^{o} degrees where 1 inch of cuttings bed deposition is expected.

For this simulation, we used a pump rate of 500GPM in order to compare the performance of the drilling fluid. Figure 47 shows the minimum flow rate required to completely transport cutting out of the well. The selected fluid with 0.25 g Nano silica provides the completely clean well with the minimum flow rate of 537 GPM. This is significantly lower than the flow rate required using three other mud systems. The reduction is 41% compared to the reference

MSc Thesis, 2015

system which will require a lower pumping capacity. One can notice that all the Nano-treated system have higher performance than the reference system.
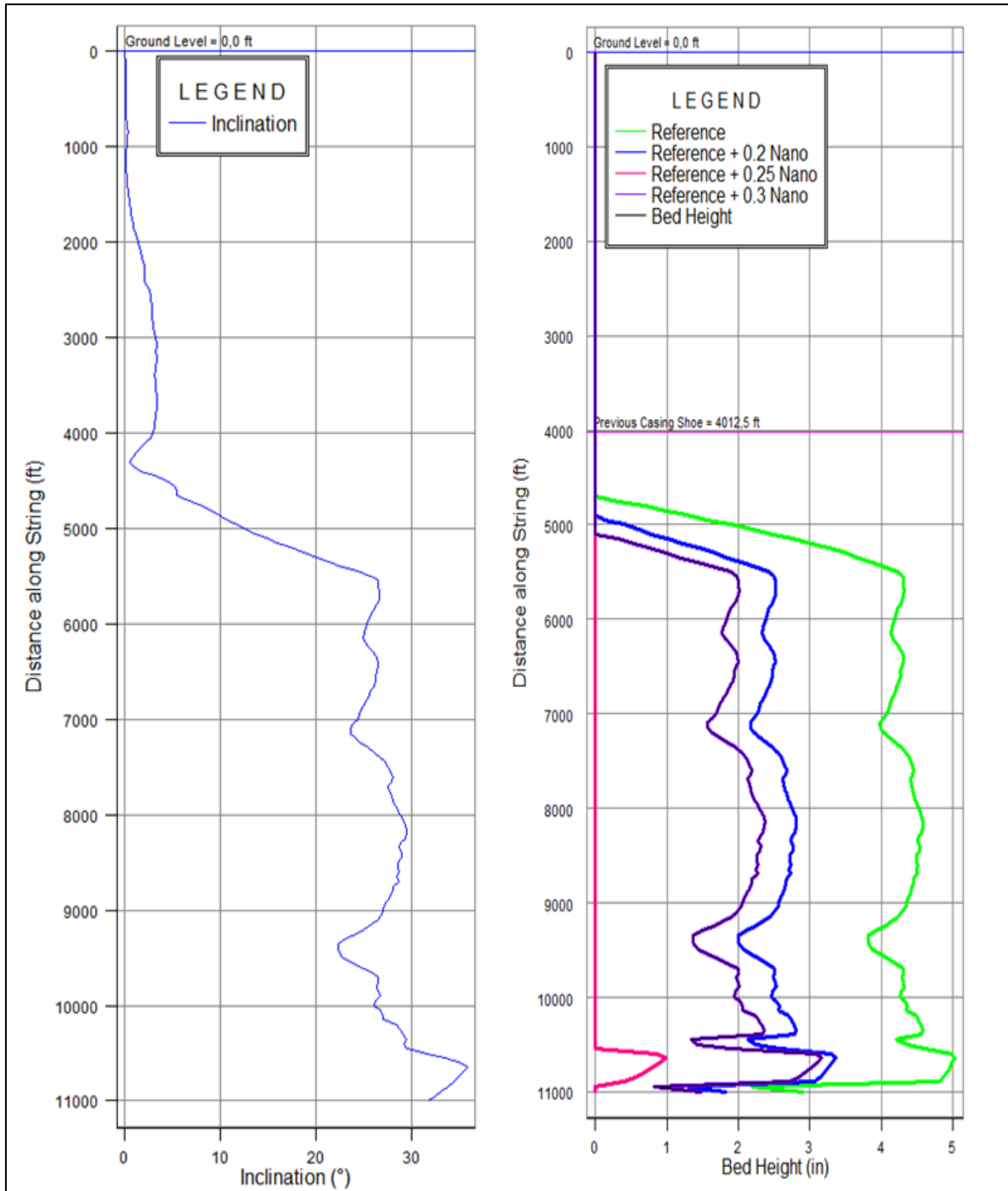
Figure 62 Well inclination and bed height for simulated drilling fluids
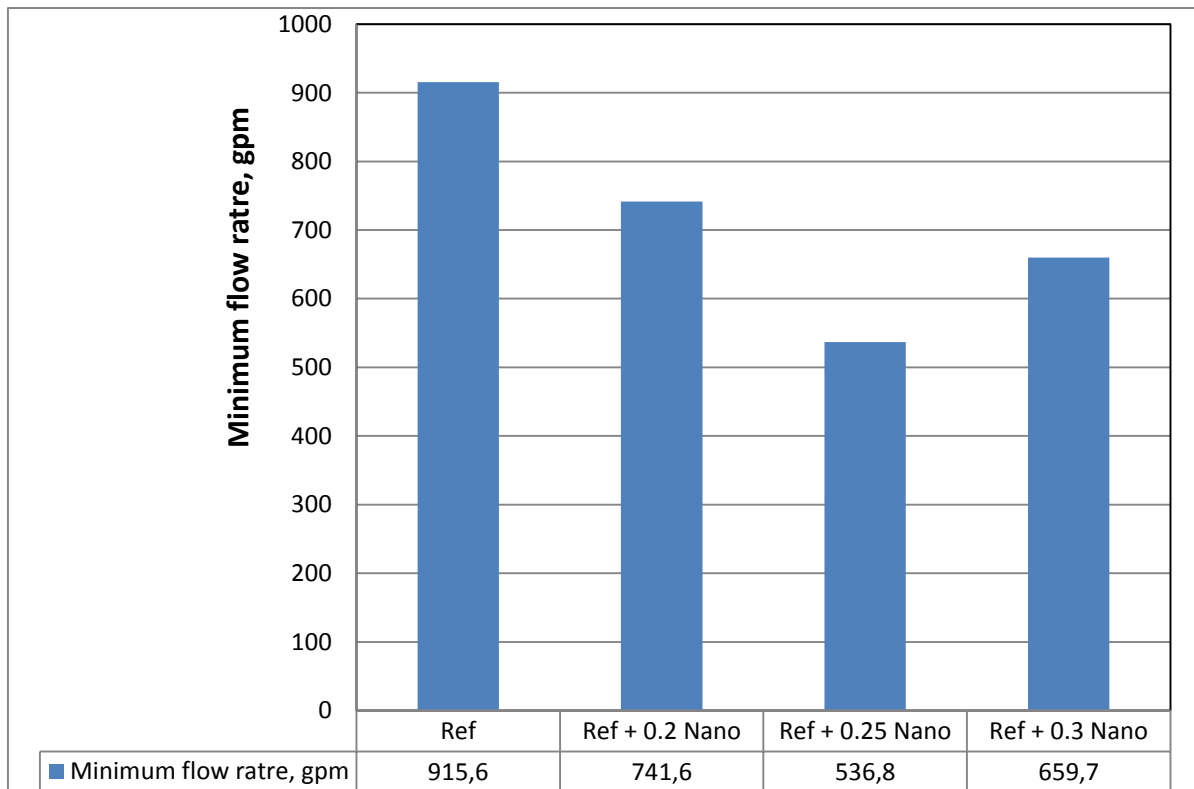
Figure 63 Comparison of minimum flow rate to transport all cuttings for simulated drilling fluids

5.1.4 Minimum flow rate

Another comparison of the minimum flow rate was performed based on the different well inclination. The simulation result is presented at figure 65. As it can be observed the most challenging inclination for the samples containing Nano silica are the horizontal section where the inclination exceeds the 85°. However the reference system demands only a flow rate of 560 gmp to ensure cutting transport for section with inclination higher than 50°. According to Torbjørnsen et al. (1994) the inclination between 40°-60° is the most difficult section in order to transport the cuttings. The reference system is

The operational parameters are presented in table 22.

Table 22 Operation parameters for the cuttings transport simulation

Cuttings diameter [in]	Cuttings density [sg]	Bed porosity [%]	ROP [ft/hr]	Rotary speed [rpm]	Bit diameter [in]	Annulus diameter [in]	Joint diameter [in]	Minimum/maximum pump rate [gpm]	Increment pump rate [gpm]
0.120 in	2.500	36.00	62.5	100	8.50	8.50	5.50	100/1000	200

Figure 64 Comparison of minimum flow rate necessary to transport all cutting in different hole angles for simulated mud systems

5.2 Hydraulics simulation study

The measurement data of the selected drilling fluid which is used for hydraulic simulation are presented in table 23. In this section we are going to simulate and compare the contribution of the drilling fluid parameters in pressure drops such as pump pressure drop and annular pressure drop. ECD which is a function of annular pressure drop is important in order to ensure well stability. The main reason of ECD calculation is to determine the contribution of the annular pressure drop in the bottom-hole pressure. There are many hydraulic models used in the industry and for the calculation of the pressure drops and in this section the unified model calculator was used due to its lower error rate. Rheological data of the selected drilling fluid are presented in table 23.

Table 23 Fann Viscosimeter measurements for the selected mud systems

RPM	REF	REF+ 0,2 Nano	REF+ 0,25 Nano	REF+ 0,3 Nano
θ600	22	24,5	31	26
θ300	16,5	19	25,5	21
θ200	14	17	23,1	19
θ100	11	14	20,5	15,8
θ6	8	10	16,5	11,5
θ3	7	9	16	11

5.2.1 Simulation setup

In order to simulate and compare the hydraulic parameters there was designed a vertical well with a depth of 12000 ft. where the last casing show is set at 8600 ft. the outer and inner diameter of the drill pipe is respectively 5´´ and 4, 8´´. The drill bit is assumed to have three nozzles of the size 28/32". The operating parameters are available in table 22. The surface pressure is assumed to be zero. The well schematic is shown in figure 66. The simulation and pressure drop calculation is done step wise by increasing the flow rate with 50 GPM at the time up to 600 GPM. The assumptions prior to simulation are an equal mud density for all samples and a concentric drill pipe.

Table 24 Operation parameters for hydraulic simulation

Well diamter	Drill pipe OD	Drill pipe ID	Well Length, ft	Bit diameter	Nozzle diameter
8,5´´	5´´	4,8´´	12000	8,5´´	28/32´´
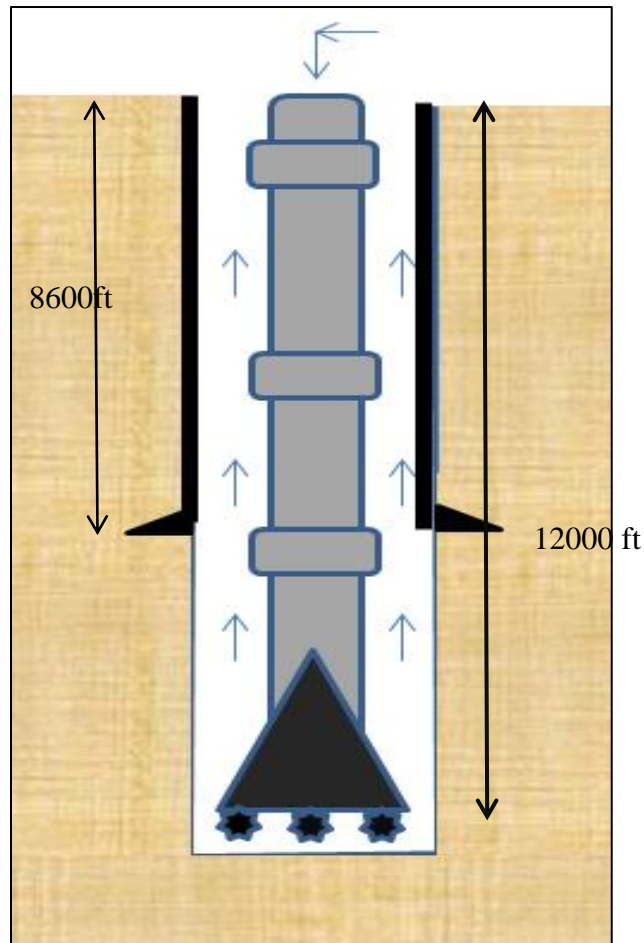
Figure 65 Schematic diagram of the designed well for the hydraulic simulation

5.2.2 Simulation result and discussion

The total pressure drop and annular friction pressure were simulated for all four samples and are shown in the figure 66 and 67. The ECD values were also calculated and plotted in order to visualize the impact of gel strength Comparison of the total pressure drop indicates the highest pressure drop for the selected drilling fluid with 0.25 g of Nano silica. The total pressure drop increases faster for other drilling fluids than the 0.25 g Nano system in a range between 300 and 600 GPM. At this flow rate the difference in pressure drop is at its lowest. However the annular pressure drop increases by same rate for all samples and a higher ECD is expected for the selected mud system. The ECD is plotted against flow rate for all 4 drilling fluids in figure 68.
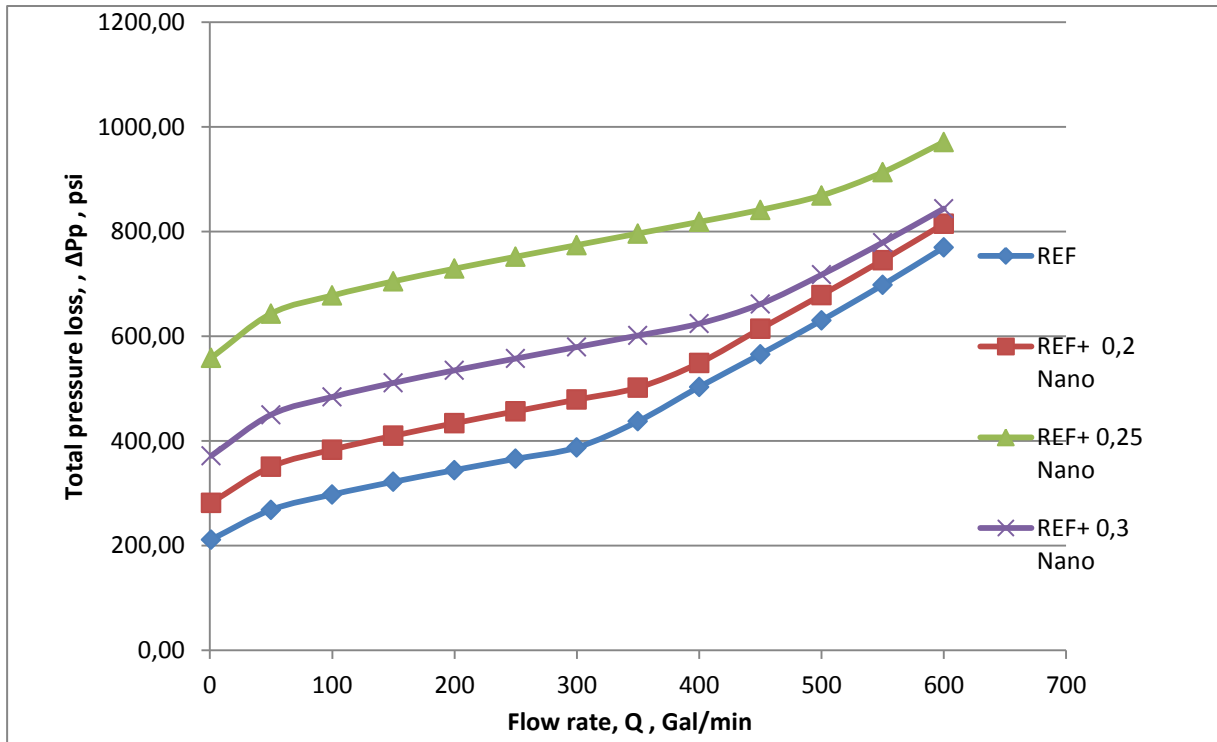
Figure 66 Comparison of total pressure loss at different flow rate for simulated drilling fluid systems
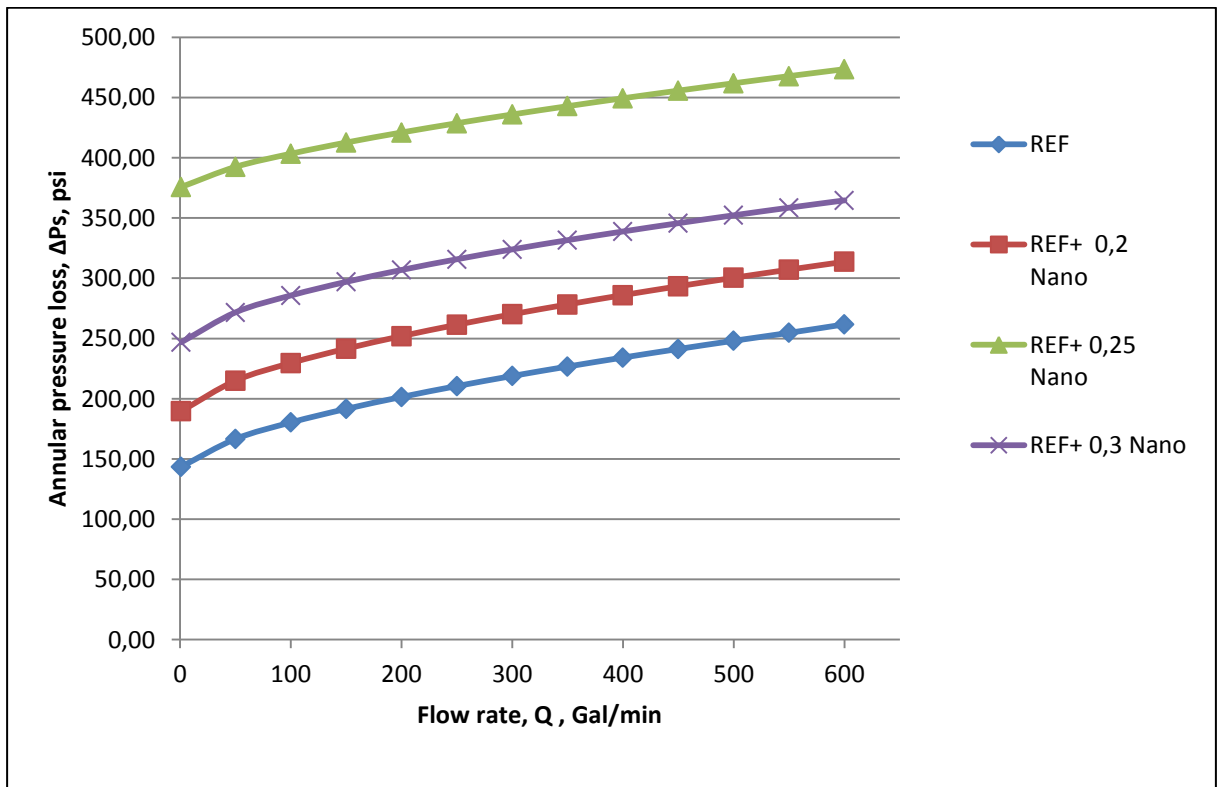
Figure 67 Comparison of annular pressure loss at different flow rate for simulated drilling fluid systems
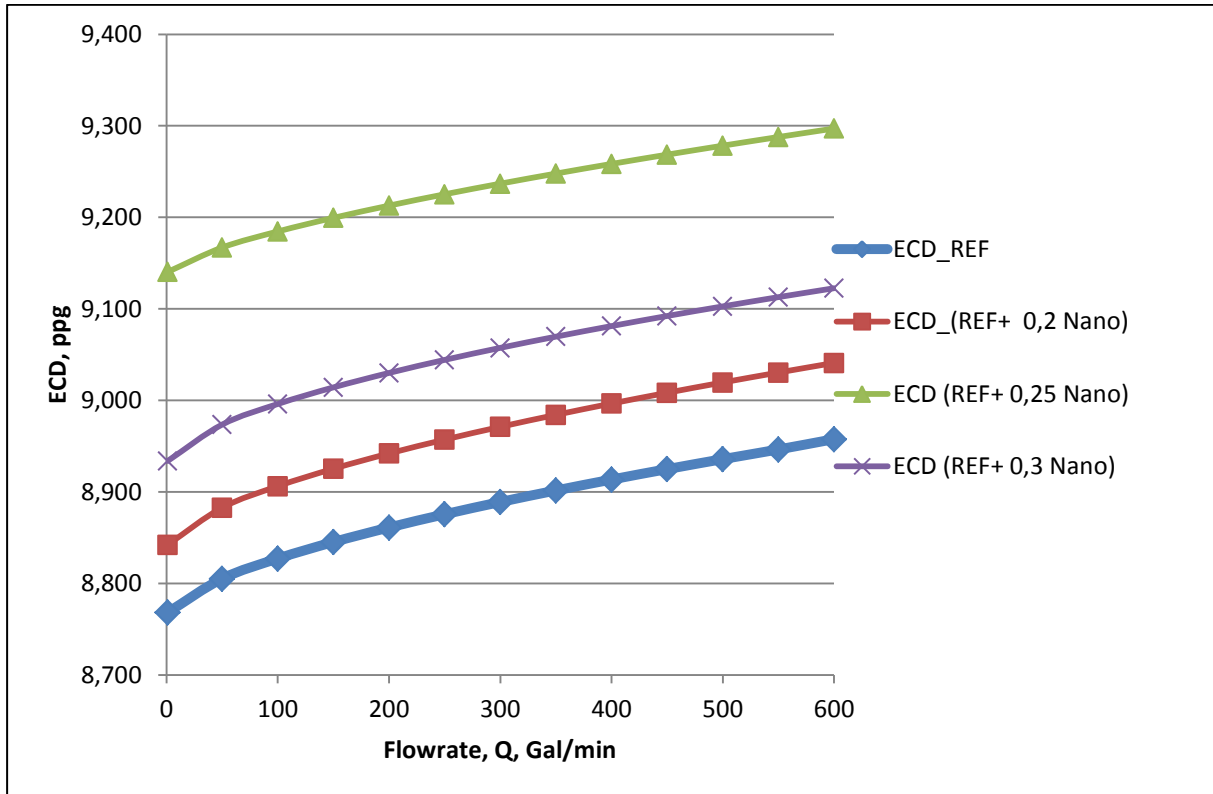
Figure 68 Comparison for ECD values at different flow rate for the simulated drilling fluid systems

6 Summary and Discussion

This chapter presents the summary and discussion for the experimental (chapter 4) and simulation part (chapter 5).The experiment part consists of rheological characterization, viscoelastic test and analysis and the flow through porous media analysis. The simulation part consist of the observation done regarding to the cutting transport, minimum flow rate and hydraulic properties which affects the ECD of the drilling fluid at different flow rate.

6.1 Effect of temperature on WBMs

The measured data at 72, 110 and 130 of indicates the high rate of error for measured showing a wavy trend for the shear rate- shear stress curve. The only sample which was must effected was the reference system (#1). It is a conservative assumption to claim that temperature does not affect the rheological behavior but wrong measured value was not able to show any specific trend. The temperature of the heater cup was not stable showing higher or lower temperature right after each measurement. Due to lack of accurate equipment the effect of temperature was not attempted for other mud system.

6.2 Effect of polymer concentration

The measured data obtained from the Fann viscometer indicate significant changes in shear stress as a result of increasing PAC concentration. In presence of the KCl, the PAC polymer had thinning effect on the mud system by decreasing the shear stress values as the concentration increased up to 0.5 g. Since the concentration of the salt was kept constant and polymer did not contributed to viscosity of the system the reduction of viscosity might be caused by a negative change in the clay platelets arrangement resulting a thinner mud system. The reduction of the YS and Gel strength indicates that the clay platelets have gone from dispersed-flocculated to aggregated-deflocculated arrangement. However the reduction in the filter loss as PAC concentration increased that PAC still acts as a filter loss controller but less effective due to deflocculated clay platelets. The concentration of the polymer was decided to maintain 0.5 g in order to reduce the filter loss as much as possible.

6.3 Effect of salt type and concentrations

The shear stress values were decreased as the salt concentration increased. Due to lower salt tolerance of the CMC polymer the $CaCl_2$ resulted to failure of the system. NaCl had less thinning effect than KCl. For the KCl both K^+ and Cl^- lead to less viscous system as both are taking part in reaction. For the NaCl only Cl^- takes part in the reaction which at the end

leads to less hydrated clay platelets. Due to shale swelling effect it was decided to use KCl as inhibitive agent by total amount of 2.5 g.

6.4 Effect of Nano silica concentration in combined polymer and combined salt

The concentration of the Nano silica was raised by 0.15 g at the time for each sample .The PAC polymer once with 2.5 g NaCl and once with 2.5 g KCl led to less favorable systems than reference system. A combination of KCl and NaCl gave almost the same effect with the PAC polymer. A combination of PAC and Xanthan XC was then used in the system with single and combined salts as follow:

- 0.4 g PAC+0.1 g Xanthan+2.5 g NaCl
- 0.3 g PAC+0.2 g Xantan+1.25 g KCl+1.25 g NaCl
- 0.3 g PAC+0.2 g Xanthan+ 2.5 g KCl

Following results were observed:

- PAC+ Nano Silica gave poor measurements as Nano silica concentration increased
- Combined salts gave higher Shear stress values than and single salt but poor values regarding to reference system.
- The more the Xanthan, the less thinning effect caused by Nano silica. XC is compatible with Nano and PAC is not.
- The increasing concentration of Nano silica from 0 to 0.45 is too high for this amount of polymer and bentonite.

By poor measurements we mean reducing the YS, LSYS values and an increase in filter loss. By keeping the salt and polymer concentration equal to 2.5 g and 0.5 g respectively, a new test matrix was prepared this time with LV CMC and Xanthan XC as polymers and KCl as salt. The following result was noticed for the 0.25 g Nano silica:

- Less filter loss
- Higher YS and LSYS
- Higher Gel strength
- Unchanged PH value close to 9.00

The shear stress value increased for 0.2 and 2.5 g Nano silica and then decreased again for the 0.3 g Nano indicating the sensitivity of the system for small amount of Nano Silica.

6.5 Flow through porous media

The porous media (sand package) filtrate invasion was different for reference and Nano treated system. The application of 0.25 g Nano silica has reduced the invasion by 47 % regarding to Nano-free system. Observation indicated a higher spurt loss in absence of Nano silica (Reference system)

6.6 Viscoelastic properties and comparison of reference and Nano-treated systems

The viscoelastic properties of drilling fluid are important to characterize the behavior of drilling fluid at different shear stress. It lets us evaluate the gel strength and YS of the drilling fluid. In this thesis the amplitude sweep and frequency sweep were carried out. A Comparison of the selected mud system with the reference system showed a clear improvement in YS and flow point after application of Nano-silica. The frequency sweep of the reference system and Nano treated system indicates the different values of storage and loss modulus. Both samples showed similar behavior with storage modulus always above the loss modulus. The decreasing slope of the complex viscosity indicates that at extremely low frequency one can expect a liquid like phase.

6.7 Effect of Nano silica on cutting transport performance

Drilling fluid rheology properties and density in addition to cutting density are essential in order to ensure cutting transport from the wellbore. Other factors such as ROP, RPM and the flow rate are easier to adjust and were kept constant during the simulation. The reference drilling fluid and other Nano containing fluid (including the selected mud system) were simulated and compared to investigate the one which gives the lowest bed height. The selected drilling fluid with 0.25 g Nano had the best performance by only a bed of 1 inch at the most inclined section (38°). It also needed the lowest flow rate among the systems to perform cuttings removal. As it was expected the selected mud system with highest YS and LSYS had the best performance.

6.8 Effect of Nano Silica on hydraulic properties

ECD management, cutting transport and pump pressure optimization are the areas where the hydraulic properties of drilling fluid play a key role. In this thesis we simulated and

compared the reference system prepared by CMC and Xanthan polymer without Nano silica with those which contained 2.0 g, 2.5 g and 3.0 g Nano silica respectively. The unified hydraulic model was used to perform the simulation. The Pump pressure, annular pressure drops and ECD was calculated for a range of flow rate from 1 GPM to 600 GPM.

The selected drilling fluid with 0.25 g Nano silica has the highest value of ECD and annular pressure drop. However the difference in total pressure drop decreases at higher flow rate close to 600 GPM. By subtracting the annular pressure drop form total pressure drop an optimization point close to 600 GPM is obtained. Based on result obtained from simulation the system with 0.25 Nano silica causes the highest pressure drop which must be taken into account.

7 Conclusion

The effect of Nano silica, polymer and salt with different concentrations on bentonite fluid system were investigated. By extensive laboratory testing the appropriate concentration of mentioned additives were determined after each rheological experiment. A final Nano-treated drilling fluid was then formulated containing the compatible type of polymer and right concentration of salt Nano silica. Rheological properties including viscoelastic characterization of the Nano-treated systems and reference system was then performed and compared.

Application of WellPlan^{TM} Simulator and Unified hydraulic model were then carried out to evaluate the performance of Nano-treated systems and the Nano free reference system in term cuttings bed height, minimum flow rate, total pressure drop and ECD. Based on the result obtained from the experimental and simulation, these thesis summaries:

- For considered temperatures (72 ^{o}F, 110 ^{o}F &130 ^{o}F), the temperature's effect is not significant in presence of PAC, Nano Silica and salt.
- Nano silica and salt shows thinning effect in presence of PAC in Bentonite mud system.
- From the overall thesis work, the best system was obtained from 0.3 g XC and 0.2 g LV-CMC polymer show compatibility with 0.25 g Nano Silica in presence of 2.5 g KCl by improving YS and LSYS values and reducing filter loss compared to reference system.
- Bentonite drilling fluid shows elastic dominating behavior which in addition of Nano silica shows an improvement in term of higher Yield Point and hence provides better cutting suspension
- The Nano treated mud system provides better cuttings removal. It also requires lower flow rate to ensure cuttings free wellbore
- The Unified hydraulic model indicated a higher annular pressure for the Nano system which means a higher ECD, compared to the reference system.

Future work

For future work this thesis proposes the investigating the effect of Nano silica in real drilling fluid.

References

[1] Aadnøy, B.S. 2010. Modern Well Design, Second edition. Chapter2.

[2] Gorge R. Gray, Composition and Properties of Drilling and Completion Fluid.

[3]. Kendall, H.A. and Goins, W.C. Jr.: "Design and Operation of Jet-Bit Programs for maximum Hydraulic Horsepower, Impact Force or Jet Velocity," SPE (Oct. 1960) 238-50; Trans., AIME, 219.

[4] Tommy M. Warren, SPE, Amoco Production Co. 1989. Evaluation of jet bit pressure losses. SPE17916.

[5] R. Subramanian, Process Engineer, Born Inc., Tulsa, Oklahoma and J. J. Azar, Mc Man Chair Professor, Petroleum Engineering, University of Tulsa, Tulsa, Oklahoma Experimental Study on Friction Pressure Drop for Non Newtonian Drilling Fluids in Pipe and Annular Flow. Nov. 2000.

[6] Practical Pressure Loss Predictions in Realistic Annular Geometries Mustafa Haciislamoglu and Ulysse Cartalos, Inst. Franqais du Petrole SPE Members, SPE 28304.

[7] M.S. Aston, P.J. Hearn, G. McGhee , Techniques for Solving Torque and Drag Problems in Today's Drilling Environment, SPE 48939.

[8] Chien, S.F. Settling velocity of irregularly shaped particles// SPE Drilling Completion, 9: 281-289. 1994.

[9] John A. Hudson, John P. Harrison, Engineering Rock Mechanics, 1997 . page 109

[10] Aadnøy, B. S., and Looyeh, R, Petroleum Rock Mechanics,2011.

[11] E. Fjær, R.M. Holt, P. Horsrud, A.M. Raaen & R. Risnes ,Petroleum Related Rock Mechanics, 2nd Edition , 1992.

[12] J. C. Jaeger, N. G. W. Cook, and R. W. Zimmerman, Fundamentals of Rock Mechanics 4th Edition, 2007.

[13] Bernt S. Aadnøy, Mesfin Belayneh, Elasto-plastic fracturing model for wellbore stability using non-penetrating fluids, Journal of Petroleum Science and Engineering 45. July 2004.

[14]Md. Amanullah, Ashraf M. Al-tahini, Nano-technology, its significance in smart fluid development in oil and gas field application. SPE-126102, May 2009.

[15] Md. Amanullah, Mohammad k. Al-arfaj, Ziad Al-abdullatif, Preliminary test results of Nano-based drilling fluids for oil and gas field application, SPE139534, March 2011.

[16] M. F. Fakoya, S. N. Shah, Rheological properties of surfactant-based and polymeric Nano-fluids, SPE 163921, March 2013 .

[17] http://www.wee-solve.de/en/amplitude-sweep.html

[18] Thomas. G. Mezger (2011). The Rheology Handbook, European coatings tech files, 3rd revised edition.

[19] "Øvinger I Bore og Brønnvæsker" (compendium in the undergraduate drilling fluid course).University of Stavanger.

[20] Van Dyke, Drilling Fluids, Austin, Texas, 2000

[21] K. Van Dyke. Drilling fluids, Mud Pumps, and Conditioning Equipment, Unit I, Lesson 7 First Edition, 1998, Austin Texas.

[22] http://www.irooildrilling.com/Viscosifier/CMC.htm

[23] V. Ershadi, T. Ebadi, A.R Rabani, L. Ershadi, H. Soltanian .The Effect of Nano silica on Cement Matrix Permeability in Oil Well to Decrease the Pollution of Receptive Environment, April 2011.

[24] Binh Bui Arild Saasen Jason Maxey Mehmet E. Ozbayoglu Stefan Z. Miska, Mengjiao Yu, Nicholas E. Takach Viscoelastic Properties of Oil-Based Drilling Fluids.

 [25] Benyounes Khaled, Benmounah Abdelbaki, Rheological and electrokinetic properties of Carboxylmethylcellulose water dispersions in the presence of salts

[26] K. Torbjørnsen , Borevæsketeknologi , 1994, chapter 1

[27] P.A. Bern, M. Zamora, K.S. Slater, the Influence of Drilling Variables on Barite Sag, SPE 36670, 1996

[28] Okrajni, S.S. and Azar, J.J. The Effects of Mud Rheology on Annular Hole Cleaning in Directional Wells. August 1986

[29] Skjeggestad , Olaf , Boreslamteknologi , 1989

[30] Statoil. 2010, Activity Program, Drilling

[31] https://www.cargillfoods.com/emea/en/products/hydrocolloids/xanthan-gum/functionality/index.jsp Cargill Corporate

[32] Aadnøy, B.S., "Geo-mechanical Analysis for Deep-water Drilling", SPE 39339 paper March, 1998

[33] http://www.separatorengineering.com/ws_tubular_centriuges.htm

[34] H. H. Rodriguez, J. B. Ramirez, D. C. Velazquez, A. N. Conejo, J. A. Martinez, "Annular flow analysis by tracers in drilling operations,2004.

[35] Chapter 5. Advanced drilling, Review of rheology, hydraulic and cutting transport, Mesfin Belayneh, University of Stavanger.

[36] MI Swaco - Engineering Drilling Fluid Manual, 1998.

[37] Mingqin Duan, Stefan Miska, Mengjiao Yu, Nicholas Takach, and Ramadan Ahmed, SPE, U. of Tulsa, and Claudia Zettner, SPE, ExxonMobil Critical Conditions for Effective Sand-Sized Solids Transport in Horizontal and High-Angle Wells, SPE 106707

[38] Decreasing Water Invasion into Atoka Shale Using Non-modified Silica Nanoparticles Jihua Cai, SPE, China University of Geosciences, Martin E. Chenevert, SPE, Mukul M. Sharma, SPE, The University of Texas at Austin, and Jim Friedheim, SPE, M-I SWACO

[39] USMS 025520 Pressure Drop Calculations for Drilling Fluids J.R. Lenschow, August 1992

[40] Kelco oil field group , Rhoelogy paper , Technical Bulletin, A Huber company

[41] Mario Zamora and David Power, "Making a Case for AADE Hydraulics and the Unified Rheological Model" April 2002

[42] I.H., Gucuyener, 1983. "A Rheological Model for Drilling fluids and Cement Slurries" March 1983 , SPE11487

[43] C. H. Van Der Zwaag, T. H. Omland, T. Vandbakk, "Dynmic filtration , Seepage losses on Tyrihans " , February 2012

[44] Versan, M. Tolga, A, "Effect of Polymers on the Rheological properties of KCl /Polymer Type Drilling Fluid," *Energy Sources*, (2005) **27**,405

Appendix

Appendix A:

Mud cake thickness:

The area A which is exposed to filtration is proportional to the volume of filtrate invading the cylindrical media:

$$A_f = 2\pi r_w h \tag{42}$$
$$Q_f \propto A_f = 2\pi r_w h C_m \tag{43}$$

Where C_m is mud cake constant, r_w is the wellbore radius and h is the height of the media. By applying material balance to the equation assuming the volume of invading filtrate V_i is equal to the volume of filtrate loss V_f.

$$V_i = \pi (r_i^2 - r_w^2) h \emptyset S_i \tag{44}$$

Time derivate of the flow rate equation becomes:

$$V_{f=} 2 r_w h C_m \, dt \tag{45}$$

By setting both equations equal to each other and knowing that C_m is time dependent:

$$\pi (r_i^2 - r_w^2) h \emptyset S_i = 2 r_w h \int C_m \, dt \tag{46}$$

Solving for radius of invasion:

$$r_i = \sqrt{r_w^2 + (\frac{2r_w}{\emptyset S_i}) \int C_m dt} \tag{47}$$

The length of invaded zone is then defined by the $d_i = ri - r_w$. Thus:

$$d_{i=} \sqrt{r_w^2 + (\frac{2r_w}{\emptyset S_i}) \int C_m dt} - r_w \tag{48}$$

By assuming that C_m no longer a function of time and using a constant value for time t_e a new equation for C_m is introduced by neglecting the explicit the time depending part. thus:

$$C_m = \frac{C_{mo}}{t+1} + C_{me} \tag{49}$$

Then the rate of the invasion is obtained by deriving the equation by time $(\frac{d}{dt})$:

$$\frac{d(d_i)}{dt} = \frac{r_w\left(C_{me} + \frac{C_m}{t+1}\right)}{\emptyset S_i \sqrt{r_w^2 + \frac{2r_w}{\emptyset S_i} + \left(C_{m0}\left(\ln\left(\frac{t+1}{t_e}\right) + \ln t_e\right) + C_{me}t\right)}} \quad (50)$$

Appendix B

Table 25 Calculated and measured data at different temperature

	#1			#2			#3			#4			#5		
RPM	72 oF	100 oF	130 oF	72 oF	100 oF	130 oF	72 oF	100 oF	130 oF	72 oF	100 oF	130 oF	72 oF	100 oF	130 oF
600	19	20	23,5	14	13	13	19	23	23	22	22	19	12	11	12
300	14,5	18	19	11	11	10	14	17	17	14	14	13	8	9	8
200	13,5	16	17,5	9	10	9	12	14	15	12	12	12	7	7	7
100	12	15,5	15,9	8	9	8	10	11	11	8	8	9	5,5	5	6
60	11	15	14	7,5	8	7	9	9	10	7	7	8	5	5	5
30	10	13,5	13,25	7	7	6,5	8	8	9	5	5	6	4,5	4,5	4
6	8,5	12	13	6,5	6,5	6	7	6,5	8,5	4	4	4,5	4	4	4
3	8	8,5	12	6	6	5	6,5	6	8	3	3	4	3	3	3
PV	4,5	2	4,5	3	2	3	5	6	6	8	8	6	4	2	4
YS	10	16	14,5	8	9	7	9	11	11	6	6	7	4	7	4
YS/PV	2,22	8	3,22	2,67	4,50	2,33	1,80	1,83	1,83	0,75	0,75	1,17	1	3,5	1
n	0,39	0,15	0,31	0,35	0,24	0,38	0,44	0,44	0,44	0,65	0,65	0,55	0,58	0,29	0,58
k	1,27	6,98	2,81	1,26	2,45	0,94	0,90	1,12	1,12	0,24	0,24	0,43	0,21	1,48	0,21
LSYS	7,5	5	11	5,5	5,5	4	6	5,5	7,5	2	2	3,5	2	2	2

Appendix C

Table 26 Measured and Calculated data for PAC+XC+NaCl systems

RPM	PAC 0.4g +XC 0.1g	NaCl 2.5 g	Nano	
	0.0 Nano+NaCl #13	0.15Nano+ NaCl #14	0.3 Nano+NaCl #15	0.45 Nano+NaCl #16
600	19	19	18	18
300	15	15	13	13
200	12	12	11	11
100	10	9	9	9
60	9	8	8	7
30	8	7	7	6
6	7	6	6	5
3	6	6	5	5
Parameter	0.0 Nano+NaCl #13	0.15Nano+ NaCl #14	0.3 Nano+NaCl #15	0.45 Nano+NaCl #14
PV	4,00	4,00	5,00	5,00
YS	11,00	11,00	8,00	8,00
YS/PV	0,36	0,36	0,63	0,63
n	0,34	0,34	0,47	0,47
k	1,79	1,79	0,70	0,70
LSYS	5,00	6,00	4,00	5,00

Appendix D

Hydraulic simulation data for CMC+XC+KCL drilling fluid systems

Table 27 Simulated annular pressure drop for CMC+XC+KCl system

Annular pressure loss				
Q	REF + 2,5 g KCl + 0,3g XC+0.2 LV CMC	REF+ 0,2 Nano	REF+ 0,25 Nano	REF+ 0,3 Nano
1	143,52	189,68	375,72	246,81
50	166,56	214,99	392,37	271,65
100	180,28	229,62	403,31	285,67
150	191,54	241,52	412,59	296,99
200	201,45	251,94	420,93	306,85
250	210,47	261,37	428,65	315,74
300	218,84	270,09	435,89	323,93
350	226,70	278,25	442,77	331,59
400	234,15	285,97	449,35	338,81
450	241,25	293,32	455,68	345,67
500	248,07	300,35	461,79	352,23
550	254,66	307,12	467,72	358,53
600	261,70	313,66	473,47	364,60

Table 28 Simulated total pressure drop for XC+CMC+KCl systems

Pump pressure loss				
Q	REF + 2,5 g KCl + 0,3g XC+0.2 LV CMC	REF+ 0,2 Nano	REF+ 0,25 Nano	REF+ 0,3 Nano
1	211,70	282,02	558,58	371,50
50	268,41	350,69	643,26	450,16
100	297,66	383,38	677,77	484,07
150	321,99	409,89	704,91	510,91
200	344,35	433,86	729,08	534,86
250	365,89	456,66	751,90	557,45
300	387,66	479,00	774,14	579,47
350	437,53	501,98	796,26	601,37
400	503,29	548,88	818,56	624,14
450	565,65	614,36	841,38	661,49
500	630,30	678,77	868,94	717,48
550	698,07	745,38	913,15	778,97
600	769,64	814,85	971,15	843,91

Appendix E

Table 29 Reference (left) and Nano-trested (right) system Amplitude sweep data

Meas. Pts.	G'' Ref	γ Ref	T Ref	G' Ref	Meas. Pts.	G''	γ	τ	G'
	[Pa]	[%]	[Pa]	[Pa]		[Pa]	[%]	[Pa]	[Pa]
1	5,98	0,000500	0,000170	33,43	1	10,14	0,0004986	3,68E-04	73,15
2	8,58	0,000697	0,000263	36,80	2	9,147	0,0006984	5,30E-04	75,28
3	4,20	0,000963	0,000358	36,96	3	7,295	0,0009721	7,16E-04	73,25
4	5,93	0,001349	0,000479	34,97	4	8,227	0,001357	1,02E-03	74,32
5	4,87	0,001872	0,000677	35,82	5	7,714	0,001892	1,44E-03	75,54
6	8,22	0,002591	0,000921	34,59	6	8,769	0,002639	1,98E-03	74,58
7	5,17	0,003619	0,001339	36,63	7	8,78	0,003677	2,80E-03	75,66
8	5,36	0,005033	0,001907	37,51	8	8,661	0,005129	3,94E-03	76,38
9	5,42	0,007000	0,002657	37,56	9	8,498	0,007154	5,51E-03	76,53
10	5,42	0,009740	0,003691	37,50	10	8,443	0,009978	7,75E-03	77,24
11	5,44	0,013540	0,005229	38,24	11	8,347	0,01392	1,09E-02	77,97
12	5,47	0,018840	0,007318	38,46	12	8,494	0,01941	1,54E-02	78,89
13	5,56	0,026190	0,010290	38,90	13	8,466	0,02706	2,16E-02	79,42
14	5,50	0,036430	0,014370	39,07	14	8,469	0,03774	3,04E-02	80,09
15	5,44	0,050670	0,020060	39,21	15	8,473	0,05264	4,28E-02	80,78
16	5,49	0,070470	0,028020	39,39	16	8,511	0,07341	6,01E-02	81,42
17	5,46	0,098020	0,039130	39,55	17	8,513	0,1024	8,44E-02	82,03
18	5,47	0,136300	0,054740	39,78	18	8,546	0,1428	1,19E-01	82,69
19	5,46	0,189600	0,076410	39,93	19	8,603	0,1991	1,67E-01	83,41
20	5,47	0,263700	0,106500	40,02	20	8,633	0,2777	2,35E-01	84,01
21	5,47	0,366800	0,148400	40,09	21	8,673	0,3873	3,30E-01	84,64
22	5,45	0,510100	0,206600	40,14	22	8,73	0,5401	4,63E-01	85,20
23	5,43	0,709500	0,287600	40,17	23	8,807	0,7533	6,49E-01	85,67

24	5,42	0,986800	0,400000	40,17	24	8,901	1,051	9,08E-01	85,98
25	5,41	1,372000	0,555500	40,11	25	9,032	1,465	1,27E+00	86,00
26	5,43	1,909000	0,770000	39,97	26	9,201	2,043	1,76E+00	85,51
27	5,49	2,655000	1,063000	39,68	27	9,439	2,85	2,42E+00	84,34
28	5,61	3,692000	1,461000	39,16	28	9,802	3,974	3,29E+00	82,30
29	5,84	5,136000	1,984000	38,18	29	10,38	5,543	4,41E+00	78,85
30	6,24	7,143000	2,650000	36,57	30	11,23	7,731	5,74E+00	73,36
31	6,87	9,937000	3,446000	33,99	31	12,43	10,78	7,16E+00	65,20
32	7,66	13,820000	4,333000	30,40	32	13,8	15,04	8,52E+00	54,95
33	8,43	19,230000	5,262000	26,04	33	14,72	20,98	9,73E+00	43,99
34	9,61	26,750000	6,074000	20,57	34	14,97	29,26	1,06E+01	33,01
35	10,57	37,190000	6,756000	14,77	35	14,09	40,8	1,10E+01	22,99
36	9,83	51,710000	7,490000	10,63	36	12,42	56,9	11,15	15,15
37	8,26	71,910000	8,067000	7,59	37	10,42	79,34	11,36	9,82
38	6,38	100,000000	8,127000	5,04	38	8,516	110,6	1,17E+01	6,31

Appendix F

Table 30 : Open hole and casing data

	Section type	Measured Depth (ft.)	Length (ft.)	Shoe Measured Depth (ft.)	Id (In)	Drift (In)	Effective Hole Diameter (In)	Friction factor	Linear Capacity (bbl/ft)	Excess (%)	Item Description
1	Casing	4012.5	4012.5	4012.5	12.250	12.459	12.615	0.25	0.1458		13 3/8in, 54.5ppf, J-55
2	Open Hole	11003.0	6990.50		12.250		12.250	0.30	0.1458	0.00	

Table 31 Drill pipe & BHA data

	Length (ft)	Depth (ft)	Body OD (in)	ID (in)	Stabilizer/tool joint Avg.joint Length (ft)	Length (ft)	OD (in)	ID (in)	Weight (ppf)	Material	Grade	Class
Drill pipe	10445	10445.00	5.0	4.276	30.00	1.42	6.406	3.75	22.26	CS_API 5D/7	E	P
Heavy weight Drill pipe	120.0	10565.0	6.625	4.5	30.00	4.00	8.25	4.5	70.50	CS_1340 MOD	1340 MOD	

Hydraulic Jar	32.00	10597	6.5	2.75					91.79	CS_API 5D/7	4145H MOD
Heavy weight Drill pipe	305.0	10902	5.0	3.0	30.00	4.00	6.50	3.063	49.7	CS_1340 MOD	1340 MOD
Bit sub	5.00	10907	6.0	2.4					79.51	CS_API 5D/7	4145H MOD
MWD tool	85.00	10992	8.0	2.5					154.36	SS_15-15LC	15-15LC MOD
Integral blade stabilizer	5.00	10997	6.25	2.0		1.00	8.453		93.72	CS_API 5D/7	4145H MOD
Bit sub	5.00	11002	6.0	2.4					79.51	CS_API 5D/7	4145H MOD
Tri-cone bit	1.00	11003	10.625						166.0		